Summer 2022

Prediction of Severity of Aviation Landing Accidents Using Support Vector Machine Models

Dezsö V. Silagyi
Embry-Riddle Aeronautical University, silagyid@my.erau.edu

Prediction of Severity of Aviation Landing Accidents Using Support Vector Machine Models

Dezsö V. Silagyi II

Dissertation Submitted to the College of Aviation in Partial Fulfillment of the Requirements for the Degree of Doctor of Philosophy in Aviation

Embry-Riddle Aeronautical University

Daytona Beach, Florida

August 2022

Prediction of Severity of Aviation Landing Accidents Using Support Vector Machine Models

By

Dezsö V. Silagyi II

This dissertation was prepared under the direction of the candidate's Dissertation Committee Chair, Dr. Dahai Liu , and has been approved by the members of the dissertation committee. It was submitted to the College of Aviation and was accepted in partial fulfillment of the requirements for the Degree of Doctor of Philosophy in Aviation.

Dahai Liu
Digitally signed by Dahai Liu
Date: 2022.09.14 17:10:58 -04'00'

Dr. Dahai Liu
Committee Chair

Dothang Truong
Digitally signed by Dothang Truong
Date: 2022.09.14 17:13:47 -04'00'

Dr. Dothang Truong
Committee Member

Steven Hampton
Digitally signed by Steven Hampton
Date: 2022.09.17 11:47:40 -04'00'

Steven Hampton, Ed.D.
Associate Dean, School of Graduate Studies, College of Aviation

Houbing Herbert Song
Digitally signed by Houbing Herbert Song
Date: 2022.09.14 20:18:34 -04'00'

Dr. Houbing Song
Committee Member

Alan J. Stolzer
Digitally signed by Alan J. Stolzer
Date: 2022.09.19 08:58:27 -04'00'

Alan J. Stolzer, Ph.D.
Dean, College of Aviation

Committee Member

Lon Moeller
Digitally signed by Lon Moeller
Date: 2022.09.19 11:42:36 -04'00'

Lon Moeller, J.D.
Senior Vice President for Academic Affairs and Provost

NEUMAN.CRAIG.HENRY.1248450076
Digitally signed by NEUMAN.CRAIG.HENRY.1248450076
Date: 2022.09.15 20:59:05 -05'00'

Dr. Craig H. Neuman
Committee Member (External)

August 17, 2022

Signature Page Date

Abstract

Researcher: Dezsö V. Silagyi II

Title: Prediction of Severity of Aviation Landing Accidents Using Support Vector Machine Models

Institution: Embry-Riddle Aeronautical University

Degree: Doctor of Philosophy in Aviation

Year: 2022

The purpose of this study was to apply support vector machine (SVM) models to predict the severity of aircraft damage and the severity of personal injury during an aircraft approach and landing accident and to evaluate and rank the importance of 14 accident factors to the severity. Three new factors were introduced using the theory of inattentional blindness: The presence of visual area surface penetrations for a runway, the Federal Aviation Administration's (FAA) visual area surface penetration policy timeframe, and the type of runway approach lighting.

The study comprised 1,297 aircraft approach and landing accidents at airports within the United States with at least one instrument approach procedure. The dataset was gathered from a combination of the National Transportation Safety Board (NTSB) accident database, the NTSB accident reports, and the FAA's Instrument Flight Procedure Gateway website. Four SVM models were developed in using the linear, polynomial, radial basis function (RBF), and sigmoid kernels for the severity of aircraft damage and another four SVM models were developed for the severity of personal injury. Five-fold cross-validation was used for testing the model accuracy and measures including evaluation of confusion matrices, misclassification rates, accuracy, precision,

sensitivity/recall, and F1-scores for model comparison. The best kernel models were selected and its model hyperparameters were optimized for the best model performance.

The SVM models using the RBF kernel produced the best machine learning models, with a 96% accuracy for predicting the severity of aircraft damage (0.94 precision, 0.95 recall, and 0.95 F1-score) and a 98% accuracy for predicting the severity of personal injury (0.99 precision, 0.98 recall, and 0.99 F1-score). The top predictors across both models were the pilot's total flight hours, time of the accident, pilot's age, crosswind component, landing runway number, single-engine land certificate, and any obstacle penetration. Specifically, the visual area surface obstacle penetration status ranked ninth across both SVM models. However, as a sub-category, an obstacle penetration on final approach was the seventh overall predictor and the second highest of the categorical predictors. The FAA visual area surface policy was ranked eighth as the overall factor, and the FAA policy from 2018 to 2019 was the third highest categorical predictor. Finally, the type of runway lighting was the sixth ranked prediction factor.

This study demonstrates the benefit of SVM modeling using the RBF kernel for accident prediction and for datasets with categorical factors. It is recommended for the NTSB to add the collection of all three new factors into the NTSB database for future aviation accident research. Lastly, flight training should include information on a pilot's susceptibility to inattentional blindness and the risks of potential obstacles in their flight path.

Keywords: aviation, accident, SVM, support vector machines, obstacle, airport, safety

Dedication

This paper is dedicated to my lovely and supportive wife, Missy, and my sons, Jack and Nate.

Acknowledgments

I would like to thank Dr. Liu, who provided inspiration and guidance throughout the dissertation process. I also want to acknowledge Dr. Song and Dr. Wang for their wisdom about machine learning and support vector machines. Next, thank you to Dr. Truong and Dr. Neuman for your insight, assistance, and suggestions as part of the committee. Lastly, I thank the best cohort ever -- Cohort 10 – for their great support and comradery throughout the classes and dissertation writing years, especially Joao Garcia for his python coding advice.

Table of Contents

Page

List of Tables

List of Figures

Chapter I: Introduction

This chapter provides an overview of this study, beginning with a background of aviation approach landing accidents, a statement of the problem regarding obstacles on final approach, and the purpose of this study. Next, it discusses the study's significance to the aviation industry and predictability research, which is followed by the three research questions guiding this study. Finally, the chapter concludes with the delimitations, limitations and assumptions, definitions, and acronyms.

Background

Commercial airlines, cargo companies, general aviation, and business aviation are all vulnerable to striking a tree, antenna, tower, pole, or other obstacles on the final approach (Huddleston, 2012; National Transportation Safety Board [NTSB], 1995, 2019). For example, according to the NTSB, in November 1995, American Airlines Flight 1572 impacted multiple treetops during the non-precision final approach and landing at Bradley International Airport, Connecticut (NTSB, 1995). The NTSB listed the obstructions on final approach to runway 15, 80-foot trees, as a finding, even though the runway had a Visual Approach Slope Indicator (VASI). United Postal Service (UPS) cargo Flight 1354 clipped a powerline and trees while on approach at Birmingham, Alabama, in August 2013, resulting in the death of all crewmembers (Aviation Impact Reform, 2013). The flight data recording revealed that the flight crew failed to perceive the obstacles in their flight path until the captain stated that they had collided with the trees (NTSB, 2014).

A general aviation flight instructor and student pilot were practicing approaches and landings when the student pilot flew the approach at higher-than-normal airspeeds

and a steeper angle because of trees at the end of the runway (Aviation Safety Reporting System [ASRS], 2021). The pilot was unable to stop the aircraft on the runway and crashed into a ditch. On September 11, 2019, two crewmembers perished when their business's cargo hauling Convair 440 impacted the tops of multiple trees on final approach at Toledo Express Airport, Ohio (NTSB, 2019b).

Pilot associations and the Federal Aviation Administration (FAA) both consider the presence of obstacles in the descent path of an aircraft on final approach as a significant problem (Airport Owners and Pilots Association [AOPA], 2016; Deener, 2013). The FAA began addressing the presence of these obstacles at the end of 2013 by removing them or installing runway approach lighting and has spent over $42 billion dollars since (FAA, 2020b, 2021a, 2021b). However, aviation landing accident research lacked any analysis addressing obstacles on final approach and landing.

The Aviation Landing Accident Problem

Every year, over 400 aircraft accidents occur during final approach and landing (AOPA, 2018). These two phases of flight account for over 65% of all aviation accidents (Airbus S.A.S., 2020; Boeing, 2019; Flight Safety Foundation [FSF], 2017; International Air Transportation Association [IATA], 2016). As the pilot departs from the decision altitude (DA) on a straight-in precision approach, or the minimum descent altitude (MDA), on straight-in non-precision or circling approach, the runway and runway environment must be in sight to continue the descent to landing (FAA, 2012, 2016b, 2016c; General Operating and Flight Rules, 2017). Typically, this transition is manually flown by the pilot or crew, even if automation was used up to the DA or MDA, to maneuver the aircraft to a position for a safe landing (Wang et al., 2018).

In addition, the final approach and landing phases have the highest workload and task saturation on a pilot or flight crew (FSF, 2017; Harris, 2011; Moriarty & Jarvis, 2014). Therefore, this period of high task saturation and hyper focus on the runway and/or runway environment may cause a pilot's or flight crew's visual routine to be impacted by inattentional blindness resulting in a missed visual area surface obstacle penetration directly in front of the descending aircraft.

Previous Landing Accident Research and Common Shortfalls

Previous human factors analysis and classification system (HFACS) research on the risks of final approach and landing accidents confirms the concerns of high task saturation on pilots and flight crews (Ancel et al., 2015; Boyd, 2019; Shappell et al., 2007; Wu, 2018). In addition, aviation landing accident research shows many common factors: environmental, aircraft, airport, and pilot characteristics (Baugh, 2020; Kushwaha & Sharma, 2014; Shappell et al., 2007; Wong et al., 2006; Wu et al., 2014). Unfortunately, there is insufficient evidence in previous research for the inclusion of the presence of obstacles on the final approach or the type of runway approach lighting.

Boyd (2019)'s results indicated that landings with higher energy levels, due to steeper flight angles or higher airspeeds, result in 38% of all landing accidents and twice the number of severe or fatal personal injuries. However, only 4% of landing accidents occurred from a shallow flight angle. If no obstacles were in the path of the aircraft, the pilot could lower the likelihood of an accident by flying at a shallower flight angle for landing. Although high energy levels have higher severity of personal injury accidents, there is a shortfall because the presence of obstacles on the final approach was not

included, which may be the cause of the steeper, faster, final approach (Valdés et al., 2011).

The majority of previous accident research was conducted using the NTSB database (Baugh, 2020; Boyd, 2019; Burnett & Si, 2017; Koteeswaran et al., 2019; Kushwaha & Sharma, 2014; Shappell et al., 2007; Wu et al., 2014). However, the database relies on the collection and input of NTSB accident investigators or investigator teams who analyze the findings and classify the accident into the database (NTSB, n.d.-d). HFACS safety classifications systems may have inter-coding and intra-coding inconsistencies because of human interpretation of the findings and taxonomy standardizations (Olsen & Sharrock, 2010). The NTSB database is not immune to these risks in which an aircraft accident during takeoff was coded as a landing accident (NTSB, 2015b). Many accident researchers indicated missing data in the NTSB database (Baugh, 2020; Boyd, 2019: Burnett & Si, 2017; Kushwaha & Sharma, 2014; Wu et al., 2014). Therefore, this study will manually review each NTSB report for missing data and taxonomy accuracy, like the previous study by Boyd (2019), to reduce any risks using the NTSB database.

In addition to missing data and the possibility of incorrect taxonomy, the NTSB database does not contain any variable information on the presence of obstacles on landing and the type of runway approach lighting, even when the accident investigation determined the aircraft impacted an obstacle on final approach and landing (NTSB, 1995, 2014, 2017a, 2017b, 2018a, 2018b). Therefore, there is a lack of previous accident research about the impact obstacles on final approach and landing due to the absence of obstacle information in the NTSB database.

Inattentional Blindness and Final Approach Obstacles

When a pilot or flight crew transitions from the DA or MDA, the focus is on locating the runway or the runway environment. This intense focus, along with the high task saturation of the final approach, may result in the pilot or flight crew missing a large obstacle directly in the descent gradient of the aircraft because of the vulnerability to inattentional blindness. The theory of inattentional blindness is when a person looks at an object directly in front of him/her but fails to process the presence of the obstacle due to focused attention (Mack & Rock, 1998; Most, 2010; Most et al., 2001; Neisser, 1979; Simon & Chabris, 1999). Wood and Simons (2019) state that an unexpected obstacle must be identified within the first 1.5 seconds of its appearance or risk inattentional blindness resulting in not recognizing the presence of the obstacle. Therefore, even if a tree or pole on final approach descent remains in view of the pilot or flight crew, it does not reduce the effects of inattentional blindness and could have disastrous consequences for the pilot and flight crew (Most, 2013). AOPA, the largest general aviation pilot organization, stated their concern to the FAA that any obstacle in the descent path of an aircraft on final approach is problematic, and the obstacle must be removed (AOPA, 2016).

However, AOPA's (2016) statement was subjective because of the lack of supporting research establishing the connection between obstacles on final approach and aviation accidents. This lack of previous research to support or refute AOPA's (2016) claim exposes a gap in accident aviation research. However, if a pilot was susceptible to inattentional blindness, resulting in a runway incursion with a vehicle or aircraft on the ground, it is reasonable to assume that the same pilot, during the final approach phase,

would be susceptible to inattentional blindness and may miss an obstacle in the aircraft flight path (Kennedy et al., 2014, 2017). Research has also shown that pilots and automobile drivers have an increased risk of inattentional blindness during periods of high task saturation (Durantin et al., 2017; Kennedy et al., 2014, 2017; Murphy & Greene, 2015, 2016; Pugnaghi et al., 2019, 2020). Therefore, this research focuses on analyzing landing accidents to determine if inattentional blindness and the possibility of missing an obstacle on the final approach are important predictors of the severity of personal injury and aircraft damage.

Statement of the Problem

The final approach and landing phases of flight account for over 65% of all aviation accidents per year (Airbus S.A.S., 2020; Boeing, 2019; FSF, 2017; IATA, 2016). Previous research has shown that this phase has high task saturation for pilots and flight crews (Ancel et al., 2015; Boyd, 2019; Shappell et al., 2007; Wu, 2018). Unfortunately, there is a lack of previous research incorporating the presence of obstacles on final approach and runway approach lighting.

However, the FAA views the presence of obstacles as a significant problem for pilots and flight crews during the final approach and landing and considers the installation of runway approach lighting to be a way to mitigate that risk. Since 2014, the FAA has spent over $42 billion dollars on approximately 2,300 airports to fund the removal of obstacles and/or the installation of runway approach lighting (FAA, 2020b, 2021a, 2021b). This significant amount of taxpayer money has been spent on reducing the number of landing accidents. However, there has been insufficient evidence in current studies to determine if the removal of obstacles or installation of runway lighting reduces

the severity of personal injury or aircraft damage. Therefore, this research filled that gap by including variables for the presence of obstacles and for runway approach lighting.

Purpose Statement

The purpose of the research was to conduct a quantitative, non-experimental research design using the support vector machine method for supervised machine learning models to predict the severity of aircraft damage and the severity of personal injury (Edmonds & Kennedy, 2017). The study incorporated 11 variables from previous aviation accident research along with three new variables that had not previously been researched. The previously researched variables were Code of Federal Regulation (C.F.R.) mission category, landing runway in use, crosswind component, number of aircraft engines, aircraft engine type, time of the accident, pilot's certificate, pilot's rating, pilot's total number of flight hours, pilot's age, and number of flight crew (Baugh, 2020; Moriarty & Jarvis, 2014; Shepell et al., 2007; Wu et al., 2014).

In addition to those 11 variables, this study was the first to incorporate the three new variables of visual area surface penetrations, corresponding FAA visual area surface penetration policies, and runway approach lighting type. These three new variables were incorporated because the theory of inattentional blindness could result in the pilot or flight crew failing to notice something unexpected, or an unexpected object, in front of the aircraft on final approach and landing (Most, 2013). Inattentional blindness has been shown to increase the possibility of runway incursions with another aircraft or vehicles during landing, so it is conceivable that the same would be true for a pilot to miss a tree, powerline, or tower on final approach (Kennedy et al., 2014, 2017). For example, inattentional blindness, and a missed obstacle, may result in an accident, like American

Airlines Flight 1572. In addition, a pilot's inattentional blindness may result in late obstacle recognition which subsequently results in an unstable approach and landing, culminating in an accident on landing (Martin, 2020; Moriarty & Jarvis, 2014; NTSB, 1995).

Incorporating all 14 variables, support vector machines (SVMs) were used to develop champion models to predict a multi-level severity of aircraft damage and multi-level severity of personal injury for aviation landing accidents in the United States. The SVM models were tested across four kernels, two of which have not been previously used in aviation accident research. The researcher used the NTSB database, a manual review of the NTSB accident reports, and additional public websites to collect and analyze landing accidents in the United States between January 2014 and December 2019 to cover the six years of the different FAA policies.

Significance of the Study

This study has practical and theoretical significance. The practical significance of the findings of this study is noteworthy to the entire aviation community. Airport owners, managers, airport designers, engineers, and consultants who pay for or conduct the removal of visual area surface obstacles are interested. If runway approach lighting is or is not a high predicting factor, this may help support their decision to install or not install runway approach lighting.

In addition, the FAA and the International Civil Aviation Organization (ICAO) may use this study to update or change orders and regulations about visual area surface obstacle removal or aircraft approach lighting requirements. Since the dataset

incorporates general aviation, business, and airlines, the results can be generalized to all facets of the aviation industry in the U.S.

The primary theoretical contribution of the study is that pilots and flight crews may gain an understanding of the dangers of inattentional blindness and its impact on approach and landing accident rates. This same understanding and knowledge may be used by aviation training companies as they update their training classes to include inattentional blindness awareness and recognizing visual area surface penetrations.

Lastly, the SVM methodology, technique, and comparison of different kernels are beneficial because these same procedures can be applied to other facets of the complex aviation environment to provide better predictability (Burnett & Si, 2017). Aviation accident research benefits from the evaluation of the new accident predictors: the presence of visual area surface penetrations for a runway, the FAA's visual area surface penetration policy timeframe, and the type of runway approach lighting. All types of predictability research, not just aviation, benefit from the general SVM methodology and kernel research because the research method and procedures could be broadly applied in other industries desiring to reduce personal injury and property damage.

Research Questions

The following research questions were investigated in this study:

RQ1

What support vector machine model is best for predicting the severity of aircraft damage and the severity of personal injury due to an aviation landing accident in the United States?

RQ2

What are the most important predictors for predicting the severity of aircraft damage and the severity of personal injury due to an aviation landing accident in the United States?

RQ3

What influence do the specific factors of the presence of visual area surface penetrations for a runway, the FAA's visual area surface penetration policy timeframe, and the type of runway approach lighting have in predicting the severity of aircraft damage and the severity of personal injury, due to an aviation landing accident in the United States?

Delimitations

The NTSB database contains all aviation accidents within the United States for this study's timeframe of January 1, 2014, to December 31, 2019, including general aviation, business, and commercial (NTSB, n.d.-a). These six years of aviation accidents were used to cover the three different FAA policies referring to the removal of obstacles on the final approach (AOPA, 2016; FAA, 2013b, 2018b, 2018c; Lebar, 2016; Namowitz, 2016; RTCA, 2016). Therefore, one delimitation was the United States-centric nature of the NTSB database because it does not contain every foreign aviation accident. However, the champion models could be used in other countries and by international aviation operators with any necessary adjustments specific to that country or operator.

The other delimitation was that this study used airport, environmental, and pilot factors. Although there are multiple factors or causes leading up to an accident, the pilot or flight crew are ultimately responsible for the safe operation of the aircraft.

Limitations and Assumptions

The study was limited to airports with at least one instrument approach procedure (IAP) because the FAA's IAP paperwork was required to verify the presence of visual area surface obstacle penetrations (FAA, 2018c). Without an IAP, the status of visual area surface penetrations would be unknown. However, with the necessary adjustment to the champion models, the results of this study can be applied to all airports, with and without IAPs, to reduce the risk of landing accidents. Airports without IAPs face many of the same cost versus benefit challenges in installing runway approach lighting, Visual Glide Slope Indicators (VGSIs), or removing obstacles (FAA, 2014a, 2014b).

It is assumed that the FAA correctly completed all the IAP visual area surface evaluations, took the appropriate regulatory action to amend the IAPs, correctly documented the results, and displayed visual area surface penetrations and approach runway lighting correctly on the IAP charts (FAA, 2018b). In addition, it is assumed all airports in the United States with IAPs have complied with the FAA requirements to identify and report obstacles around an airport, especially those obstacles in the visual area surface, whether or not they penetrate the visual area surface (FAA, 2014b).

Summary

The background discussed how the approach and landing phase of flight account for the majority of aviation accidents and how inattentional blindness impacted a pilot or flight crew's ability to detect visual area surface obstacle penetrations during final

approach and landing (Airbus S.A.S., 2020; Boeing, 2019; FSF, 2017; IATA, 2016). Although the FAA has spent billions at airports to install runway approach lighting and remove obstacles there is no evidence that research was conducted to determine if these changes impacted final approach and landing accidents. This research was the first to incorporate visual area surface penetrations, the different FAA policies, and runway approach lighting, along with other factors, to conduct a holistic evaluation of factors impacting approach and landing accidents. Also, it used support vector machine modeling and four different kernel functions to develop and compare high dimensional, linear and non-linear algorithms. The modeling determined how these factors predict the severity of aircraft damage and the severity of personal injury.

The next chapter provides a review of the relevant literature on inattentional blindness and aviation accidents. Then, Chapter III examines the development of the dataset and the use of support vector machine modeling to develop, test, fine tune, and validate the best model for predicting the severity of aircraft damage and another model for predicting the severity of personal injury. Finally, Chapters IV and V describe the results, followed by a discussion of the results, recommendations, and conclusion.

Definitions of Terms

20:1 Slope — An imaginary surface that starts 200 feet prior to the approach end of a runway and increases one foot in altitude for every 20 feet of distance, until reaching the location of the DA, for precision approaches, or VIP, for non-precision approaches (FAA, 2018b).

34:1 Slope — An imaginary surface that starts 200 feet prior to the approach end of a runway and increases one foot in altitude for every 34 feet of

distance, until reaching the location of the DA, for precision approaches, or VIP, for non-precision approaches (FAA, 2018b).

Attentional Misdirection When a person purposefully manipulates another person's attention away from seeing an unexpected object (Kuhn & Tatler 2005; Tatler & Kuhn, 2007).

Decision Altitude Specific altitude on a precision final approach where the pilot must have the runway environment in sight in order to continue to land (FAA, 2017).

Hyperplane An imaginary line used by SVMs to separate a set of data points based on their classification (Navlani, 2019).

Inattentional Blindness When a person either fails to perceive or fails to remember a large object due to a lack of focused attention (Mack & Rock, 1998; Most, 2010; Most et al., 2001; Neisser, 1979; Simon and Chabris, 1999).

Kernel Algorithm Used by SVMs to help maximize the margin between classifications by transforming nonlinear separable data classifications into a new higher dimensional space (Berwick, 2003; Navlani, 2019).

Margin The gap between the closest datapoints of different classifications and the hyperplane (Berwick, 2003; Navlani, 2019). The goal of a SVM model is to maximize this margin.

Minimum Descent Altitude The lowest altitude pilots are allowed to descend to on a non-precision final approach before having the runway environment in sight in order to continue to land (FAA, 2017).

Non-Precision Approach Instrument approach that only provides lateral guidance (Safe, Efficient use, and Preservation of the Navigable Airspace, 2020).

Obstacle Any temporary or permanent fixed object or movable object that is a hazard to navigation, extends above a slope or surface designed to protect flight operations, or is located on or around aircraft movement areas (ICAO, 2018).

Precision Approach Instrument approach that provides both lateral and vertical guidance (Safe, Efficient use, and Preservation of the Navigable Airspace, 2020).

Support Vectors These are the data points that are closest to the hyperplane and are most relevant to the development of the hyperplane (Berwick, 2003; Navlani, 2019).

Visual Area Surface Begins 200 feet before the runway threshold and extends until the DA, for precision approaches, or the VDP, for non-precision approaches. This area should not have 20:1 or 34:1 obstacle penetration (FAA, 2018c).

List of Acronyms

ACARS Aircraft Communications Addressing and Reporting System

ANN Artificial Neural Networks

ANOVA	Analysis of Variance
AOPA	Airport Owners and Pilots Association
ATC	Air Traffic Control
C.F.R.	Code of Federal Regulations
CT	Computed Tomography
DA	Decision Altitude
DV	Dependent Variable
FAA	Federal Aviation Administration
FSF	Flight Safety Foundation
fMRI	Functional Magnetic Resonance Imaging
HFACS	Human Factors Analysis and Classification System
IAP	Instrument Approach Procedure
IATA	International Air Transportation Association
ICAO	International Civil Aviation Organization
IV	Independent Variable
K	Kernel
KNN	K-Nearest Neighbors
NTSB	National Transportation Safety Board
MANOVA	Multivariate Analysis of Variance
MDA	Minimum Descent Altitude
NAS	National Airspace System
NOTAM	Notice to Airmen
PAPI	Precision Approach Path Indicator

RBF	Radial Basis Function
ROS	Random Over-Sampling
RTCA	Radio Technical Commission for Aeronautics
RUS	Random Under-Sampling
SEM	Structural Equation Modeling
SEMMA	Sample, Explore, Modify, Model, and Assess
SPSS	Statistical Package for the Social Sciences
SMOTE	Synthetic Minority Over-Sampling Technique
SVM	Support Vector Machine
UTC	Coordinated Universal Time
VASI	Visual Approach Slope Indicator
VDP	Visual Descent Point
VGSI	Visual Glide Slope Indicator

Chapter II: Review of the Relevant Literature

The chapter begins with an investigation of aviation landing accident research, followed by a discussion of the aviation landing accident factors, and a description of the three new variables introduced in the study. The next section provides an overview of support vector machines (SVM), including SVM calculations and their utilization in predictability research. The final sections provide an overview of the theory of inattentional blindness, inattentional blindness comparison to attentional misdirection, inattentional blindness in safety research, and how inattentional blindness supports the three research questions.

Aviation Accidents on Landing

As the pilot departs from the DA or MDA, the runway and runway environment must be in sight to continue the descent to landing (FAA, 2012, 2016b, 2016c; General Operating and Flight Rules, 2017). This transition is typically manually flown by the pilot or crew even if automation was used up to the DA or MDA (Wang et al., 2018). Between 2008 and 2018, 3,608 general aviation accidents have occurred during the approach and landing (AOPA, 2018). In commercial aviation, approach and landing accounts for roughly 65% of accidents and almost half of all fatalities (Boeing, 2019; FSF, 2017; IATA, 2016). The phase of flight from approach to landing has the highest workload and task saturation on a pilot or flight crew (FSF, 2017; Harris, 2011; Moriarty & Jarvis, 2014). Therefore, this period of high task saturation and hyper focus on the runway and/or runway environment may cause a pilot's or flight crew's visual routine to be impacted by inattentional blindness resulting in a missed visual area surface obstacle penetration directly in front of the descending aircraft.

Lasty, research has shown that landings with higher energy levels due to steeper flight angles or higher airspeeds result in 38% of the landing accidents (Boyd, 2019). However, if no obstacles were present, the pilot could lower the likelihood of an accident by flying a shallower flight angle for landing. Only 4% of landing accidents occurred from a shallow flight angle (Boyd, 2019). In addition, steeper final approaches result in twice the number of severe or fatal injuries. Many of these accidents can be contributed to the presence of visual area surface obstacles requiring the flight crew to avoid them or cause an actual collision with the aircraft. These obstacles may also result in steeper final approaches and landing overruns (Valdés et al., 2011).

Aviation Landing Accident Factors

Aviation landing accident research shows that there are many factors that seem to be common among general aviation and commercial airlines. These factors, listed in the following sections, include environmental, aircraft, airport, and pilot characteristic (Baugh, 2020; Kushwaha & Sharma, 2014; Shappell et al., 2007; Wong et al., 2006; Wu et al., 2014). This study combined the significant landing accident factors from previous research with the new variables of the presence of visual area surface penetrations, the FAA's visual area surface penetration policy timeframe, and the type of runway approach lighting.

Environmental Factors

Environmental factors include anything external to the aircraft including, but not limited to, light, weather, noise, atmospheric conditions, volcanic ash, and temperature (Kushwaha & Sharma, 2014). In aviation, environmental factors such as weather, crosswind component, lighting, and time of day are commonly listed as factors impacting

aviation accident rates (Baugh, 2020; Kushwaha & Sharma, 2014; Shappell et al., 2007; Wong et al., 2006).

Wong et al. (2006) used the NTSB database to assess four types of takeoff and landing accidents at nine major airports in the months of February, May, August, and November. The environmental factors reviewed were airport ceiling and visibility, general weather, temperature, crosswind component, and tailwind component. Chi-square and t-test statistical results showed landing accidents were more likely to occur at airports with instrument meteorological conditions rather than visual meteorological conditions. The results support this study, because obstacles around an airport could pose a potential safety hazard as aircraft arrive on an instrument approach procedure. However, they found no significant difference in crosswind component, which was contrary to their literature review. Even with their results, their literature research revealed the need for a crosswind component variable in this study.

Although the goal was to look only at the specific months of seasonal change, the location of the nine major airports differed across the United States, resulting in different seasonal changes. Therefore, Wong et al. (2006) could have analyzed additional airports and gathered accident data for all twelve months. Lastly, the researchers only conducted statistical analysis and did not conduct any type of predictive analysis.

The accident time of day variable was shown to be significant with aviation accidents for airlines and on-demand commuter aircraft (Shappell et al., 2007). Shappell et al. (2007) reviewed the NTSB database for 1,020 commercial accidents from 1990 to 2002. The statistical analysis showed accidents were five times more likely to occur when the pilot's visibility was diminished during nighttime, dusk, and dawn. Although the

research did not include general aviation or business aircraft and did not focus specifically on landing accidents, the research supported the necessity for time of day to be included as a variable in this research.

Aircraft Factors

Additional categories of aircraft type, C.F.R. mission type, and the number of engines on the aircraft also factor into aviation accidents because of the complexity of the aircraft, flight deck instruments, and type of mission (Shappell et al., 2007). This increased complexity may result in the pilot multitasking or being distracted from primary functions. These same issues, plus environmental and human factors, contributed to unstable approaches in commercial airlines and increased inattentional blindness (Moriarty & Jarvis, 2014).

For example, Boyd (2019) evaluated the aircraft's engine type and number to discover that single piston-engine aircraft were statistically more likely to have greater descent and landing airspeed resulting in an unsafe situation and higher injury severity. The research covered general aviation aircraft landing accidents at runways shorter than three thousand feet in length, from 1997 to 2016, using the NTSB database. Although the research included several aircraft variables, only a statistical evaluation was conducted, instead of predictability. Another shortfall was the limit to only runways less than three thousand feet, which eliminated many general aviation landing accidents. However, this study still included the variables of aircraft engine type and number of engines because of their statistical findings.

Moriarty and Jarvis (2014) conducted a qualitative study interviewing 25 airline pilots from one airline. The pilots were asked eight questions about stabilized precision

instrument approaches and the interaction with the aircraft, air traffic control, and crew members. Coding the interviews with NVivo 9 software, they discovered only a few pilots were adhering to the airline's standard operating procedures for stabilized approaches. Instead, competing priorities between air traffic control's desire for sequencing and the crew's desire to descend as fast as possible to the lowest allowed altitude increased the crew's task saturation. The increased task saturation also increased the crew's risk of inattentional blindness and exposed them to possible obstacles on final approach. In addition, the researchers uncovered how pilots were reluctant to go around from an unstable approach if the pilot or crew believed they could regain aircraft control. Although the study was limited to a single airline and a small sample the research supports the pilot's high task saturation on final approach and the human factors impact between the pilot and aircraft. This supported the use of variables in this study of mission category, number of engines, and aircraft engine type because these variables may increase complexity for the pilot and crew.

Airport Factors

To support the earlier discussion of the crosswind component, this research included the landing runway in use as a tool for calculating the crosswind component (Wong et al., 2006). The crosswind component was computed by calculating the sine of the difference between the wind direction and the landing runway, then multiplied against the wind velocity (FAA, 2014a). Although the landing runway in use could be kept as a hidden value in the calculation, it was included as a separate airport variable.

Pilot Characteristic Factors

Human factors research about aviation accidents lists factors such as pilot flight hours, pilot certificate, pilot rating, number of crew in the aircraft, and age of the pilot (Baugh, 2020; Shappell et al., 2007; Wu et al., 2014). As the pilot's experience increases, the risk for an accident typically decreases, which is why airlines and business aviation typically have fewer accidents than general aviation. However, airlines and business aviation are still susceptible to multiple human factors that impact unstable approaches (Moriarty & Jarvis, 2014). Therefore, these human factors variables were used in this study.

Specifically, Boyd (2019) conducted a Pearson Chi-Squared test to evaluate the different pilot and aircraft variables on high-speed landing accidents. In addition to the aircraft variables mentioned earlier, the research evaluated a pilot's highest certificate, pilot's rating, and pilot's total time. Through a combination of 1,392 surveyed pilots and 235 NTSB landing accidents, the lower the pilot's flight time, the more statistically significant the likelihood of a high-speed landing. However, the higher the pilot's flight time also revealed the pilot was more likely to attempt to recover a high-speed landing and continue the landing instead of initiating a go-around. Therefore, this research used variables of pilot total flight hours, certificate, and rating.

Using data mining techniques, Koteeswaran et al. (2019) reviewed 1,379 aviation accidents in all phases of flight from 1919 to 2014 using the FAA aviation accident dataset. Reviewing for 231 features, their top accident feature was pilot error followed by landing accidents. Although Koteeswaran et al.'s (2019) study did not look at specific accident variables, pilot error can result from numerous variables including pilot's age

and experience (Kennedy et al., 2010). One factor reviewed by Koteeswaran et al. (2019) was crew resource management, which was found to lower the risk of an aviation accident. Koteeswaran et al.'s (2019) results supported the variable for number of flight crew in this study because having multiple crew members may offset the severity of personal injury or aircraft damage during final approach and landing accidents because multiple crew members may be more likely to detect obstacles on final and not be as susceptible to inattentional blindness (Carpenter, 2001; Kreitz, Furley, et al., 2015).

Pilot's flight hours were also listed as a factor in research about general aviation accidents during all phases of flight (Baugh, 2020). Using the NTSB database, 26,387 accidents were pulled from 1998 to 2018. The data were evaluated using a combination of text mining and various machine learning models for a data, text, or combination model for predicting personal injury severity. Logistic Regression resulted in the best predictive model for the severity of personal injury with the lowest misclassification rate of 0.098. In addition, two of the top six variables were weather and pilot total flight hours, which were included in this study.

However, Baugh's (2020) predictive study differs from the Code of Federal Regulations and FAA, which separates personal injury into the four categories of none, minor, serious, and fatal (FAA, 2018b; "Notification and Reporting of Aircraft Accidents or Incidents", 2020). Instead of using a complex machine learning model to evaluate a multi-level dependent variable (DV), Baugh (2020) changed the DV into a binary variable by combining fatal and severe accidents into one level and combining minor and none into the other level. A minor injury is hospitalization of up to 48 hours, first degree burns, or external cuts, which no pilot would consider equal to an accident with no

injuries (FAA, 2018b; “Notification and Reporting of Aircraft Accidents or Incidents”, 2020). The researcher also included all phases of general aviation accidents, which explains why four of the top six significant variables apply to enroute phase of flight and does not apply to takeoff or landing (Baugh, 2020). Lastly, Baugh’s (2020) research successfully evaluated 21 different machine learning techniques; however, neither support vector machines nor kernel techniques were used in any of the 21 methods.

Another predictive research on personal injury and general aviation accidents in all phases of flight, used multiple machine learning techniques and various models composed of 64 variables (Burnett & Si, 2017). The research concluded that artificial neural networks had the highest predictability of accident fatalities and the highest predictability of a combination of accident injuries and fatalities. However, the research did not include accidents with minor or no personal injuries. Although the study did include support vector machine models with linear and polynomial kernels, the sigmoid or RBF kernels were not evaluated. The research also did not evaluate the sensitivity or importance of each factor. However, in the development of the different models, the variables included pilot certification, pilot’s age, pilot’s total flight hours, pilot rating, time of day, number of aircraft engines, and type of aircraft engine.

New Accident Variables

Three new variables, status of visual area surface penetrations, FAA visual area surface policy timeframe, and runway lighting types, were incorporated in this research. All three of these variables have not been assessed in previous aircraft accident research because the variables are not part of the NTSB database and thus require manual research

and coding (NTSB, n.d.-b). Therefore, the following section discusses their inclusion in this study.

Status of Visual Area Surface Penetrations. Although the majority of the final approach may be flown in clouds, the FAA (2012, 2017, 2020a) requires pilots and flight crew to be clear of clouds to begin descent from the DA on a precision approach, or MDA on a non-precision approach, through the landing. Since this maneuver from the DA or MDA to landing is conducted visually by the pilot, the FAA (2012, 2017, 2020a) also requires the pilot to see and avoid any ground obstacles (i.e., trees, towers, and buildings) that may be in the flight path of the aircraft. Even autopilot, or other automation, used for stabilized descent on the final approach does not guarantee the avoidance of obstacles (Huddleston, 2012).

During the visual maneuver from DA or MDA to landing, the FAA (2018c) has a visual area surface, as shown in Figure 1, that should be clear of ground obstacles. The visual area surface exists for precision approaches, non-precision approaches, and circling approaches. If an obstacle does exist in the visual area surface and the pilot or flight crew experience inattentional blindness, an accident may result (Durantin et al., 2017; Kennedy et al., 2014, 2017). The flight crew of American Airlines Flight 1572 may have experienced inattentional blindness, which is why they did not perceive the 80-foot-tall trees that penetrated the visual area surface by 55 feet (NTSB, 1995).

Figure 1

Circling and Straight-in Visual Area from FAA Order 8260.3D

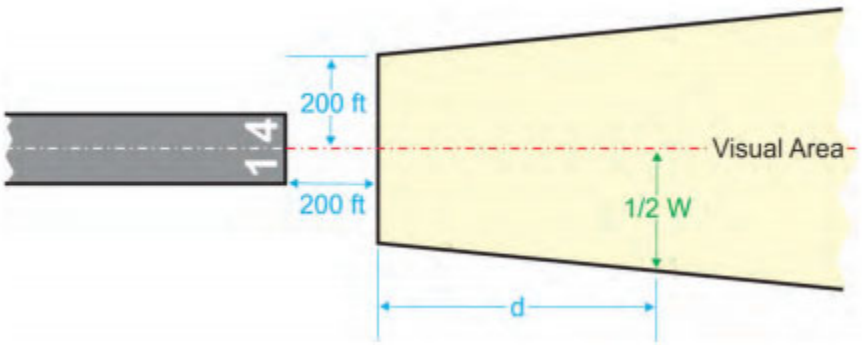

Note. The Visual Area begins 200 feet before the runway threshold and extends, as shown, until the DA, for precision approaches, or the VDP, for non-precision approaches and circling approaches. This area should not have 20:1 or 34:1 obstacle penetration (FAA, 2018c).

Previous research examined the impacts of inattentional blindness on flight crews during all phases of flight. Durantin et al. (2017) concluded that during times of high task saturation, pilots who suffered from inattentional blindness resulted in significantly missing flight deck cues and warnings. In addition, the likelihood of inattentional blindness increased when the pilots were also displaying poor flying performance; for example, struggling to stay on the final approach course or keeping the aircraft on a stable descent to landing. Research on runway incursions concluded that participants were prone to inattentional blindness on landing in both high task saturation (manual flying) scenarios and low task saturation (full automation) scenarios (Kennedy et al., 2014, 2017). Just as a pilot was unable to recognize an impending collision with a vehicle or aircraft on a runway, it is possible that a pilot would be just as susceptible to inattentional blindness and fail to notice a tree, pole, or tower directly in the flight path of

the aircraft. Even if the pilot was slightly affected by inattentional blindness and had a delayed recognition of the obstacle on final approach, the late recognition could result in an unstable approach that concludes with an accident on landing, as shown in Figure 2 (Martin, 2020).

Figure 2

Unstable Approach as a Result of Late Recognition of Trees on Final

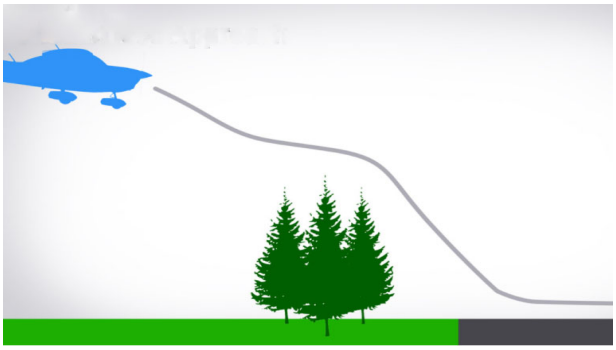

Note. The pilot's inattentional blindness may cause late recognition of obstacles on final approach, thus culminating in an unstable approach and an accident (Martin, 2020).

When a pilot or flight crew notices an obstacle in the visual area surface or directly in the flight path, the presence of the obstacle could increase pilot task saturation during an already critical phase of flight (FSF, 2017; Harris, 2011; Huddleston, 2012; Moriarty & Jarvis, 2014). This may impact pilots because when transitioning visually from the DA, on a precision approach, or MDA, on a non-precision straight-in or circling approach, a pilot and crew's primary focus is on the runway and the runway environment (FAA, 2012, 2016b, 2016c; General Operating and Flight Rules, 2017). Airline Owners & Pilots Association (AOPA, 2016) stated the increased risk of obstacle penetrations to the visual area surface was unacceptable and called on airport owners and managers to remove all of the penetrations. Their reasoning aligns with the theory of inattentional

blindness because a 20:1 or 34:1 obstacle penetration in the visual area surface penetration was an unexpected object directly in front of the flight path of the aircraft and may not be perceived by the pilot resulting in an accident. Even if the pilot detects the obstacle late, the aircraft is placed into an unsafe situation which could result in a hard landing, overrun, or landing accident (Valdés et al., 2011; Wong et al., 2006).

FAA Visual Area Surface Policy Timeframe. The final approach and landing phases of flight are only a fraction of the entire mission; however, this short phase accounts for roughly 65% of commercial aviation fatalities and almost 400 general aviation accidents per year (AOPA, 2018; Boeing, 2019; FSF, 2017; IATA, 2016). The FAA has launched numerous initiatives over the past couple of decades to reduce aviation accidents. With the support of the General Aviation Joint Steering Committee (2016), the FAA launched a goal to reduce general aviation accidents by 10% from 2009 to 2018. In the 2010s, the FAA also had yearly initiatives to reduce aviation fatalities for business and commercial aviation (Performance.gov, n.d.).

In September 2013, the Instrument Landing System (ILS) approach at New York's LaGuardia Airport was out of service, impacting major airlines and flight operations in the Northeast of the United States (National Business Aviation Association [NBAA], 2013). This instrument approach was shut down because an obstacle was erected that penetrated the visual area surface, rendering the final approach unsafe.

Therefore, in November 2013, due to political pressure and the FAA's desire to decrease approach and landing accidents, the FAA developed a two-year interim policy period to protect an aircraft on an Instrument Approach Procedure (IAP) as it descended from the DA or MDA to the runway (Deener, 2013; FAA, 2013b). The interim policy

stated that no obstacles should penetrate the 20:1 or 34:1 slopes in the visual area surface, as shown in Figure 1 (FAA, 2019b). These 20:1 and 34:1 slopes were imaginary surfaces that started 200 feet prior to the approach end of the runway and increased one foot for every 20 feet or 34 feet until the location of the DA or, for MDA non-precision approaches, the visual descent point (VDP). This area would be evaluated by the FAA at least every two years to prevent obstacles from being built or vegetation growing into the potential flight path of a landing aircraft (FAA, 2018b).

Unfortunately, some airports could not or chose not to adhere to the FAA interim policy to prevent obstacles from penetrating the visual area surface, or to remove obstacles that already penetrated the visual area surface. For example, an airport may not be able to remove trees due to environmental concerns, impacting endangered species, or historic preservation (Bruggers, 2016; Hart, 2018). Other times, trees which were once lowered have since regrown (Lyte, 2014). Lastly, some airport owners or property owners refuse to allow their trees to be lowered or obstacles to be removed (Gannon, 2009; Ryser, 2016). Therefore, the interim policy outlined a process that the airport owner or manager had to follow if the airport had a runway end with a 20:1 or 34:1 visual area surface penetration (FAA, 2013b). If the airport did not adhere to the interim policy, then the FAA stated they would issue a Notice to Air Missions (NOTAM) removing night operations to that runway (FAA, 2016b).

During the interim policy period, the FAA asked the Radio Technical Commission for Aeronautics (RTCA) to evaluate and recommend improvements to their interim policy. The RTCA evaluated the FAA's visual area surface obstacle penetration plan, mitigation procedures, and risk reduction for low visibility and night operations

(FAA, 2013a). The FAA's interim policy letter was effective on January 6, 2014. A month later, the RTCA recommended the FAA retain the low, medium, and high-risk categories for visual area surface penetrations but suggested the FAA conduct additional stakeholder outreach (RTCA, 2014). As part of the outreach, the FAA reminded all of their federal airport personnel, state agency airport personnel, individual airport owners, and individual airport managers to protect the visual area surface from obstacle penetrations (FAA, 2015). Lastly, the RTCA required the FAA to provide them all of the data and results once the two-year interim policy period was completed. These results included the FAA's evaluation of every airport runway end's visual area surface that had at least one IAP in the National Airspace System (NAS). During the interim period, the FAA evaluated over 16,000 IAPs at over 3,000 airports.

After the two-year interim policy ended in January 2016, the FAA moved to an assessment period with new policy guidance based on the results from the interim period (AOPA, 2016; Lebar, 2016; Namowitz, 2016; RTCA, 2016). During the two-year assessment period, the FAA allowed airport owners and managers 30 days to remove or light any visual area surface obstacle penetrations once they were discovered. If the airport owner or manager needed an extension to the 30-day policy, a request needed to be submitted to an FAA review board for approval. The FAA again reviewed over 16,000 IAPs at over 3,000 airports during this period.

After the two-year assessment phase ended in January 2018, the FAA moved to a final policy state where they added visual area surface guidance into their airport and instrument procedures development orders and regulations (FAA 2018b, 2018c). The final policy included an increase in IAP's visibility and removal of the VDP for non-

precision approaches when an obstacle penetrated the visual area surface. Although the FAA considered these steps a solution, AOPA (2016) stated any solution that allows obstacles to penetrate the visual area surface was problematic and should not be allowed.

The FAA changed the policy toward visual area surface penetrations three times over a six-year period from 2014 to 2020 (AOPA, 2016; FAA, 2013b, 2018b, 2018c; Lebar, 2016; Namowitz, 2016; RTCA, 2016). Changing aviation policy may have a significant impact on aviation landing accidents (Ancel et al., 2015). Previous human factors analysis and classification system research has shown how changes to FAA aircraft maintenance policies and oversight have shown to be a factor in maintenance accidents. The changes in policy resulted in confusion or misapplication in the airline companies' management conditions. The AOPA stated the FAA's interim policy, 2014 to 2016, was helpful but lacked easy to understand language for the general aviation pilots, and hoped the assessment period policy, 2016 to 2018, would provide much needed clarification (Namowitz, 2016). The AOPA did not state after the assessment period policy was published if the new policy solved the ambiguities in the interim policy. Therefore, the FAA Visual Area Surface Policy Timeframe variable were added to the study to determine if changing policies had an impact on the understanding or removal of visual area surface penetration by pilots and airport owners and operators.

Runway Lighting Types. The new factor of runway lighting types is included because of how environment lighting can factor into aviation accidents (Baugh, 2020; Shappell et al., 2007; Wong et al., 2006). As mentioned previously, Shappell et al. (2007) conducted a human factors analysis and classification system of airlines and commuter aircraft accidents in all phases of flight. Time of day was considered a significant factor

for these accidents. To mitigate this increased safety risk of night, dawn, and twilight approach and landing, airport owners and managers may choose to install runway lighting.

In addition to the environmental impact of lighting, inattentional blindness correlates to the presence and type of runway lighting because if an unexpected object is outside of the focus of the primary task, the inattentional blindness rates are significantly higher than if the object is inside the primary task focus (Kreitz et al., 2020). At an airport, runway lighting is installed to assist pilots during approach and landing, to find the airport in low light and low visibility weather conditions, and to establish lower visibility minimums (FAA, 2012, 2016b, 2016c). However, runway lighting types may have an unintentional negative consequence because the presence of the lighting could cause pilots to focus on the airport lighting type instead of focusing on the broader runway environment, thus inadvertently impacting the pilot's visual routine. This failure to notice something unexpected, or an unexpected object, can have serious consequences for pilots on approach and landing (Most, 2013). Therefore, the new variable for runway lighting type was included in this research to determine if the type of runway lighting installed predicts aircraft damage or personal injury.

Visual Routines

Since a pilot must have the runway and runway environment in sight to depart the MDA or DA, identification of the runway, runway environment, and any obstacles in the aircraft's glide path requires visual observation (FAA, 2012, 2016b, 2016c; General Operating and Flight Rules, 2017). However, Ullman (1996) states that there are four main problems with visual routines. The first problem is identifying the basic set of

operations that compose a visual routine (i.e., comparing one shape to another). Second is the integration of the different basic operations. Next is how the different operations are triggered and what determines their order. Last is how new visual routine operations are created and merged with known operations.

Roelfsema et al. (2000) stated that even if an object is seen, there are still possibilities of neuron delays impacting the ability of the person to see and process the seeing of the object. Therefore, pilots and flight crews experienced in visual routines on landing are still susceptible to missing an object on final approach and landing. Research confirmed this suspicion, showing how participants suffered from inattentional blindness by not visually detecting a possible runway incursion on landing (Kennedy et al., 2014, 2017).

Support Vector Machines

This section covers an overview of machine learning, then an overview of support vector machines (SVM). This is followed by SVM calculations and previous SVM predictability research.

Machine Learning Overview

Machine learning can be grouped into three different categories: supervised learning algorithms, unsupervised learning algorithms, and semi-supervised learning algorithms (Franchitti, n.d.). Unsupervised machine learning techniques include clustering, artificial neural networks, and radial basis functions. Semi-supervised machine learning techniques combine functions from the previous two categories, that is, clustering and regression. Supervised machine learning techniques include different types of regression, k-nearest neighbors (KNN), support vector machines, decision trees,

random forest, gaussian, and Bayesian. Therefore, support vector machines are a supervised machine learning algorithm used for solving problems that involve two group classifications (Franchitti, n.d.; Stecanella, 2017).

Support Vector Machine Overview

Support vector machines are a machine learning technique based on Vapnik's statistical learning theory, which allows for the generalization of multidimensional calculations (Vapnik, 1999). These multidimensional calculations, sometimes referred to as a black box because of the obscure or hidden processes, are used to determine the relationship between the input factors, independent variables (IVs), and outcomes, DVs (Dinov, 2018). The goal of SVM is to create a separation, called a margin, between categorical classification starting with the lowest dimension, two-dimension linear regression, and progressively increasing dimensions to three-dimensional space, four-dimensional space, and incrementally onward (Berwick, 2003; Navlani, 2019). Each increase in dimension is evaluated to maximize the margin between categorical classifications (Gandhi, 2018). This margin maximization concept is calculated for each variable to create a model that has a high accuracy of prediction (Dibike et al., 2001; Jeeva, 2018). The goal of SVM is to maximize the margin, the yellow shaded area, as depicted in Figure 3 (Marius, 2020).

Figure 3

Support Vector Machine Mechanics

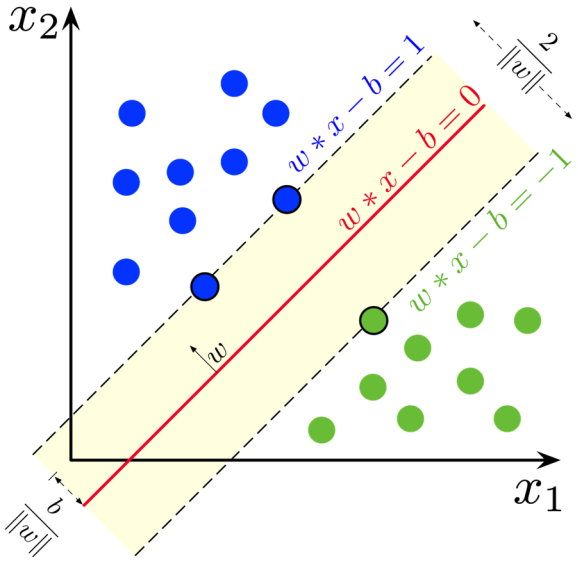

Note. w is the vector perpendicular to the hyperplane (red line); x is the input vector; b is the bias used to separate the two classifications (Marius, 2020).

Support Vectors. SVM begins with the opposing categorical data points that are closest to each other and are most relevant to the development of the hyperplane (Berwick, 2003; Navlani, 2019). These datapoints are used to create perpendicular support vectors that influence the development and orientation of the hyperplane. In Figure 2, the support vectors are the two blue dots and one green dot shown with a dark circular outline and are on the edge of the margin, or yellow area.

Margin. The margin is the gap between the closest datapoints, or support vectors, of different classifications (Berwick, 2003; Navlani, 2019). This is the yellow shaded area shown in Figure 2. The goal of a SVM model is to maximize this margin.

Hyperplane. The hyperplane is an imaginary line that separates a set of data point based on their classification (Navlani, 2019). The hyperplane is in the margin and is

depicted as the red line in Figure 2. The hyperplane acts as a decision boundary. Future datapoints that fall on one side of the hyperplane or the other are then classified as the attributes of that category. Therefore, in a margin maximization concept, the optimum hyperplane is established.

Kernels. A kernel algorithm helps SVM incrementally transform nonlinear classifications into separable data through the use of mathematical algorithms (Berwick, 2003; Navlani, 2019). SVM begins at the lowest dimension, two-dimensions, and progressively increases dimensions based on the specific kernel formula to transform the nonlinear classifications into a higher than three-dimensional space. Support vector machines models use a variety of different kernel algorithms to help maximize the margin between classifications. The four most common kernel calculations are the linear kernel, polynomial kernel, sigmoid kernel, and RBF kernel, as shown in Table 1 (Erdem et al., 2016; Jiang et al., 2016; Lin & Lin, 2003; Sánchez-González et al., 2018; Vapnik, 1999; Yang et al., 2019).

Table 1

Common Kernel Functions Used in Support Vector Machines

Kernel	Formula
Linear kernel	$K(x, x_i) = sum(x \cdot x_i)$
Polynomial kernel	$K(x, x_i) = \left((x \cdot x_i) + 1\right)^d$
Sigmoid kernel	$K(x, x_i) = \tanh\left(\gamma(x^T \cdot x_i) + r\right)$
Radial basis function (RBF) kernel	$K(x, x_i) = \exp\left(- \|\|x - x_i\|\|^2 / 2\sigma^2\right)$

Note. D is the degree polynomial, and γ and σ are the kernel parameters. Therefore, this study used all four kernel functions on each factor to find the maximized margin.

Figure 4 provides a depiction of the four different kernels (Marius, 2020; Scikit-learn, 2020). To answer all of the research questions, this study used all four common kernel functions to find the maximized margin for each variable and model.

Figure 4

Depiction of the Four Kernel Functions Used in this Study

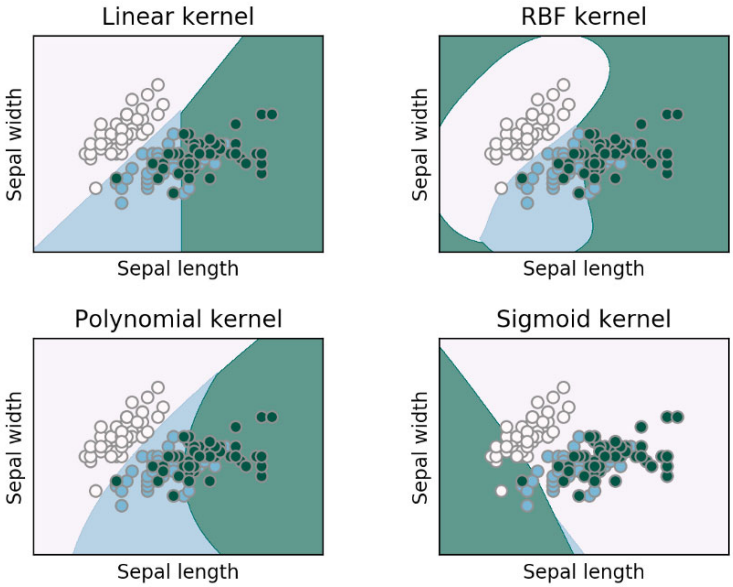

Note. Adapted from "Support Vector Machines" by Scikit-learn, 2020 (https://scikit-learn.org/stable/modules/svm.html). In the public domain.

Support Vector Machine Calculations

Support vector machines classify an individual data point as (x, y), or for an infinite amount of datapoints as (x_i, y_i), as seen in Equation 4, where i is each individual data point in a dataset up to the last data point N (Vapnik, 1999). To calculate a hyperplane,

$$w * x - b = 0 \quad (1)$$

where:

w = vector perpendicular to the hyperplane.

x = input vector.

b = bias used to separate the two classifications.

Sometimes this same formula is expressed by the addition of b, however the outcome is identical. For each new data point, if $w * x > b$, then the data point would belong to one of the classifications, while if $w * x < b$, then the data point would belong to the opposite classification (Melgani & Bruzzone, 2004). To calculate the optimum hyperplane (theta, θ),

$$\theta(w) = \frac{1}{2} \| w \|^2 \quad (2)$$

Since the optimum hyperplane is not automatically known, the solution to optimize the hyperplane lies in the Lagrangian (L) and Euler-Lagrange equations which subtracts potential energy (T) from kinetic energy (V) (Morin, 2007):

$$L = T - V \quad (3)$$

Substituting the Lagrangian formula for the hyperplane:

$$L = \frac{1}{2} \| w \|^2 - \sum_{i=1}^{N} \alpha_i [(w * x_i - b) y_i - 1] \quad (4)$$

where:

α_i = Lagrange multipliers.

α_i is replaced by ${\alpha_i}^0$ at the optimum hyperplane where vector w_0 meets the requirements (Vapnik, 1999):

$$\sum_{i=1}^{N} {\alpha_i}^0 y_i = 0 \quad and \quad {\alpha_i}^0 \geq 0 \ and \ i = 1, 2, 3, \ldots, N \quad (5)$$

At the optimum hyperplane location, using the Euler-Lagrange equation, the requirements are written (Dibike et al., 2001; Morin, 2007; Vapnik, 1999):

$$\frac{\partial L}{\partial x} = \frac{\partial L\,(w_0, b_0, a^0)}{\partial b} = 0 \quad \text{and} \quad \frac{\partial L\,(w_0, b_0, a^0)}{\partial w} = 0 \tag{6}$$

In addition, the support vectors at the optimum hyperplane location are:

$$w_0 = \sum_{i=1}^{N} {\alpha_i}^0 y_i x_i \;\; and \;\; {\alpha_i}^0 \geq 0 \tag{7}$$

Substituting w_0 into the above Lagrangian equation, still assuming ${\alpha_i}^0 \geq 0$, results in:

$$w(a) = \sum_{i=1}^{N} \alpha_i \; - \frac{1}{2} \sum_{i,j}^{N} \alpha_i \alpha_j y_i y_j (x_i * \; x_j) \tag{8}$$

This can then be displayed as a function in the original dimension using Equation 1 as:

$$f(x) = sign\,(w_0 * x - b_0) \tag{9}$$

Substituting w_0 for the support vectors at the optimum hyperplane at the original dimension:

$$f(x) = sign\,\left(\sum_{i=1}^{N} {\alpha_i}^0 y_i (x_i \; * x\right) + b_0) \tag{10}$$

When dealing with categorical data classification, SVM allows the adjustment of the hyperplane width through the parameter C (Fan, 2018; Kuhn & Johnson, 2016; Scikit-learn, 2022d; Vapnik, 1999).

$$\theta(w) = min\,\frac{1}{2} \parallel w \parallel^2 + C \sum_{i=1}^{N} \zeta \quad and \quad \zeta \geq 0 \tag{11}$$

A low value of C produces a larger margin while a larger value of C produces a hyperplane with a smaller margin width (Fan, 2018; Scikit-learn, 2022d, Wang, 2014). The change of C is a tradeoff between data categorical errors in the training set or test set. A low C value may have more errors in the training model while performing better with a test set. Conversely, with categorical data, a high C allows SVM to develop a model with improved nonlinear data separation at the risk of possible overfitting with numerous

errors in the test set. When optimizing a SVM model, C is one of the adjustable parameters in Google Colaboratory (2022).

The benefit of SVM is the ability to change the classification of categories from the original dimension into increased or higher dimensions using various kernel (K) functions (Dibike et al., 2001; Morin, 2007; Vapnik, 1999). Therefore, transitioning the support vector function at the original dimension to any higher dimension using a kernel function can be shown as:

$$f(x) = sign\left(\sum_{i=1}^{N} \alpha_i{}^0 y_i K(x_i * x\right) + b_0) \quad (12)$$

Any type of K function can be used in this formula to change the categorization to a higher dimension. In this research, the four kernel algorithms to be tested, as shown in Table 1, were the four most common kernel calculations: linear kernel, polynomial kernel, sigmoid kernel, and RBF kernel, as shown in Table 1 (Erdem et al., 2016; Jiang et al., 2016; Lin & Lin, 2003; Sánchez-González et al., 2018; Vapnik, 1999; Yang et al., 2019). Google Colaboratory (2022), similar to many python applications, has default values for the different kernel parameters. The application allows the user to change the value of the kernel parameters γ and σ to optimize the kernel's performance in the SVM model.

Therefore, the purpose of SVM is to maximize the hyperplane for the categorical separation in higher dimensional space (Melgani & Bruzzone, 2004; Vapnik, 1999):

$$w(a) = \sum_{i=1}^{N} \alpha_i - \frac{1}{2}\sum_{i,j}^{N} \alpha_i \alpha_j y_i y_j K(x_i * x_j) \quad (13)$$

$$\sum_{i=1}^{N} \alpha_i{}^0 y_i = 0 \ and \ \alpha_i{}^0 \geq 0 \ and \ i = 1, 2, 3, \ldots, N$$

Support Vector Machines in Predictability Research

Machine Learning in Aviation. The use of SVM in aviation accident research has only occurred over the past few years. Burnett and Si (2017) evaluated aviation fatalities using SVM, KNN, Artificial Neural Networks (ANN), and Decision Trees. These different prediction techniques were used to appraise general aviation accidents from 1975 to 2002. Comparing over 64 different variables, their research concluded that ANN had the highest predictability of fatalities and the combination of injuries and fatalities. Although ANN had a percentage of approximately 91% for fatalities and 78% for injuries and fatalities, it only outperformed the other machine learning techniques by 1%-4%. Decision Trees and KNN had the lowest predictability percent for both evaluations. However, Burnett and Si's research only used SVM modeling with the linear and polynomial kernels and did not evaluate the sigmoid or RBF kernels. Although they did not report on specific individual factors' ability to predict injuries and fatalities, they did state the likelihood these modern machine learning techniques are able to provide better predictability in the complex aviation environment. They also stated the research should be conducted using more recent accident data than 2002.

Around the same time, Koteeswaran et al. (2019) compared many of these same machine learning techniques on aviation accidents from 1991 to 2014. Their dataset, based on the Flight Safety Foundation, evaluated only aviation accidents that had listed both a primary and secondary cause. Instead of researching only human factors impacting accidents, this study focused on all factors: 231 reported probable causes, such as engine fire, wing icing, fatigue, and corrosion. They concluded that pilot error was the leading

cause of accidents followed by crashing during the landing phase. K-Nearest Neighbors has the highest predictability over SVM and ANN; however, at over 99% accurate, the KNN model risked overfitting.

Of late, various machine learning techniques were used to identify maintenance hazards with the aircraft's auxiliary power unit (Zhou et al., 2020). There were 1,244 events in the Aircraft Communications Addressing and Reporting System (ACARS) dataset used across 10 different parameters. Applying a 10-fold cross-validation, their predictability research discovered that SVM had the highest accuracy over Decision Trees, Artificial Neural Networks, Logistic Regression, KNN, and Linear Discriminant. In other aviation research, SVM has been used to evaluate the impacts of fatigue in Air Traffic Controllers (Shen et al., 2020). Using the RBF kernel and a six-fold cross-validation, SVM predicted fatigue accuracy higher than almost 93% in Air Traffic Controllers.

Support Vector Machines in Accident Research. Although the full use of SVM for predicting aviation accidents has yet to be utilized, SVM has been widely used in modeling automobile accidents and their injury severity. Li et al. (2008) stated SVM offered both the best performance for predicting automobile accidents, the fastest results, and reduced the risk of overfitting. Their research compared four variable factors during 88 traffic accidents in Texas. The RBF kernel was used to compare three different training and validation sample sizes. The training size of 80% had the best prediction accuracy. Based on their findings, the authors suggested continued evaluation against other highway datasets.

Li et al. (2012) continued their automobile accident research by analyzing approximately 5,500 automobile crashes across 10 variables to determine if SVM was suitable in predicting injury severity levels. Injury severity was listed as the DV broken up into five categories ranging from no injury to a fatality. The RBF kernel produced the best prediction behavior using 80% of the data toward the training set. The leading factors impacting injury severity levels were the number of freeway lanes and the type of business/residential area surrounding the intersection. This study was the closest in similarity to Li et al.'s (2012) research except using aviation landing accidents instead of freeway intersection accidents.

Gaps in the Literature

Research of the predictability of aircraft accidents in all phases of flight currently exists and is expected to continue (Burnett & Si, 2017; Valdés et al., 2011). However, as previously discussed, there is a limited amount of research predicting aviation accidents using SVM (Burnett & Si, 2017; Koteeswaran et al., 2019). Burnett and Si (2017), Baugh (2020), and Koteeswaran et al. (2019), who explored aviation accidents across all phases of flights, restricted their dataset to general aviation only and were subject to a lack of current accident data. They also adjusted their DV to a binary variable instead of the original multi-level variable as defined by the FAA (2018b; "Notification and Reporting of Aircraft Accidents or Incidents", 2020). In addition, SVM kernels were limited to the linear and polynomial kernels and did not explore the RBF or sigmoid kernels. Therefore, this study narrows the focus of aviation accidents to those that occurred only during the approach and landing phase and explores all four SVM kernels to predicted severity as a multi-level DV.

The reason for narrowing to the approach and landing phase of flight was because this portion has resulted in 3,608 general aviation accidents between 2008 and 2018 and roughly 65% of accidents, and half of all fatalities, in commercial aviation (AOPA, 2018; Boeing, 2019; FSF, 2017; IATA, 2016). Koteeswaran et al. (2019) stated that landing accidents were the second ranked attribute of aviation accidents behind pilot error. The closest approach and landing research was flight simulator experiments that determined participant susceptibility to inattentional blindness when flying an approach and landing manually or with automation (Kennedy et al., 2014, 2017). These studies used analysis of variance (ANOVA) to determine if there was a significant difference and did not do any modeling for predictability. Therefore, this research combined general aviation, business, and airline missions because they all have the highest percentage of accidents during the final approach and landing. In addition, this same phase of flight imposes a high task saturation on pilots and flight crews, causing a higher likelihood of inattentional blindness.

Not only did this research narrow the focus of aviation accidents, but this research also introduced factors that have not been previously researched. The theory of inattentional blindness supports the addition of the three new factors of visual area surface penetrations, runway lighting, and FAA policy timeframe because of the possibility of the pilot or flight crew missing an obstacle directly in the flight path of the aircraft. These three new factors were incorporated with previous factors to develop a holistic model to predict aviation accidents on final approach and landing. Lastly, previous research on automobile accidents has shown the ability for SVM to accurately predict the severity of injury (Li et al., 2012). Therefore, the research method and design

filled the gap in research by creating a comprehensive model, using factors never evaluated before, to predict both the severity of aircraft damage and the severity of personal injury.

Theoretical Framework – Inattentional Blindness

The human factors theory of inattentional blindness is demonstrated when a person looks at something unexpected directly in front of him/her but fails to notice it due to preoccupation (Mack & Rock, 1998; Most, 2010; Most et al., 2001; Neisser, 1979). Simon and Chabris (1999) define inattentional blindness as a person either failing to perceive or failing to remember a large object due to a lack of focused attention. This identification of an unexpected object must occur during the first 1.5 seconds the object appeared, or most likely the participant continued to suffer from inattentional blindness no matter how long the unexpected object remained in view (Wood & Simons, 2019).

When transitioning from DA, for precision approaches, or MDA, for non-precision straight-in or circling approaches, a pilot's primary focus is on the runway and the runway environment. Inattentional blindness could cause the pilot to miss a large obstacle directly in the descent gradient of the aircraft, such as a tree or pole. Even though a tree or pole is a large object and may remain in view, it does not reduce the possibility of inattentional blindness. This failure to notice an unexpected object could have serious consequences for the pilot and flight crew (Most, 2013).

Inattentional Blindness Research

In one of the earliest inattentional blindness studies, participants counted the number of passes by a basketball team but failed to notice a woman carrying an umbrella walking through the back of the scene (Neisser, 1979). Simons and Chabris (1999)

reproduced the study but replaced the woman carrying an umbrella with a person in a gorilla costume. Almost half of the participants failed to notice the gorilla while counting passes. The researchers determined that the ability to notice an unexpected object, like an obstacle in the flight path on final approach, is dependent on how difficult the primary task is for the participant. Unfortunately for pilots, special proximity of the unexpected event does not deter inattentional blindness, which means even if a pilot detects events around the aircraft and runway, the pilot may not see an obstacle directly in the flight path.

One could argue that the gorilla study does not impact pilots because pilots are engaged in a routine occurrence, flying an approach and landing, as opposed to an unexpected event. However, expert radiologists were asked to review chest computed tomography (CT) scans for lung-nodule detection, a routine task for radiologists (Drew et al., 2013). In one of the CT scan groupings, the image of a gorilla, 48 times larger than any lung-nodule, was inserted into the area of the lung. To avoid a sudden onset, the gorilla image was faded into the position in the lung during multiple image slices of the lungs. The same thing was repeated with the gorilla fading out of the lung over multiple CT slides. Even with the gorilla in multiple images and 48 times larger than any lung-nodule, 83% of the expert radiologists suffered from inattentional blindness and did not see the gorilla. Eye track monitoring showed that many of the radiologists looked directly at the gorilla but still did not observe the gorilla. Therefore, even experts conducting routine operations, such as expert pilots flying an approach and landing, are vulnerable to inattentional blindness.

Similar to the gorilla studies, Oktay and Congoz (2018) tested participants on their ability to recognize Zorro during a video. The difference is that Oktay and Congoz changed the backgrounds of the videos to show a positive background scenario, neutral scenario, and negative scenario. Participants did not notice Zorro in the positive background 60% of the time and negative background 58% of the time. When the background was empty (neutral), participants did not notice Zorro 48% of the time, which was the lowest inattentional blindness of the study. This could impact how a pilot recognizes obstacles on approach, depending on whether the pilot considers the airport scenario as a positive or negative background. Unfortunately, there are no scenarios for pilots where the background is clutter free, or neutral.

To determine how different stimuli threats impact inattentional blindness, researchers conducted an experiment asking participants to identify different symbols and displays while interjecting threatening and non-threatening words (Beanland et al., 2018). After the experiment, each participant was asked to describe the different symbols, displays, and possible words. The researchers found that 22% of the participants recognized at least one word, 19% recognized the threatening word, 11% recognized the non-threatening word, and only 8% recognized both. Therefore, the researchers concluded that although all groups were impacted by inattentional blindness, participants were more likely to recognize a threat over a non-threat. This could benefit pilots if the pilots perceived the landing phase as a threat.

This experiment was repeated using pictures of threatening spiders instead of random objects (New & German, 2015). Again, all participants were affected by inattentional blindness; the threatening spiders were discovered more often than the

neutral objects and pictures. However, the results from Stothart et al. (2017) stated that there was no significant difference in the amount of inattentional blindness between the high and low threat groups. Their research, comparing high cost (threat) and low cost (non-threat) words and pictures, found that all groups were equally influenced by inattentional blindness.

Lastly, if the unexpected object is outside of the focus of the primary task, the inattentional blindness rates are significantly higher than if the object is inside the focus of the primary task (Kreitz et al., 2020). This may impact pilots because during the landing phase, pilots are focused on the runway end instead of a broader runway environment scan. Therefore, the pilot could miss an unexpected object in the flight path of the aircraft and even more likely to miss an obstacle slightly off the flight path, such as a tree or telephone pole, while also missing the tree branch or telephone wire directly in the flight path.

However, not all experiments provided significant differences in inattentional blindness. Research attempting to distinguish if personality traits impacted inattentional blindness did not find a significant impact on inattentional blindness levels (Kreitz Schnuerch, et al., 2015). Also, a person's cognitive ability did not differentiate inattentional blindness levels (Kreitz, Furley, et al., 2015). Finally, if a participant was given multiple classic attention capture practice problems prior to the inattentional blindness experiment, the added perception knowledge did not improve inattentional blindness levels (Wright et al., 2018). These studies show that participants of every age, cognitive ability, and persona are susceptible to inattentional blindness.

Inattentional Blindness versus Attentional Misdirection

Researchers of the theory of inattentional blindness have differing opinions than those of the theory of purposeful attention misdirection. Attentional misdirection is when a person purposefully manipulates another person's attention away from seeing an unexpected object (Kuhn & Tatler 2005; Tatler & Kuhn, 2007). For example, magicians use attentional misdirection to prevent an audience from seeing how a magic trick was accomplished.

Attentional misdirection researchers criticize inattentional blindness research stating that the unexpected object, like a gorilla appearing during teams passing basketballs, does not mirror real life, whereas studying magicians and audience eye movement closely imitates real life (Kuhn & Tatler 2005; Kuhn et al., 2008; Tatler & Kuhn, 2007). In essence, these researchers state that the theories of inattentional blindness and attentional misdirection are actually the same in application. In these attentional misdirection experiments, participants' eye movements were monitored; those who did not know the magic trick were compared to those who were informed of the upcoming misdirection (but not where or how the misdirection would occur). As expected, those participants who knew of the misdirection looked toward that location significantly earlier than those who were not informed. This confirmed that a person's attention remained primarily on the object even when the magician tried to divert the participant's eyes away from the object.

In response to these theory of attentional misdirection experiments, Memmert (2010) countered that the two theories are not similar and proposed four distinctions between the two theories. First was that the attentional misdirection theory provided

foreshadowing of the unexpected event compared to the inattentional blindness, which allowed no foreshadowing. Second, inattentional blindness experiments were full-attention trials that provided the entire scenario for the participant to view compared to the attentional misdirection trials that only accounted for the participant observing the specific trick instead of also mirroring the same conditions without misdirection. Memmert's third difference stated that there was no workload assigned to the participants in the attentional misdirection experiments. The inattentional blindness experiments included the opportunity for the participant to be distracted by a primary task while the attentional misdirection experiment asked the participants to watch the magician. Lastly, the inattentional blindness experiments involved an unexpected object, something not relevant to the primary task, to test participant's perception, while the attentional misdirection experiments' unexpected object was part of the magic trick and not actually unexpected. Therefore, Memmert concluded that inattentional blindness and attentional misdirection were not the same.

After Memmert published his argument, Kuhn and Tatler (2011) rebutted the four differences stating that the magician's ability to create misdirection removed any difference of foreshadowing and no foreshadowing. In addition, the researchers of attentional misdirection compared the eye movements of the group that were told to look for the unexpected object and the participants that were not told. Their third rebuttal was that an unexpected object, such as a gorilla, was so unexpected that participants did not recognize it because it was not realistic to any real-world scenarios. Lastly, Kuhn and Tatler (2011) stated the purpose of a magician was to keep the audience from knowing the method of the trick and thus creating the unexpected event. Their refutation

concluded again stating that the theory attentional misdirection was similar to the theory of inattentional blindness.

While the argument between attentional misdirection and inattentional blindness transpired, Most (2010) suggested that the disagreement highlighted at least two different forms of inattentional blindness, spatial inattentional blindness and central inattentional blindness. Spatial inattentional blindness was defined as the concealed misdirection of a participant's attention, while central inattentional blindness was defined as a failure of a later stage in visual processing and visual memory which prevents the participant from recognizing the unexpected event. Therefore, instead of completely separating or combining attentional misdirection and inattentional blindness, Most (2010) posited that these experiments revealed two of the different types of inattentional blindness. Whether the different experiments showed single or multiple facets of inattentional blindness, there is no magician purposely moving the attention of the pilot away from perceiving an obstacle in the flight path. Therefore, the theory of inattentional blindness remained the theoretical framework for this study.

Inattentional Blindness in Aviation

The main aviation study of inattentional blindness was a flight simulator experiment for runway incursion detection (Kennedy et al., 2014, 2017). The experiment measured the relationship between flight deck automation and inattentional blindness. Using non-pilots, each participant was asked to fly, in random order, a final approach and landing configured for full automation, partial automation, and no automation. During the landing phase, multiple aircraft and vehicles were in view, but there was either an aircraft or vehicle which created a runway incursion event. After the flight simulator, each

participant filled out a questionnaire to determine what was perceived or not perceived to evaluate inattentional blindness. Each type of automation configuration was flown twice. The overall number of inattentional blindness occurrences were 70% during the first approach, and decreased to 50% on the second approach. Partial automation approaches had the lowest inattentional blindness on the first attempt, and full automation had the lowest inattentional blindness on the second attempt. Only full automation had a significant decrease in inattentional blindness between the first and second attempt, most likely because the participants recognized their automation complacency on the first attempt. However, none of the approach types had a significant difference in inattentional blindness compared to the other approach types. Therefore, the researchers concluded both high and low workload conditions induced inattentional blindness.

Researchers have also studied air traffic controllers, their display screens, and their warnings for the possibility of inattentional blindness (Imbert et al., 2014). The current display plus four different displays, with varying visual and notification designs, were used to determine each setup's ability to capture the controller's attention and reduce inattentional blindness. This included eye movement tracking, performance measures, and other reports to determine where the controller's attention was focused. The results showed controllers did not respond as well to color or animation, but instead to different methods of aircraft notification symbols (e.g., pulsating box). Unfortunately, these notification symbols impaired other task performance. Therefore, it was identified that controllers were impacted by inattentional blindness in their current system display design and recommended a new design that balanced notifications and performance.

Another aviation study close to inattentional blindness was about inattentional deafness: flight deck auditory warnings missed by pilots during increased workload conditions (Durantin et al., 2017). Researchers conducted a flight simulation experiment where pilots were asked to fly an air racecourse and then asked to push a button on their joystick when they heard the audible warning. To map brain activity, the participants donned a functional magnetic resonance imaging (fMRI). The fMRI revealed a significantly increased activity in the superior medial frontal cortex and right inferior frontal gyrus when inattentional deafness occurred. If the participants also displayed poor flying performance (e.g., missed air racing gates), the pilots were more likely to also have inattentional deafness.

Inattentional Blindness in Drivers

Unlike aviation, inattentional blindness has been studied more robustly in automobile drivers. Pammer et al. (2018) conducted an experiment to test the inattentional blindness of automobile drivers and their failure to detect motorcycles. Through three different experiments, the researchers showed participants different city driving scenarios on laptop computers while interjecting pictures of motorcycles and taxis. From their experiments, they discovered participants had double the likelihood of failing to notice the motorcycle over the taxi. If the motorcycle was placed at an intersection by itself, with the possibility of an accident, the participants had a significantly higher detection rate. However, if both a taxi and a motorcycle were at the same intersection posing the same threat, participants recognized the taxi while inattentional blindness impacted the recognition of the motorcycle. Therefore, the

experiment showed automobile drivers have a high probability of inattentional blindness sharing the road with motorcyclists.

Color may also play into inattentional blindness. Most and Astur (2007) conducted driving simulator experiments where they used different colored arrows telling the driver which way to turn. They also interjected motorcycles with either the same color or different color than the arrow at the same intersection. Their research concluded collision rates were higher when the motorcycle was a different color than the direction arrow. This matched non-driving experiments that showed participants had a larger inattentional blindness when the unexpected obstacle was a completely different color than the stimuli, rather than unexpected objects with the same or slightly different colors than the stimuli (Horstmann & Ansorge, 2016; Webster et al., 2018). Unfortunately, obstacles on final approach may not be the same color as the runway.

In addition to color, researchers experimented to determine if age impacted the level of inattentional blindness in drivers (Saryazdi et al., 2019). The experiments used driving simulations to determine if the participants noticed different stimuli (i.e., people, vehicles, advertisements, and more) on the side of the road. Results showed both young and older adults suffered from inattentional blindness. However, older adults had a higher level of inattentional blindness than younger drivers, and older adults did not improve throughout each experiment as the younger drivers did. In other research, children also suffered from inattentional blindness (Zhang et al., 2018). These studies suggest that pilots of all ages are susceptible to inattentional blindness. Even as pilots gain experience, typically making them safer, their increase in age may contribute to higher levels of inattentional blindness, offsetting that experience.

The same type of driving scenarios were used in additional experiments to determine task loading and inattentional blindness (Murphy & Greene, 2015, 2016; Pugnaghi et al., 2019, 2020). These experiments aligned with other research that showed drivers had a higher probability of inattentional blindness when under a heavy task load versus a low task load. When a higher task load was combined with other types of stimuli (e.g., heat, noise, etc.), the participants over-corrected their driving during the scenarios and showed increased inattentional blindness levels (Dattel et al., 2015). This same combination of high task load and additional stimulus may impact pilots on final approach and landing because of additional stimuli of aircraft noise, flight deck instruments, and possible changes of flight deck temperatures.

Inattentional Blindness and Smartphones

In addition to testing inattentional blindness in drivers, researchers experimented on the inattentional blindness of pedestrians. Pai (2016) had participants cross an intersection while texting, listening to music, talking on the phone, or without phone use. In addition to videoing their crossing behaviors, an unexpected stimulus of a clown was added to the intersection. The video displayed participants of all three types of distractions had a significantly higher rate of failure to look both ways and obey traffic lights when crossing the intersection. In addition, all three types of distractions had significant inattentional blindness, missing the clown, compared to the pedestrians not engaged with their phones. Texting participants had the highest rate of inattentional blindness. Therefore, this study demonstrates phone use of any kind can cause both distractions and inattentional blindness.

This finding was verified in a second study including popular gaming apps, which showed how both texting and playing gaming apps cause significant inattentional blindness for pedestrians (Chen & Pai, 2018). Pilots and flight crews on final approach are already engaged in multitasking between flight controls, radio calls, and concentrating on the runway environment. During this same phase, pilots may use additional tools to assist in displaying the instrument approach, such as electronic flight bags, tablets, or digital flight deck displays, which may inadvertently increase the risk of inattentional blindness.

Research Questions and Support

This study used a combination of previous aviation accident variables along with additional variables not previously researched. The first and second research questions explored aviation accidents by evaluating a dataset from January 1, 2014, to December 31, 2019 (Burnett & Si, 2017; Koteeswaran et al., 2019). This research used SVM to evaluate the predictability of the severity of personal injury and the severity of aircraft damage. Unlike other aviation accident research, this research restricted the dataset to the approach and landing phase. In addition, this study combined the lessons learned from research on the severity of personal injury during automobile accidents with a new output variable of severity of aircraft damage. Lastly, the predictability was evaluated using multiple kernels to determine which algorithm had the most accurate prediction of severity of aircraft damage and severity of personal injury.

The third research question specifically evaluated the three new variables to determine their impact on the predictability of aircraft damage and personal injury. The status of the visual area surface penetrations can create unexpected events and increased

task saturation during an already critical final approach and landing phase of flight (FSF, 2017; Harris, 2011; Huddleston, 2012; Moriarty & Jarvis, 2014). This reasoning aligns with the theory of inattentional blindness because a 20:1 or 34:1 obstacle penetration in the visual area surface penetration is an unexpected object directly in front of the flight path of the aircraft.

Since 2012, the FAA has changed policy related to visual area surface penetration three times (AOPA, 2016; FAA, 2013b, 2018b, 2018c; Lebar, 2016; Namowitz, 2016; RTCA, 2016). Previous research has shown how FAA aircraft maintenance policies and oversight are a factor in maintenance accidents (Ancel et al., 2015). It is currently unknown if changing policies had an impact on the understanding or removal of visual area surface penetration by airport owners and operators. Therefore, the different FAA policies referring to the removal of obstacles on the final approach was added as part of the third research question for this study.

The new variable of runway lighting was included because of inattentional blindness and because environment lighting can factor in aviation accidents (Baugh, 2020; Shappell et al., 2007; Wong et al., 2006). Inattentional blindness relates to the presence and type of runway lighting because if the unexpected object is outside of the focus of the primary task, the inattentional blindness rates are significantly higher than if the object is inside the primary task focus (Kreitz et al., 2020). This may impact pilots because when transitioning from the DA to MDA, a pilot and crew's primary focus is on the runway and the runway environment (FAA, 2012, 2016b, 2016c; General Operating and Flight Rules, 2017). To assist a pilot in locating the runway and runway environment, many airports use a runway lighting system. The brightness of a runway lighting system

allows the airport to also have lower approach minimums. However, this brightness could cause pilots to focus on the runway lighting system, instead of focusing on the broader runway environment, thus inadvertently impacting the pilot's visual routine. This change in visual routine may cause a pilot to miss a visual surface obstacle penetration in the flight path of the aircraft. This failure to notice something unexpected, or an unexpected object, can have serious consequences for pilots on approach and landing (Most, 2013). Therefore, the third research question determined if inattentional blindness and the FAA's policy timeframe, presence of obstacles, and the type of runway lighting effect the pilots' ability to avoid obstacles, thus predicting the severity of aircraft damage and the severity of personal injury.

Summary

Although there is existing research predicting aviation accidents and addressing the factors causing those accidents, there is limited research using SVM methodology. Following a review of aviation landing accident literature was an overview of SVM and machine learning in aviation. Next was a history of the theory of inattentional blindness succeeded by a comparison to attentional misdirection. This subsequent section details how inattentional blindness supports the different research questions as a result of a pilot missing a visual area surface penetration while focused on the runway environment. Therefore, the theory of inattentional blindness supported the addition of these factors as possible predictors to the severity of personal injury and the severity of aircraft damage resulting from aviation landing accidents.

Chapter III: Methodology

This chapter outlines the methodology for predicting the severity of aircraft damage and for predicting the severity of personal injury for aircraft landing accidents using support vector machines (SVMs). It also covers the population and variables used in the aircraft landing accident dataset followed by how the dataset was gathered, organized, cleaned, and coded. With a completed dataset, the next sections outline the SVM workflow to develop and test the models for prediction.

Research Method Selection

The purpose of this study was to develop a classification model using SVM methodology to predict the severity of aircraft damage and the severity of personal injury during aviation landing accidents. Additionally, all input variables were evaluated for factor contribution and sensitivity (Burnett & Si, 2017; Valdés et al., 2011).

This study was comprised of $N = 1{,}297$ approach and landing accidents. Support vector machines have the ability to evaluate medium to small data, combined with SVM's ability to quickly separate nonlinear variables with the different kernel algorithms, thus allows SVM to have a faster processing time for real life evaluations (De Luca, 2020; Dibike et al., 2001; Jeeva, 2018; Vapnik, 1999). Since this research had categorical variables such as approach runway lighting type, visual area surface penetrations, FAA policy timeframe, aircraft mission, pilot rating, and the output factors of personal injury and aircraft damage, SVM was deemed appropriate as a machine learning method for classification.

In addition, SVM, although not the only machine learning technique to be able to evaluate multi-level variables, was the only machine learning method that had been used

by researchers to predict three or more categorical levels of the severity of personal injuries (Li et al., 2012). Support vector machines were used previously, assessing 326 automobile accidents using the RBF kernel to evaluate 18 IVs, many categorical, for a five-level severity of personal injury scale. Researchers found SVM accurately predicted the correct injury severity approximately 80% of the time (Li et al., 2012). Although the study lacked a larger amount of data, the researchers concluded the severity of personal injury could be predicted by SVM.

Similarly to Li et al.'s (2012) research, the goal of this study was to evaluate a four-level DV and compare the predictability of four different kernel functions. Therefore, SVM methodology was selected because the dataset had various numerical and categorical variables.

Population/Sample

The database population and sampling timeframes for this study are presented in this section.

Population and Sampling Frame

The population is all approach and landing accidents. For this study, the representative sample of the population was all aviation accidents during the approach and landing phase of flight in the United States at an airport with at least one instrument approach procedure from 2014 through 2019. The data were collected from a variety of databases and public websites, beginning with an initial data pull from the NTSB (n.d.-a) database. Then additional variables were coded into the accident dataset with information from the FAA's Instrument Flight Procedures Gateway website (FAA, n.d.-b), AirNav.com (n.d.), and reading the individual NTSB accident reports (n.d.-c). This study

did not consider foreign accidents because the information is not available in the NTSB database (n.d.-a).

To ensure the findings can be generalized for pilots and flight crews, the researcher removed any non-pilot caused accidents (e.g., gear malfunction or engine failure). These types of accidents were removed because they have no possibility of influence by the pilot's inattentional blindness during the approach or landing. Even though the aircraft malfunctions were removed, aircraft manufacturers and aircraft designers can use the results of this study to improve machine and human interfaces to reduce the possibility of inattentional blindness.

The sampling timeframe for this study consisted of approach and landing aviation accidents in the United States from January 1, 2014, to December 31, 2019. This sample was chosen to cover the two years of the FAA's interim visual area surface memorandum, the two years of the FAA's assessment period, and the first two years of the FAA's final policy period (AOPA, 2016; FAA, 2013b, 2018b, 2018c; Lebar, 2016; Namowitz, 2016; RTCA, 2016).

Data Collection Process

The data were collected from the NTSB database and filtered for only aircraft accidents or incidents that occurred on approach or landing in the United States (NTSB, n.d.-a). Although the majority of the variables were in the NTSB database, each accident was reviewed as part of the analysis to prevent missing data (NTSB, n.d.-c). From this review, the reason and location of the accidents were evaluated for applicability to this study. In addition, the manual review added, or confirmed, the landing runway number, wind direction and velocity (to calculate crosswind component), local time of the

accident, the pilot's age, the pilot's total flight hours, the pilot's certificate, and the pilot's rating. Once completed, the FAA's Instrument Flight Procedures Gateway (FAA, n.d.) website was used to determine if the airport had at least one IAP. The Instrument Flight Procedures Gateway (FAA, n.d.-b) was then used to annotate in the dataset the status of any visual area surface penetrations and the type of approach runway lighting for the runway of record for the accident. If the approach runway lighting was not listed by the FAA, then AirNav.com (n.d.) was used to code the variable in the dataset. Once all of this information was combined, the dataset collection was completed.

Design and Procedures

To determine predictability of the severity of personal injury and the severity of aircraft damage during aviation landing accidents, this study used a quantitative, non-experimental, research design using SVM (Edmonds & Kennedy, 2017). This was selected as the most appropriate type of statistical analysis because of the multitude of ordinal and interval factors/IVs involved in aviation landing accidents. Also, as discussed earlier, SVM was compared to other types of machine learning techniques, and had the ability to separate categorical variables into higher than three-dimensional space using kernel algorithms (Byrne, 2016; Jeeva, 2018).

Ethical Consideration

The NTSB database removed all of the pilot's personal identification information from the accident reports to prevent any type of ethical repercussions (NTSB, n.d.-a). The dataset contained the airport's three letter identification code, airport name, city, and state. This airport name, city, state, or code was not used in the computations or results, but was required to discover each accident's landing runway, runway lighting type, and

status of the visual area surface penetrations. The NTSB accident reports contained the name of the accident investigator, but this name was not collected as part of the dataset (see Appendix B). Also, the FAA Instrument Approach Procedure forms contained names of individuals from the FAA, but this information was not collected as part of the dataset (see Appendix A). Only the status of the visual area surface penetrations and runway lighting types were retrieved from those forms, thereby eliminating any possibility of personal ramifications. There would be minimal positive or negative impact to the FAA based on the results and their interim, assessment, or final policies. Therefore, the ethical considerations for this research were minimum since the information was pulled from public websites.

Measurement Instrument

The dataset was collected in Microsoft Excel. Once complete, the descriptive statistics were compiled using IBM's Statistical Package for the Social Sciences (SPSS) statistics software (IBM, n.d.). The remainder of the study and all of the research questions were originally attempted in Anaconda Navigator suite of tools (Anaconda Inc., 2021) but completed using Google Colaboratory (2022) using Scikit-learn python coding (Pedregosa et al., 2011).

Variables and Scales

The IVs for this study were the status of visual area surface penetrations, mission C.F.R. category, approach runway lighting types, landing runway in use, crosswind component, number of aircraft engines, aircraft engine type, FAA policy timeframe, time of the accident, pilot's certificate, pilot's rating, pilot's total number of flight hours, and

pilot's age. The DVs were severity of aircraft damage and the severity of personal injury. All variables are listed in Table 2.

Table 2

Variables of the Dataset

Variable	Scale or Categorical	Type
Status of visual area surface penetrations (IV)	3 Categories	Nominal
Mission C.F.R. category (IV)	4 Categories	Nominal
FAA Visual Area Surface Policy Timeframe (IV)	3 Categories	Nominal
Runway lighting types (IV)	6 Categories	Nominal
Landing runway in use (IV)	01 to 36	Interval
Crosswind Component (IV)	0.00 to 180.00	Interval
Aircraft engine type (IV)	3 Categories	Nominal
Number of aircraft engines (IV)	1 to 8	Interval
UTC time of accident (IV)	0001 to 2400	Interval
Pilot's certificate (IV)	6 Categories	Nominal
Pilot's rating (IV)	3 Categories	Nominal
Pilot's total number of flight hours (IV)	Unlimited	Ratio
Pilot's age (IV)	Unlimited	Ratio
Number of flight crew (IV)	4 Categories	Interval
Severity of aircraft damage (DV)	4 Categories	Ordinal
Severity of personal injury (DV)	4 Categories	Ordinal

Note. IV = Independent variable or predictors. DV = Dependent variable or target variable.

For the categorical input variables, the goal of SVM was to maximize the margin between categorical classification, starting with the lowest dimension and progressively increasing into a higher dimensional space (Berwick, 2003; Navlani, 2019). Each DV category was evaluated separately. Therefore, each DV had four separate evaluations by the machine, one for each ranking.

Definition of Variables and Constructs. This section provides the definitions for each variable used in this study.

Status of Visual Area Surface Penetrations (IV). The status of the visual area surface penetration was listed as either an obstacle penetration of the 34:1 surface, both 20:1 and 34:1 surface, or no surface penetrated. These surfaces defined the number of feet from the threshold (20 feet or 34 feet) for every one foot in elevation. Therefore, when the 20:1 surface was penetrated, the 34:1 surface was also penetrated. These surfaces were evaluated by the FAA during IAP development and were documented on the IAP forms and charts shown in Appendix A (FAA, 2018b, 2018c).

Mission Code of Federal Regulation Category (IV). The C.F.R. establishes the type of operations for an aircraft owner or company (NTSB, n.d.-b). This is broken into C.F.R. Parts 91, 121, 135, and 137. The typical general aviation aircraft operates under 14 C.F.R. Part 91 (General Operating and Flight Rules, 2017). Domestic airlines operate under 14 C.F.R. Part 121 (Operating Requirements: Domestic, Flag, and Supplemental Operations, 2020). Smaller commercial aircraft operate under 14 C.F.R. Part 135 (Operating Requirements: Commuter and On Demand Operations and Rules Governing Persons On Board Such Aircraft, 2020). Lastly, agriculture aircraft operate under 14 C.F.R Part 137 (Agricultural Aircraft Operations, 2020).

FAA Visual Area Surface Policy Timeframe (IV). The aircraft accidents were grouped into one of three two-year periods based on the type of policy the FAA had in effect about visual area surface obstacle penetrations. Accidents from January 1, 2014, to December 31, 2015, were coded into the interim policy category (FAA, 2013b). Aviation accidents from January 1, 2016, to December 31, 2017, were coded in the assessment period category (AOPA, 2016; Lebar, 2016; Namowitz, 2016; RTCA, 2016). The last

category was coded as the FAA final policy from January 1, 2018, to December 31, 2019 (FAA, 2018b, 2018c).

Runway Lighting Types (IV). Runway approach lighting were composed of different VGSI and approach lighting systems (FAA, 2012, 2016b, 2016c). This variable had six categories: no approach lighting, Precision Approach Path Indicator (PAPI) system with two lights, PAPI system with four lights, Visual Approach Slope Indicator (VASI) system with two lights, VASI system with four lights, and approach lighting system. This variable was coded for multiple selections if an approach lighting system also had a VGSI.

Landing Runway in Use (IV). This was the approach landing runway at the time of the accident. The runway numbers ranged from 01 to 36 and were retrieved from the NTSB database and NTSB accident reports (See Appendix B).

Crosswind Component (IV). This was the amount of crosswind, in knots, for the landing runway at the time of the accident. The wind direction and wind velocity were retrieved from the NTSB database. Crosswind component was computed by calculating the sine of the difference between the wind direction and the landing runway, then multiplied against the wind velocity (FAA, 2014). Results were reported to the nearest hundredths. Winds reported as "calm" during the time of the accident were coded at three knots and 20 degrees off of the landing runway (FAA, 2020a).

Aircraft Engine Type (IV). This was the type of engines on the aircraft listed on the accident report (NTSB, n.d.-b). The NTSB database and NTSB accident reports listed engine types as reciprocating, turbo fan, turbo jet, and turbo prop. Some reports stated

the aircraft model instead of the engine type. When this occurred, the aircraft model was researched, and the engine type was coded appropriately.

Number of Aircraft Engines (IV). This was the number of engines on the aircraft listed on the accident report (NTSB, n.d.-b). This information was provided by the NTSB database and NTSB accident reports.

Coordinated Universal Time (UTC) of Accident (IV). This variable was added to account for different risks associated with night landings (FAA, 2016b). This variable was retrieved from the NTSB accident reports and logged as UTC, a 24-hour format from 0000 to 2359 hours.

Pilot's Certificate (IV). This was the certificate held by the pilot as defined in the C.F.R. (General Definitions, 2020). The NTSB reports the information of the pilot flying the aircraft at the time of the accident. For example, if a student was flying the aircraft with a flight instructor, pilot in command, the student's information was reported as the pilot while the flight instructor was listed as a second pilot. A pilot's certificate ranged from the lowest, student, to sport pilot, recreational pilot, private pilot, commercial pilot, and then the highest certificate, airline transport pilot (Certification: Pilots, Flight Instructors, and Ground Instructors, 2020). Only the pilot's highest certification was recorded. Pilots that held an additional flight instructor certificate were coded as both flight instructor and the highest of the certificates held above.

Pilot's Rating (IV). This was the rating held by the pilot flying the aircraft at the time of the accident as defined in the C.F.R. (General Definitions, 2020). Pilot ratings ranged from single-engine, multiengine, instrument, or a combination thereof (Certification: Pilots, Flight Instructors, and Ground Instructors, 2020).

Pilot's Total Number of Flight Hours (IV). This was the total number of flight hours, rounded to the nearest whole number, for the pilot, controlling the aircraft at the time of the accident, as defined in the C.F.R. (General Definitions, 2020). Total number of flight hours was listed as one of the significant human factors for predicting aviation accidents (Baugh, 2020; Burnett & Si, 2017; Liu et al., 2013).

Pilot's Age (IV). This was the age of the pilot flying the aircraft at the time of the accident as defined in the C.F.R. and reported as a whole number from the NTSB accident report (General Definitions, 2020). Age was considered one of the human factors that impacted the predictability of aviation accidents (Baugh, 2020; Burnett & Si, 2017; Liu et al., 2013).

Number of Flight Crew (IV). This was the total number of the flight crew in the flight deck at the time of the accident.

Severity of Aircraft Damage (DV). The FAA and49 C.F.R list aircraft damage in four categories: none, minor, substantial, and destroyed (FAA, 2018b; "Notification and Reporting of Aircraft Accidents or Incidents", 2020). Aircraft with minor damage were repaired easily before the aircraft was restored to airworthy condition. Substantial damage was structural or impacted the aircraft's flight characteristics. Lastly, destroyed aircraft were impracticable or impossible to repair to airworthy conditions.

Severity of Personal Injury (DV). The FAA 49 C.F.R list individual injury during an aviation accident as none, minor, serious, and fatal (FAA, 2018b; "Notification and Reporting of Aircraft Accidents or Incidents", 2020). Minor injury was a hospitalization of up to 48 hours, first degree burns, or external cuts. Serious injury was the loss of a limb, bone fracture, second- or third-degree burns, or more than 48 hours of

hospitalization. Fatal injury was the death of a crew member or passenger. If an accident had multiple levels of personal injury, only the highest severity was coded. Each accident was weighted and coded as one person to prevent an airline accident from skewing results.

Data Analysis Approach

The SEMMA process consists of five steps to prepare and assess a database or dataset: Sample, Explore, Modify, Model, and Assess (SAS Institute, 2013). The first step, Sample, was used to develop a sample of the dataset to ensure it contains the input variables and information needed for the research. For this research, the NTSB database was used to begin the development of a sample dataset (NTSB, n.d.). For the second step, the entire sample dataset was compiled and explored for anomalies like missing variables (SAS Institute, 2020). Once the NTSB sample dataset was downloaded from the NTSB database, the information was combined with data manually gathered from the NTSB accident reports, FAA's Instrument Flight Procedures (IFPs) Gateway website, and AirNav.com website (AirNav.com, n.d.; FAA, n.d.-b; NTSB, n.d.-c). After this was completed for a sample dataset, this process was repeated to compile the entire dataset covering 1 January 2014 through 31 December 2019.

Once the entire dataset was assembled and explored, during the Modify step the dataset was cleaned and filtered to remove aviation approach and landing accidents that did not occur at an airport or were not due to an approach or landing problem. For example, aircraft that attempted to land on a road or open field because of an engine failure, engine fire, aircraft ran out of fuel, or controlled flight into terrain, are removed from the dataset. Aviation accidents due to aircraft malfunction, gear malfunctions,

collision with an animal on the runway, or pilot failure to lower the gear, are also removed from the dataset. The next organization and cleaning of the dataset removed accidents at airports that did not have at least one IAP because an IAP was required to determine if there were any visual area surface penetrations.

The last organization step was to partition the dataset into a training dataset and validation dataset (Shmueli et al., 2016). Although there was no required partition percentage, previous research recommends partitioning 80% toward the training dataset and the remaining 20% for the validation dataset (Draelos, 2020; Li et al., 2008, 2012). Therefore, for this research, an 80% training and 20% validation partition is used. In addition, for this research, multiple dataset partitions were evaluated using the confusion matrix to determine error rate and avoid overfitting (Yang et al., 2019). Confusion matrix evaluated observations into true positives, true negatives, false positives, and false negatives to calculate the accuracy of each training set (Nalepa & Kawulok, 2018; Scikit-learn, 2021). Once this was completed, the dataset was ready for the final two SEMMA steps: Model and Assess using SVM.

The SVM process for the final two SEMMA steps, Model and Assess the dataset, consisted of retraining the models, evaluation of the models, and cross-validation (Scikit-learn, 2019). Once the specific training partition was selected, the partition and the various kernel functions were coded into the SVM to evaluate each variable separately for the prediction. The SVM machine modeling starts at a low dimension and systematically increased to a higher dimension to maximize the margin between the categories (Yang et al., 2019). Then, the SVM model coding maximized the margin and evaluated the specific factors for the predictability against the DV (Li et al., 2012). After

completing this for each individual factor, the SVM model was coded to report each model's accuracy, precision, sensitivity, and F1-score.

To Assess the model, a cross-validation was coded into the SVM to evaluate the model's ability to predict (Brownlee, 2018; Igel et al., 2008; Scikit-learn, 2019). Based on the results of the cross-validation, the researcher adjusted the SVM and kernel parameters and repeated the process until a model with the lowest cross-validation error rate was designed. The model was then validated using the validation partition to calculate the accuracy of the prediction (Hair et al., 2010; Nalepa & Kawulok, 2018).

Support Vector Machines (SVM) Model Development

The first SVM models were developed using the initial workflow. After the dataset was augmented, the machine learning models were coded using the final SVM workflow and optimization.

Initial SVM Workflow. Using the workflow in Figure 5, the SVM models were coded into Google Colaboratory (2022) and ready to separate positive and negative samples from each variable/factor to create a hyperplane and develop different predictive models (Dibike et al., 2001; Jeeva, 2018; Scikit-learn, 2019).

Figure 5

Initial Support Vector Machine Workflow

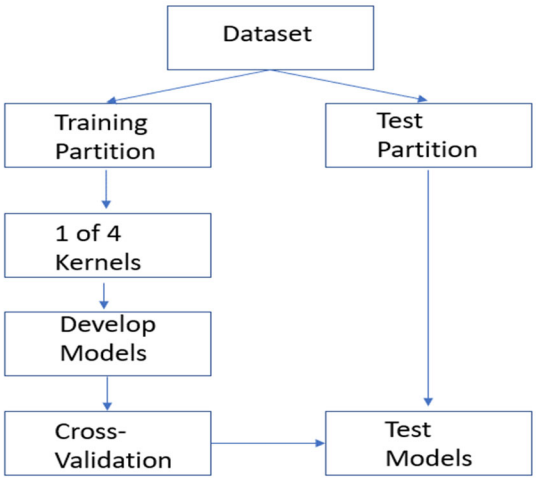

With a completed dataset, the first step in the SVM workflow was to load the dataset into Google Colaboratory (2022), shuffle the dataset, and divide the dataset into the training and validation partition. Since this was the first research using SVM to predict aviation landing accidents, there was not equivalent research to predetermine the optimum partition percentage. The closest research about injury severity in automobile accidents compared multiple partitions splits (Li et al, 2008; Li et al., 2012). The automobile accident research discovered that the 80% training to 20% validation provided the highest accuracy. Therefore, this study also used an 80% training partition and 20% test partition for both the severity of personal injury and the severity of aircraft damage of aviation landing accidents. Then, the confusion matrix was used to determine minimum error rate while avoiding overfitting (Yang et al., 2019). Confusion matrix evaluated observations into true positives, true negatives, false positives, and false

negatives to calculate the accuracy of each training set (Nalepa & Kawulok, 2018; Scikit-learn, 2021).

After the appropriate training partition was selected, the next step was to process the training partition in SVM using the kernel functions on each variable to systematically increase categorization from a low dimension to a higher dimension to find the minimum error rate and maximum margin (Yang et al., 2019). The kernel evaluation began with the linear kernel, and then increasingly progressed through the polynomial kernel, sigmoid kernel, and finally the RBF kernel. The kernel with the maximized margin was recorded for each factor.

Once each factor was evaluated to maximize the margin between the variable's categories, the SVM was coded to evaluate the specific IV for the predictability against the specific DV (Li et al., 2012). After each variable was evaluated for predictability separately, the SVM models were coded to create a model based on the separate prediction accuracies, or misclassification rates. Once a model was developed, the researcher programed the SVM to do a cross-validation of the model, discussed in the next section, to evaluate the model's ability to predict (Brownlee, 2018; Igel et al., 2008; Scikit-learn, 2019). Based on the results of the cross-validation, the SVM model parameters and kernel parameters were adjusted before restarting the evaluation and cross-validation again. To ensure reliability, in addition to the cross-validation, the final model was evaluated through the use of the validation partition to determine each model's confusion matrix, classification report, and misclassification rate or accuracy to discover which model was the best for predicting the severity of aircraft damage (Hair et

al., 2010). This process was also used to develop the best model for predicting the severity of personal injury.

Final SVM Workflow. After development and testing of the initial SVM models, analysis revealed the models were heavily impacted due to the slanted dataset towards substantial aircraft damage and no personal injury. Therefore, the SVM workflow was adjusted to incorporate dataset augmentation and optimization (see Figure 6).

Figure 6

Final Support Vector Machine Workflow

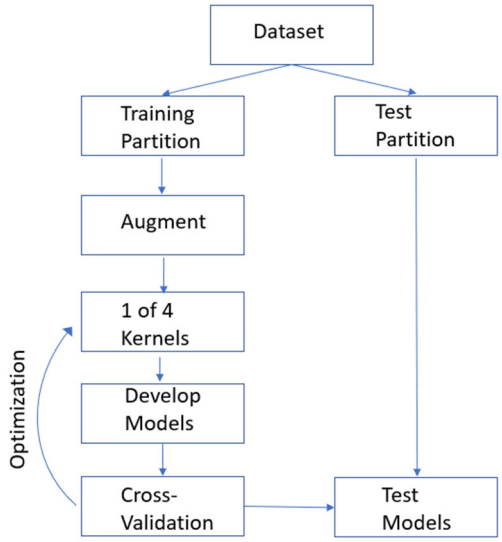

Unlike the initial SVM workflow, the dataset was shuffled in Microsoft Excel and then split into the training and test partitions The same 80/20 split was used. Once the training partition was separated, the dataset was augmented (to be discussed in further detail in the next section) to provide roughly the same amount of none, minor, substantial, and destroyed aircraft damage accidents. Once complete, the augmented

training partition and the original test partition were loaded into Google Colaboratory (2022) for SVM development.

The SVM model development, use of kernels, and cross validation remain the same as the initial workflow. After comparing the final models for the severity of aircraft damage and the severity of personal injury, the SVM models with the highest accuracy, precision, sensitivity/recall, and F1-score are selected (Geron, 2017; Kuhn & Johnson, 2016). That specific model and kernel will then be optimized by adjusting the SVM parameter and kernel parameter to fine tune the model and improve predictability. Once the models are optimized, they are compared to the test dataset and again evaluated for reliability and validity. The models are compared and the best model for predicting the severity of aircraft damage and the best model for predicting the severity of personal injury are chosen.

SVM Model Optimization. Support vector machine models allow for optimization through modifying the C parameter. The C parameter adjusts the width of the margin surrounding the hyperplane. Low value of C produces a larger margin, while a larger value of C produces a smaller margin (Fan, 2018; Scikit-learn, 2022d, Wang, 2014). The value for the C parameter also teaches the SVM model how it handles misclassifications of data. Since SVM goal is to maximize the margin, a low C value allows the model to accept individual misclassified data points thus having a model with low variance and high bias (Albon, 2017; Brownlee, 2021b; Fan, 2018; Kumar, 2018). However, a large C value assumes any misclassified point as a penalty and therefore attempts to not allow any misclassified data points thus producing a model with high variance and low bias.

As stated earlier, one of the benefits of SVM is the ability to separate categorical data through the use of different kernels. Many of the kernels, but not all, have a variable that can be adjusted within the coding (Albon, 2017; Brownlee, 2021b; Fan, 2018; Kumar, 2018). For the polynomial kernel, d is the kernel parameter, while γ is the sigmoid kernel parameter and σ is the RBF kernel parameter. Some researchers use γ and σ interchangeably between the RBF and sigmoid kernels (Geron, 2017; Kuhn & Johnson, 2016).

For the polynomial kernel, d is the degree of freedom. When d is a value of one, the polynomial kernel and linear kernels match (Fan, 2018; Scikit-learn, 2020). As d is increased, the kernel changes the hyperplane to a more complex shape attempting to separate the categorical data. There is no maximum for the d parameter, however, the higher the value the increased risk of overfitting.

Both the sigmoid and RBF kernels can use gamma (γ or σ) to optimize the kernel (Wang, 2014; Vapnik, 1999). By increasing the value of gamma, the hyperplane increases conformity to the support vectors, thus attempting to limit the amount of misclassified data points (Albon, 2017; Brownlee, 2021b; Fan, 2018; Kumar, 2018). The gamma parameter can range from any positive value above zero with no maximum. However, as gamma increases, there is a risk of overfitting as the SVM model attempts to separate each categorical data point individually rather than as a whole (Geron, 2017; Kuhn & Johnson, 2016; Scikit-learn, 2022d).

Once the initial SVM models, with either the linear, polynomial, RBF, or sigmoid kernel, are developed and compared, the one with the best ability to predict is selected. Then, the selected SVM model is optimized by incrementally increasing the SVM and

kernel parameters, either through manually changing the value or coding a loop function in Google Colaboratory (Geron, 2017; Google, 2022; Kuhn & Johnson, 2016; Scikit-learn, 2022d). Once the optimized SVM model outputs are compared, the best performing model must be evaluated using the test dataset to ensure overfitting did not occur and the model achieved approximately the same accuracy, precision, sensitivity/recall and F1-scores.

Data Augmentations

Before and during SVM model development, the dataset underwent augmentations of normalization and expansion.

Variable Normalization. After the dataset was collected, the variables of pilot's total number of flight hours, crosswind component, and pilot's age required normalization. Normalization is when a variable scale is converted from the raw data to a common scale while keeping the range differences between events (Jiang et al., 2016; Kuhn & Johnson, 2016; Microsoft, 2021). Flight hours ranged from six hours to 40,000 hours. Crosswinds ranged from 3 knots, calm, to 39 knots. Pilot's age ranged from 16 years old to 91 years old. All three variables were normalized to a scale from 0.0 to 1.0 range using the following formulas:

$$Flight\ Hour\ Norm = \frac{Flight\ Hours}{Max\ Flight\ Hours} \tag{14}$$

$$Crosswind\ Norm = \frac{Crosswinds}{Max\ Crosswinds} \tag{15}$$

$$Pilot\ Age\ Norm = \frac{Pilot\ Age}{Max\ Pilot\ Age} \tag{16}$$

These new variables were used in the SVM modeling in place of the original values.

Dataset Expansion. Augmenting a dataset for machine learning is not considered uncommon, especially when dealing with categorical variables. (Geron, 2017; Kuhn & Johnson, 2016). For example, a medical study attempting to predict a rare form of cancer would not expect a balanced dataset but would expect almost all patients to test negative for cancer (Leevy et al., 2018). Therefore, this study considered three types of dataset augmentation: Gathering additional accident data outside the 2014 – 2019 range; data-algorithm methods; or data-sampling methods (Leevy et al., 2018). For this study, the major levels were no personal injury and substantial aircraft damage while the rest were considered as minor or limited levels.

Since the goal of aviation safety is to eliminate fatalities, expanding the years would only gather more data with the expected same level percentages (FAA, 2021c). Thus, the first data augmentation method would not solve the imbalance. The data-algorithm method, synthetic minority over-sampling technique (SMOTE), uses a random sample from the minor levels to develop an algorithm (Korstanje, 2021). Once the algorithm is developed, SMOTE creates new events, or in this study, accidents, to remove the offset balance between the DV levels. This method was not used because creating random data could impact the factor importance of the three new variables.

The data-sampling methods are broken down into random over-sampling (ROS) and random under-sampling (RUS) (Leevy et al, 2018). RUS would randomly remove accident data from the major severity levels. Randomly removing data were not considered viable for this study because there were concerns it would impact the three new variables in the study.

After the elimination of SMOTE and RUS, ROS was the remaining augmentation available. Random over-sampling increases the minor or limited without modifying or varying the internal characteristics of an event or accident (Hayati et al., 2021). Leevy et al. (2018), stated that ROS yielded better results than SMOTE or RUS for machine learning modeling. Random over-sampling could be accomplished through random selection or using a fixed method (Khoshgoftaar et al., 2007; Van Hulse et al., 2007). Random selection duplicates exampling in the minority class through random selection while fix method duplicates examples through a user directed selection (Brownlee, 2021a; Korstanje, 2021). For multi-level DVs with multiple minor levels, fixed method is preferred because random selection may only increase some, not all, of the minor levels. Therefore, for this dataset, the ROS fixed method was used on each minor level through user specified duplication of accident data.

Reliability Assessment Method

Cross-Validation. Cross-validation, sometimes called k-fold cross-validation, is a technique to evaluate a model's performance or ability to predict and, if necessary, adjust the model's hyperparameters (Brownlee, 2018; Igel et al., 2008; Scikit-learn, 2019). This process eliminates one of the concerns with SVM, which is the potential for overfitting the predictability of the data (Sánchez-González, 2018; Vapnik, 1999). Overfitting is when the matching learning program goes from dataset point to dataset point to create a training model that has a very high predictability or "fit", but then fails to allow for enough generality to be used against any other dataset. To avoid overfitting, SVM uses the k-fold cross-validation to split the training dataset into different sections and then develops multiple models using all but one of the sections (Brownlee, 2018; Igel et al.,

2008; Scikit-learn, 2019). Once the models are developed, they are compared on their estimation and performance (Kuhn & Johnson, 2016).

The k-fold cross-validation process evaluates a specific model's ability to predict the desired DV, for example, the severity of aircraft damage or the severity of personal injury. The model is evaluated against only one DV at a time. To cross-validate, SVM takes the entire dataset and splits it into equal partition subsets and then randomly assigns each event to one of the subsets. There is no formal number of subsets (k) to split, but typically a k of 10 is used to reduce the bias of technique, that is, the difference between estimating and true performance (Kuhn & Johnson, 2016). Each model subset is evaluated for cross-validation performance and cross-validation error. Then, the subset with the lowest error rate is used to retrain the original SVM model developed using the training partition (Hastie et al., 2008). For this study, based on the size of the dataset, a k of five was used to avoid overfitting.

Validity Assessment Method

This study desires a predictive model with low misclassification rate, high accuracy, high precision, high sensitivity/recall, high specificity, and high F1-score. There is no desire to have only a high precision or only a high sensitivity/recall because incorrectly assessing a non-injury accident as fatal or a fatal accident as non-injury is not deemed acceptable (Branco, et al., 2015; Brownlee, 2020a; Geron, 2017; Kuhn & Johnson, 2016; Leevy, et al., 2018; Sofaer et al., 2019).

Confusion Matrix. A confusion matrix records the true positive, false positive, true negative, and false negative returns for the specific model (Geron, 2017; Kuhn & Johnson, 2016; Scikit-learn, 2021). These results are then used to calculate the precision,

recall, F1-score, and specificity. For a binary classification, Table 3 depicts the confusion matrix (Kuhn & Johnson, 2016).

Table 3

Binary Confusion Matrix Example

Predicted Values	Actual Values: Positive (1)	Actual Values: Negative (0)
Positive (1)	TP	FP
Negative (0)	FN	TN

Note. TP = True positive; FP = False positive; FN = False negative; TN = True negative.

However, for a multi-class DV, the confusion matrix expands the display by the number of columns and rows equal to the number of levels in the DV (Kuhn & Johnson, 2016; Mohajon, 2020). The true positive, false positive, true negative, and false negative are separately calculated for each level as shown in Table 4.

Table 4

Multi-Class Confusion Matrix Example

Aircraft Damage Predicted Values	Aircraft Damage Actual Values: None	Minor	Substantial	Destroyed
None	A	B	C	D
Minor	E	F	G	H
Substantial	I	J	K	L
Destroyed	M	N	O	P

With a multi-class DV, the confusion matrix calculations are as follows:

$$True\ Positive = A \tag{17}$$

$$True\ Negative = F + G + H + J + K + L + N + O + P \quad (18)$$

$$False\ Postive = B + C + D \quad (19)$$

$$False\ Negative = E + I + M \quad (20)$$

For simplicity, a confusion matrix table can be graphically displayed as a black and white image in Google Colaboratory (Geron, 2017). The darker the square, the worse the machine learning model predicted true positives. Conversely, the whiter the square the better the model predicted true positives. A balanced confusion matrix image displays white squares on a diagonal from upper left to lower right, reflecting a model that accurately predicted high true positive values (see Figure 7).

Figure 7

Multi-Class Confusion Matrix Image Example

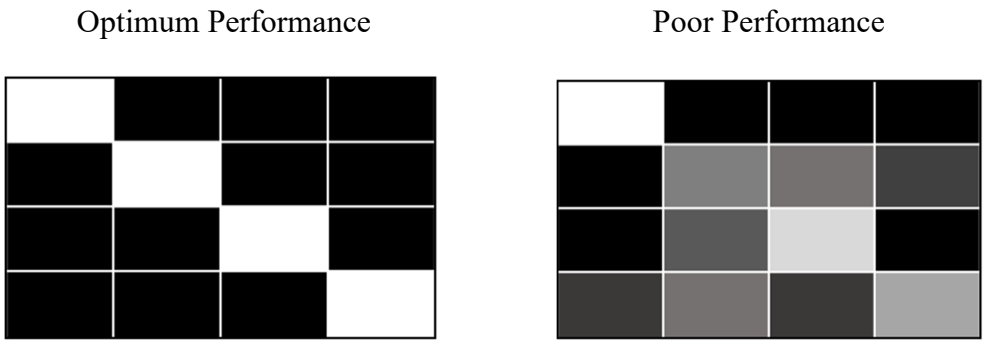

The optimum performing machine learning model on the left contains a pure white diagonal from upper left to lower right. This reveals a model that correctly predicted 100% true positives. However, a 100% performing model is unrealistic. The right confusion matrix image contains a model that correctly predicted the true positives for the first level of the DV, however it poorly predicted the true positives on levels two

through four. The different shades of gray show the false positives in the model, where it incorrectly predicted a true positive.

Misclassification Rates. Finally, the validation partitioned data evaluates using the final model to assess for predictability of the severity of personal injury and the severity of aircraft damage as a result of aviation landing accidents. Validity is tested by comparing the predicted model developed using the training partition with the validation partition (Yang et al., 2019). These models evaluate using misclassification rates, which display the number of correct and incorrect predictions by the final SVM model (Nalepa & Kawulok, 2018). The lower the misclassification rates, the higher the accuracy of prediction (Hair et al., 2010; SAS Institute, n.d.). Misclassification rates are evaluated for each DV at the four different levels from none to fatal/destroyed. The final SVM model composition reveals which input factors have the most impact on predictability of the severity of aircraft damage and the severity of personal injury, answering the second and third research questions. At the same time, the best models answered the first research question for both the predictability of the severity of aircraft damage and the severity of personal injury.

$$Misclassification\ Rate = \frac{(FP+FN)}{(TP+TN+FP+FN)} \tag{21}$$

Accuracy. The opposite of misclassification rates. Although there is no set minimum accuracy for a good model, a minimum of 80% accuracy is used for this study (Geron, 2017; Kuhn & Johnson, 2016). To calculate accuracy:

$$Accuracy = 1.0 - Misclassification\ Rate \tag{22}$$

Sensitivity/Recall. Considered the true positive rate, sensitivity, also referred to as recall, is the rate that a specific model correctly predicts the outcome (Kuhn & Johnson, 2016; Mohajon, 2020). To calculate sensitivity/recall:

$$Sensitivity = \frac{TP}{(TP+FN)} \tag{23}$$

Where *TP* is the number of true positive results and *FN* is the number of false negative results.

Specificity. Another validity calculation is the specificity rate, or true negative rate (Kuhn & Johnson, 2016; Mohajon, 2020). To calculate specificity:

$$Specificity = \frac{TN}{(TN+FP)} \tag{24}$$

Where *TN* is the number of true negative results and *FP* is the number of false positive results. For medical research, where the goal is disease free patients (i.e., true negatives), specificity is a great indicator (Parikh, et al., 2009). However, for multi-level DVs, specificity cannot be used as a single source validation. In this study, random selection produced a model with a specificity of 75%, the ability to select a true negative in three out of the four variable levels.

Precision. This determines the ability of the model to correctly predict positive results (Kuhn & Johnson, 2016; Mohajon, 2020). To calculate precision:

$$Precision = \frac{TP}{(TP+FP)} \tag{25}$$

When the precision and sensitivity/recall both perform well (i.e., close to one), then the model is predicting accurately (Scikit-learn, 2022a).

F1-Score. This combines the results of precision and sensitivity/recall to create a holistic evaluation of the model (Kuhn & Johnson, 2016; Mohajon, 2020). F1-score ranges from best (one) to worst (zero). To calculate F1-score:

$$F1 - Score = 2 * \frac{(Recall * Precision)}{(Recall + Precision)} \quad (26)$$

Classification Report. This report is a combination of accuracy, precision, sensitivity/recall, and F1-score for the DV (Kohli, 2019; Kuhn & Johnson, 2016; Scikit-learn, 2022a). For this study, the classification report displayed four sets of values since severity of personal injury and severity of aircraft damage are both a four level multi-class DV.

Factor Contribution and Sensitivity Analysis

Once the SVM models are reviewed for reliability and validity, the next process is to code the factor importance by analyzing factor contribution and sensitivity. Factor importance determines the value of a specific variable in development of the predictive model (Kuhn & Johnson, 2016). The factor importance for the severity of aircraft damage and the severity of personal injury are developed separately using python coding and Google Colaboratory (Geron, 2017; Google, 2022).

Although there are numerous ways to code factor importance, the Scikit-learn random forest classifier is widely used and considered stable and versatile both for categorical and integral variables because it uses multiple trees to develop the factor importance (Booth, et al., 2021; Malik, 2020; Ronaghan, 2018; Zhao, et al., 2022). Random forest classifier uses the number of tree nodes used by a specific variable and weighs it against the number of samples in the training partition which use the specific node (Brownlee, 2020b; Geron, 2017; Gupta & Sehgal, 2021). The larger the sensitivity analysis value, the more important the specific value is to the predicted model. The total of all factor importance values equals one, allowing a simplistic yet powerful evaluation.

For the specific Scikit-learn calculations to determine factor importance, the machine learning algorithm uses random forest classifier to calculate each node, assuming a binary tree (Gupta & Sehgal, 2021; Ronaghan, 2018; Shen, et al., 2007). The basis for the classifier begins with the gini index (Geron, 2017; Kuhn & Johnson, 2016; Strobl et al., 2007). Gini index determines the impurities for a particular node ($G_i = 0$ is a pure node) which determines how a node on the random forest classifier branches (Burnett & Si, 2017; Geron, 2017; Schott, 2019; Scikit-learn, 2022b).

$$G_i = 1 - \sum_{k=1}^{n} \left(p_{i,k}\right)^2 \tag{27}$$

where:

$p_{i,k}$ = The frequency or ratio of the particular class k in the i^{th} node of the tree.

n = The number of classes.

From there, Scikit-learn uses the gini index to develop an algorithm for the node importance (Geron, 2017; Ronaghan, 2018; Saini, 2021; Scikit-learn, 2022b). The node importance at a specific node is:

$$ni_j = \frac{N_t}{N}\left[G_i - \left(\frac{N_{t(right)}}{N_t} * \ G_{i(right)}\right) - \left(\frac{N_{t(left)}}{N_t} * \ G_{i(left)}\right)\right] \tag{28}$$

where:

N_t = The number of rows for a specific node.

N = The total number of rows in the data.

$N_{t(left/right)}$ = Number of nodes in the left/right node split.

Once calculated, the feature importance is calculated using the node importance as follows:

$$fi_i = \frac{\sum_{j:node\ j\ splits\ on\ feature\ i} ni_j}{\sum_{k \varepsilon all\ nodes} ni_k} \tag{29}$$

To ensure the feature importance is normalized between zero and one, the following calculation is applied:

$$normalizedfi_i = \frac{fi_i}{\sum_{j \varepsilon all\ features} fi_j} \quad (30)$$

Finally, the random forest algorithm calculates the final factor importance by averaging the factor importance calculations for a specific variable across all of the trees:

$$Ffi_i = \frac{\sum_{j \varepsilon all\ trees} normalizedfi_i}{T} \quad (31)$$

where:

T = The total number of trees in the random forest. The final factor importance is then displayed in Scikit-learn as individual values for each variable and combined in a graph.

Summary

Chapter III covered the use of SVM as the basis of the research methodology. Support vector machines are a relatively new process used for creating prediction models that require in-depth analysis and higher calculations than many other forms of machine learning techniques (Byrne, 2016; Craven & Shavlik, 1997; Vapnik, 1999). This chapter discussed the use of SVM as the appropriate machine learning technique and how it aligned to previous research of approximately 5,500 automobile crashes across ten variables (Li et al., 2012). That research predicted personal injury severity as the DV ranging from no injury to a fatality. Similarly, this study had a DV for severity of personal injury and a DV for severity of aircraft damage across fourteen IVs.

Next, the chapter covered the development of the aircraft landing accident dataset based on many of the previous factors found to influence aviation accidents, including accidents on landing, which had not been evaluated with complex SVM machine learning

techniques. The chapter defined the different variables of this dataset and how the dataset was initially formed by pulling aircraft landing accident information from the NTSB database. Then, the dataset was expanded through manual additions from the FAA website, including area surface penetrations, runway approach lighting, and FAA obstacle policy timeframe. Although many of these variables, including the two DVs, were categorical, SVM had the ability to use the different kernel functions to separate categorical variables and maximize the margins of each category (Dibike et al., 2001; Jeeva, 2018; Vapnik, 1999).

Once the dataset was complete, Chapter III discussed the SVM workflow to develop, test, and validate each SVM model. This workflow started with partitioning the dataset into various training and validation sets and evaluating the multiple training and validation sample sizes to find out which proportion produces the best model (Li et al., 2008). It also discussed processing the training dataset using one of the four different kernel functions and concluded with the reliability and validation process measuring cross-validation and misclassification rates. Finally, the chapter discussed the use of SVM models to answer each of the research questions.

Therefore, Chapter III covered how SVM was the correct model for predicting the severity of aircraft damage and predicting the severity of personal injury. Chapters IV and V describe and discuss the results, recommendations, and conclusion.

Chapter IV: Results

The purpose of this research was to develop SVM models to predict the severity of personal injury and the severity of aircraft damage from an aircraft accident on approach and landing. At the same time, the researcher sought to evaluate the statistical findings for factor importance of 14 different variables to the severity including three new variables the status of visual area surface penetrations, corresponding FAA visual area surface penetration policies, and runway approach lighting type. This chapter analyzes the results from the different SVM models developed per the methodology, SEMMA process, and SVM workflow outlined in Chapter III.

Dataset Collection and Organization

The initial NTSB database pull had 6,806 accidents. During the Modify step in the SEMMA process, the dataset was cleaned and filtered to remove accidents that did not occur at an airport or did not occur during approach and landing. For example, a pilot that attempted an emergency landing on a road or open field because of an engine failure, engine fire, or fuel starvation, were removed from the dataset. In addition, accidents that occurred at an airport without at least one IAP were also removed. As discussed in Chapter III, this study required an airport to have at least one IAP to determine if the accident runway had visual area surface penetrations. This cleaning removed 3,738 accidents from the dataset.

Next, a manual review was conducted of the remaining 3,068 NTSB accident records to examine the HFACS accident taxonomy, confirm the landing runway, wind direction, wind velocity, and code any missing values from the initial NTSB database pull. During this evaluation, 1,771 accidents were removed from the dataset because the

accidents had the wrong taxonomy (i.e., the accident occurred after takeoff on a touch-and-go, occurred while taxiing to/from the runway, etc.), were due to mechanical failure prior to landing (i.e., engine failure, gear failure, etc.), or could not have occurred because of inattentional blindness and obstacles (i.e., fuel starvation, failure to lower the landing gear, collision with an animal on the runway, etc.). The final dataset was comprised of N = 1,297 approach and landing accidents at airports with at least one IAP.

This amount of data were considered to be sufficient to allow SVM to develop models to create high reliability for prediction because the amount of data is similar to previous studies used to predict automobile accidents using SVM (Li et al., 2008; Li et al., 2012). Lastly, the sample size of N = 1,297 was large enough to allow SVM to separate each categorical variable to develop the different predictive models (Dibike et al., 2001; Jeeva, 2018).

Demographics Results

With the dataset complete, the sample size of N = 1,297 was loaded into SPSS (IBM, n.d.) for statistical analysis. The age of the pilots ranged from 16 to 91 (M = 53.90, SD = 17.01) years with frequencies as shown in Figure 8. The pilot's total number of flight hours were between six and 40,000 (M = 2836.45, SD = 5397.38) hours.

Figure 8

Frequency of Variable: Pilot's Age Distribution

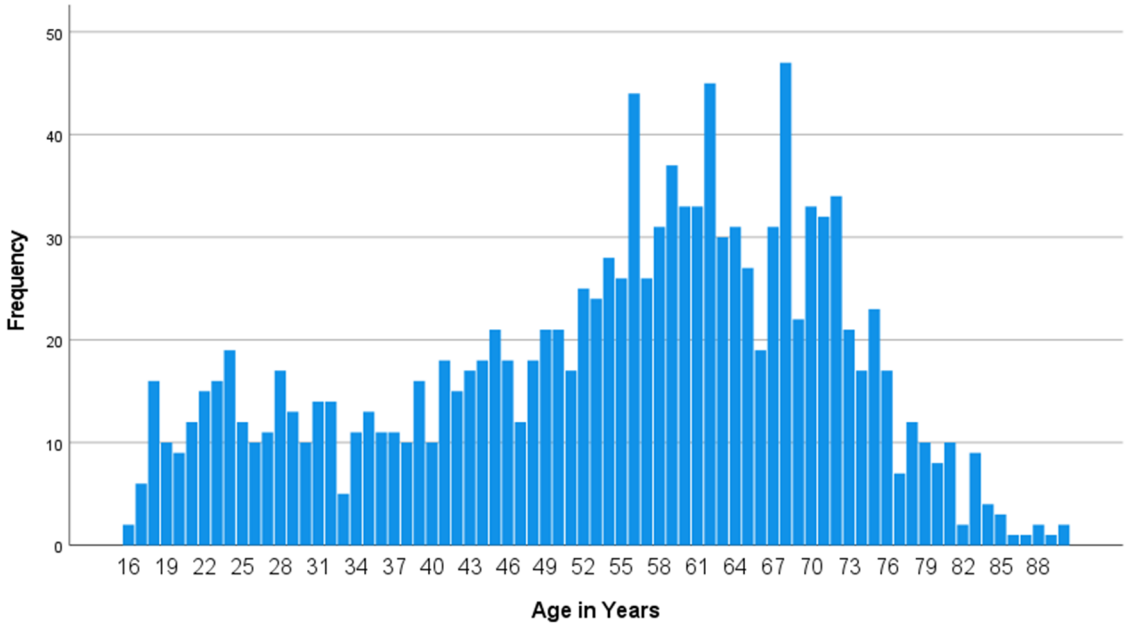

The pilot's certificate ranged from student to airline transport pilot and included flight instructor certificate. When the pilot held multiple certificates, only the highest certificate, from student to airline transport pilot, was coded. However, when a pilot held an additional flight instructor certificate, both the highest, from student to airline transport pilot, and flight instructor were coded. Figure 9 shows the frequency and distribution of the pilot's certificate and Appendix C has the actual numbers.

Figure 9

Frequency of Variable: Pilot's Certificate

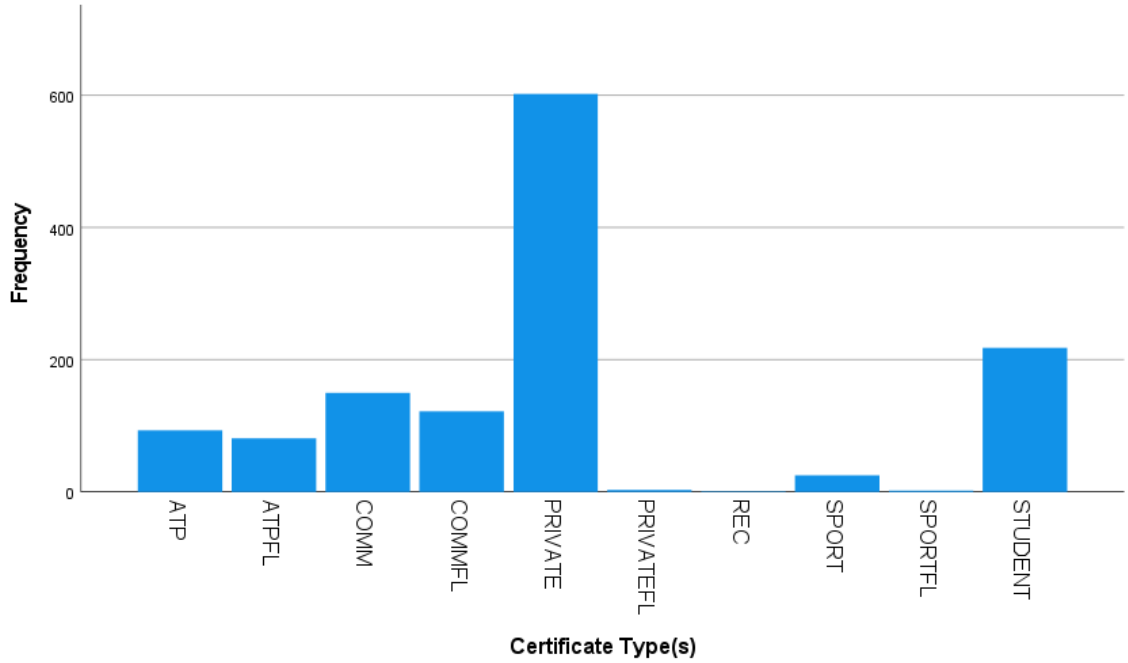

Note. ATP = Airline Transport Pilot; ATPFL = Airline Transport Pilot plus Flight Instructor; COMM = Commercial; COMMFL = Commercial plus Flight Instructor; PRIVATEFL = Private plus Flight Instructor; SPORTFL = Sport plus Flight Instructor.

An addition to the pilot's certificate, the variable of pilot's rating was able to have multiple selections. Pilot's rating was coded as single-engine, multiengine, instrument, or a combination. If the pilot held both a single-engine and multiengine, then only the higher rating of multiengine was coded. Instrument rating was added in addition to single-engine or multiengine rating. Figure 10 depicts the frequency of the pilot's rating, and the specific numbers are located in Appendix C.

Figure 10

Frequency of Variable: Pilot's Rating

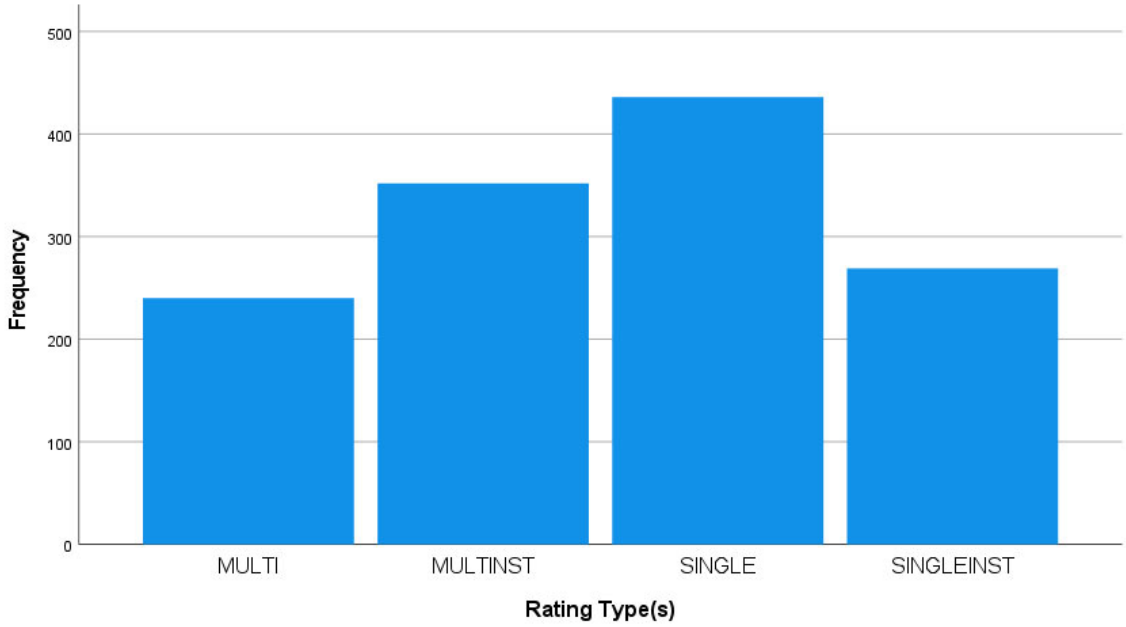

Note. MULTI = Multiengine; MULTINST = Multiengine with Instrument; SINGLE = Single-engine; SINGLEINST = Single-engine with Instrument

Lastly, the majority of the landing accidents had only one crew member in the aircraft ($n = 1274$) while only $n = 23$ had two crew members ($M = 1.02$, $SD = 0.13$). There were no reported accidents with more than two crew members.

Descriptive Statistics

This study proposed three new variables that had not been used in previous research: status of visual area surface penetrations, runway lighting types, and FAA visual area surface policy timeframe. Status of visual area surface penetrations were coded based on the worst obstacle penetration for the landing runway of the accident. This information was retrieved from the FAA's Instrument Flight Procedures Gateway

website (FAA, n.d.-b). Each IAP form, as show in Appendix A, was manually reviewed for the obstacle penetration status and subsequently manually coded into the dataset as both a 20:1 and 34:1 obstacle surface penetration, only a 34:1 obstacle surface penetration, or no obstacle surface penetrations. Figure 11 and Table 5 depict the frequency results of this variable.

Figure 11

Frequency of Variable: Status of Visual Area Surface Penetrations

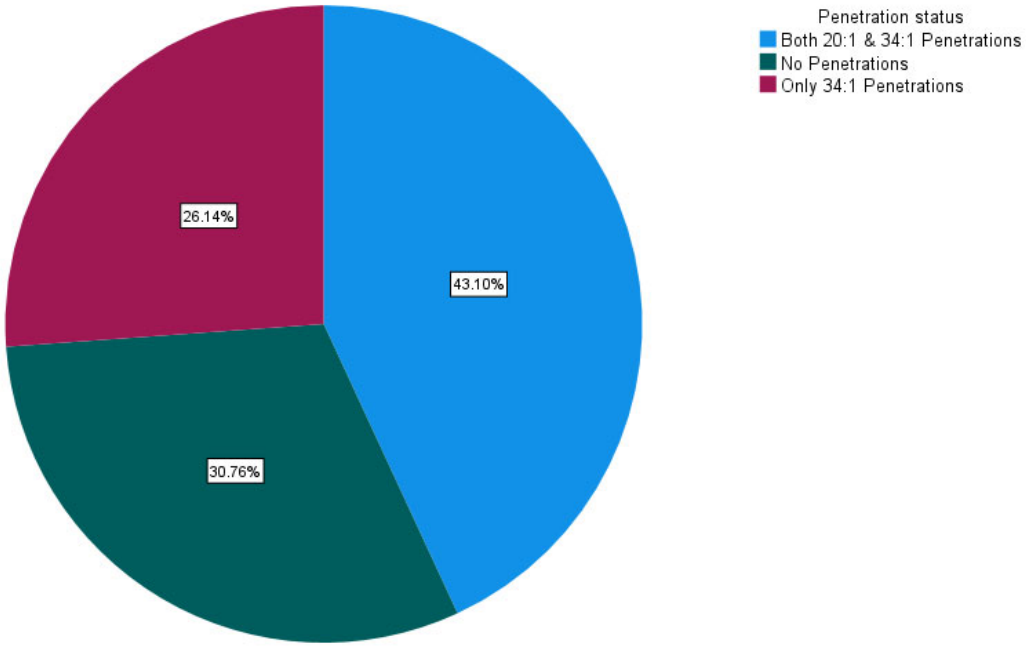

Note. There were no missing data for the status of visual area surface penetrations variable.

Table 5

Numerical Table of Status of Visual Area Surface Penetrations

Type of Visual Area Surface Penetration	*N*	Percentage
No Obstacle Penetrations	399	30.8%
Only 34:1 Obstacle Penetrations	339	26.1%
Both 20:1 & 34:1 Obstacle Penetrations	559	43.1%
Total	1297	100.0%

Note. There were no missing data for the status of visual area surface penetrations variable.

Of the dataset landing accidents, the majority (43.1%) of the landing runways had both 20:1 and 34:1 obstacle penetrations of the visual area surface. Overall, 69.2%, (898) of the landing runways had an obstacle penetration of the visual surface. The researcher broke down this variable and compared it to the different DVs, severity of personal injury and severity of aircraft damage. Table 6 shows the dispersion of the status of visual area surface penetrations against the different categories of severity of aircraft damage.

Table 6

Frequency of Status of Visual Area Surface Penetrations Compared to Severity of Aircraft Damage

Severity of Aircraft Damage	Both 20:1 & 34:1 Penetrations	No Penetration	Only 34:1 Penetration
None	1	1	0
Minor	2	3	1
Substantial	541	384	326
Destroyed	15	11	12

Note. There were no missing data for the status of visual area surface penetrations or severity of aircraft damage variables.

Of the 1,251 approach and landing accidents, 96.5% resulted in substantial aircraft damage. When the aircraft was substantially damaged, 43.2% (541) of those accidents had a landing runway with both a 20:1 and 34:1 obstacle penetration. Sixty-nine percent (867) of the landing runways had an obstacle penetration. No matter the amount of aircraft damage, the landing runway was more likely to have an obstacle penetration than no obstacle penetration. Only minor aircraft damage had an equal amount of landing runways with an obstacle penetration compared to no obstacle penetration (three total).

When comparing the status of visual area surface penetration to the severity of personal injury, the statistics are similar to aircraft damage. Table 7 displays the comparison of these two variables. The majority of approach and landing accidents did not result in an injury (1,060 accidents or 81.7%). However, as seen in the severity of aircraft damage, the majority of accidents had both 20:1 and 34:1 obstacle penetrations. Specifically, 69.0% (731) of accidents with no personal injury, 71.3% (97), of accidents with a minor personal injury, 62.2% (45) of accidents with serious personal injury, and 75.0% (42) of accidents with a fatal injury had a runway with at least one obstacle penetrating the visual area surface.

Table 7

Frequency of Status of Visual Area Surface Penetrations Compared to Severity of Personal Injury

Severity of Personal Injury	Both 20:1 & 34:1 Penetrations	No Penetration	Only 34:1 Penetration
None	442	329	289
Minor	70	39	27
Serious	22	17	6
Fatal	25	14	17

Note. There were no missing data for the status of visual area surface penetrations or severity of personal injury variables.

The next new variable introduced in this study was the runway lighting types. Figure 12 and Appendix C show the frequency distribution of this variable. The majority of approach and landing accidents did not result in an injury (1,060 accidents or 81.7%). However, as seen in the severity of aircraft damage, the majority of accidents had both 20:1 and 34:1 obstacle penetrations. Specifically, 69.0% (731) of accidents with no personal injury, 71.3% (97) of accidents with a minor personal injury, 62.2% (45) of accidents with serious personal injury, and 75.0% (42) of accidents with a fatal injury had a runway with at least one obstacle penetrating the visual area surface.

Figure 12

Frequency of Variable: Runway Lighting Types

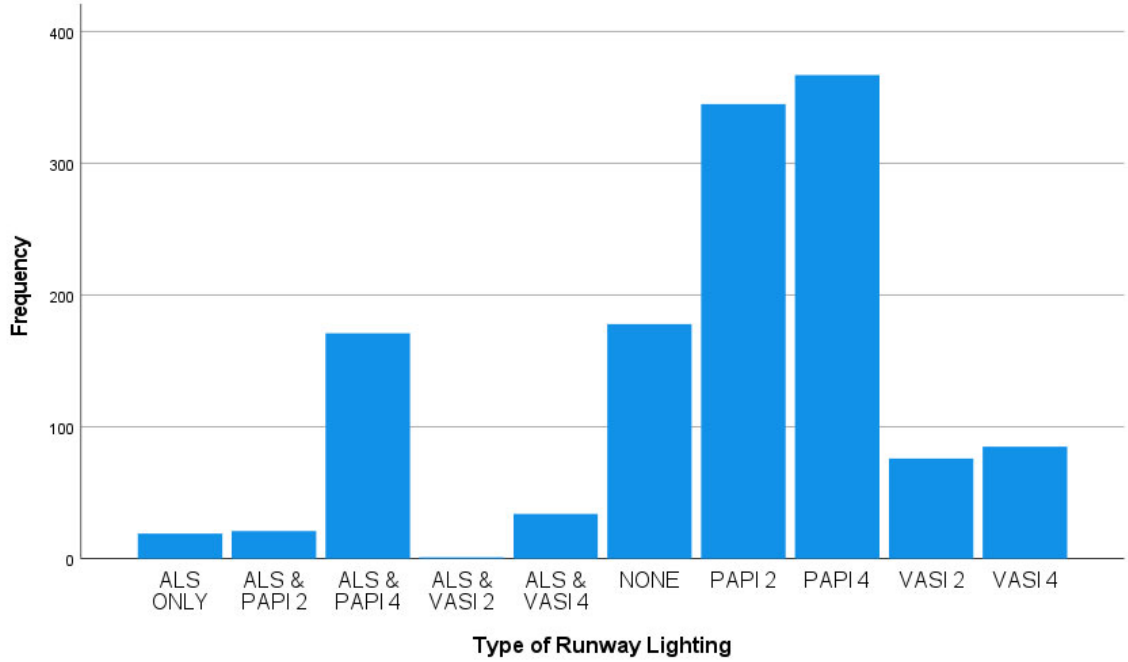

Note. ALS = Approach Lighting System. PAPI = Precision Approach Path Indicator. VASI = Vertical Approach Slope Indicator. There were no missing data for the runway lighting types variable.

The most common type of approach lighting was a four light PAPI system followed by a two light PAPI system. The least common lighting scenario was a runway with an approach lighting system with a two light VASI system. These statistics were expected because the FAA stated in 1985 that the PAPI systems were to replace the VASI systems (Federal Funding of Visual Glideslope Indicators, 1985). At that time, the PAPI systems were expected to cost an airport approximately $7,000 less than the VASI systems. Therefore, almost 35 years later, the PAPI systems are widely used at airports in the United States.

The third new variable for this study was the FAA visual area surface policy timeframe. Since each timeframe covered a two-year period, it was expected that each timeframe had roughly the same number of approach and landing accidents. However, Figure 13 and Appendix C show that the middle, two-year assessment policy period had 93 more accidents than the initial interim policy and 67 more accidents than the final policy period.

Figure 13

Frequency of Variable: FAA Visual Area Surface Policy Timeframe

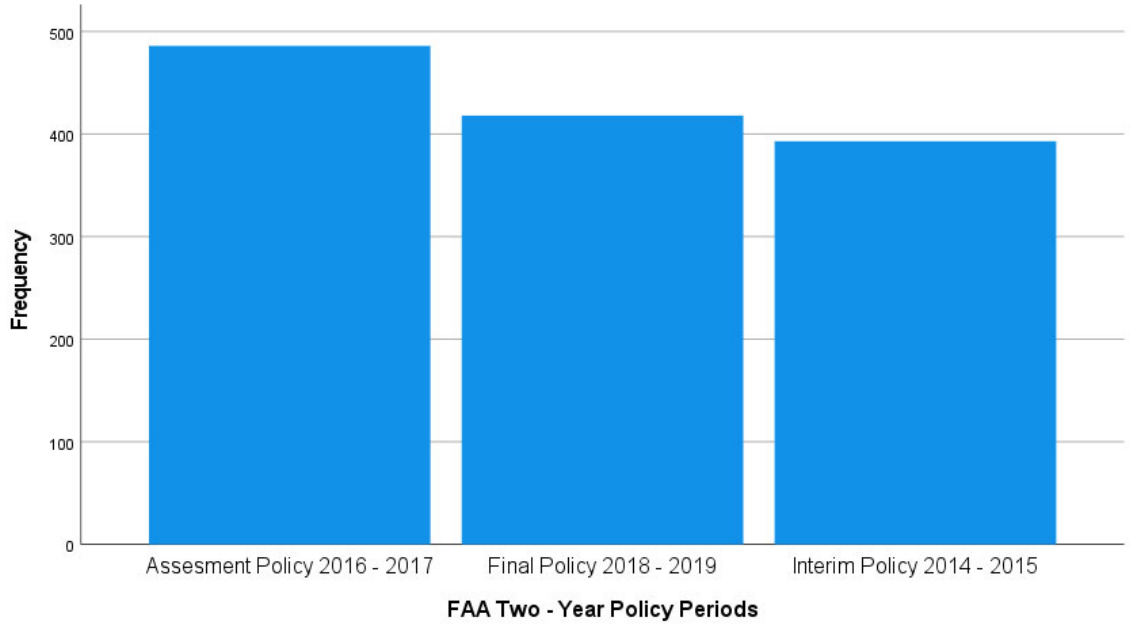

Note. Each policy period began on January 1st of the first year and ended on December 31st of the following year. There were no missing data for the FAA visual area surface policy timeframe variable.

Although not a specific variable for this study, Appendix C displays the frequency of landing accidents by the individual states. California had the highest number of

landing accidents at 144 while Maine had the least number of accidents at three. Every state had landing accidents except for Delaware.

The remaining six variables were mission C.F.R. category, landing runway in use, crosswind component, aircraft engine type, number of aircraft engines, and UTC time of accident. Table 8 depicts the frequency of the mission C.F.R. category depicting that general aviation accidents comprised of 96.5% of all approach and landing accidents in this dataset.

Table 8

Numerical Table of Mission C.F.R. Category

Aircraft's Mission (14 C.F.R.)	*N*	Percentage
Part 91 – General Aviation	1252	96.5%
Part 135 – Business Aviation	18	1.4%
Part 137 – Agricultural Aviation	5	0.4%
Part 121 – Airline Aviation	22	1.7%
Total	1297	100.0%

Note. There were no Part 129 accidents – foreign air carriers or cargo – in the dataset. There were no missing data for the mission C.F.R. category variable.

The next variable was the landing runway in use. Figure 14 and Appendix C display the frequency based on the two-digit runway designator (i.e., runway 180 was recorded as runway 18). All runway directions were represented in the dataset. Runway 18 had the highest number of approach and landing accidents with 64 (4.9%). The next highest was runway 17 with 56 accidents (4.3%). The lowest was runway 06 at 16 accidents (1.2%), and then runway 02 with 18 accidents (1.4%).

Figure 14

Frequency of Variable: Landing Runway in Use

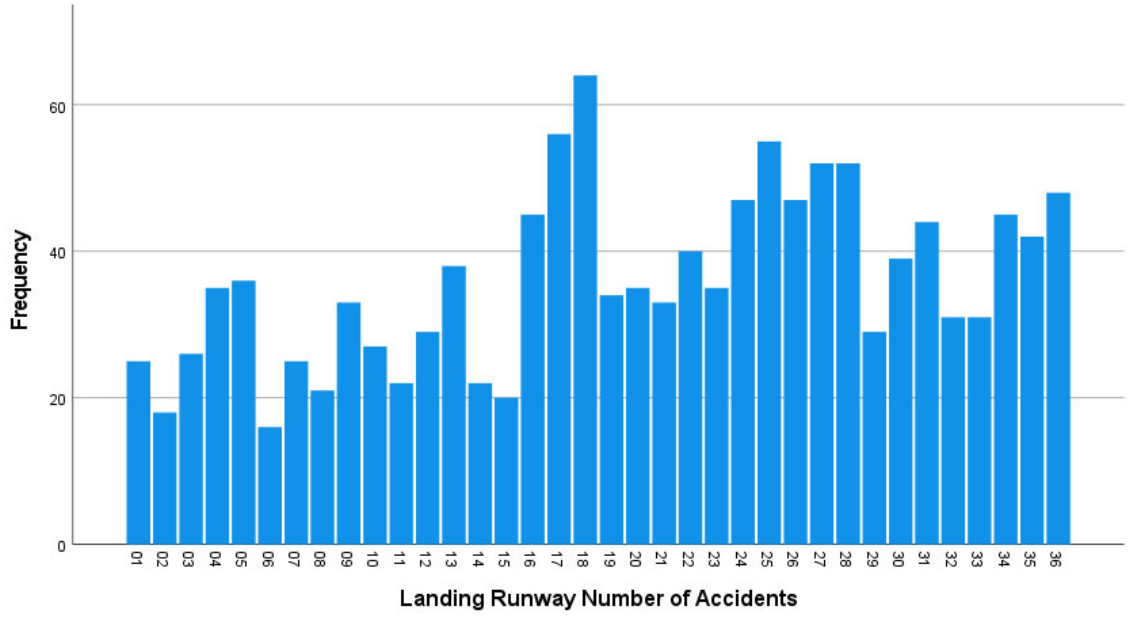

Note. Runway approach ends are designated from 010 to 360 and were recorded from 01 to 36. There were no missing data for the landing runway in use variable.

Crosswind component was the next IV which was a combination of the reported wind speed, in knots, and wind direction. The reported wind velocity ranged from calm up to 39 knots. Calm winds had the highest frequency at 248 accidents. One thousand forty-seven accidents (80.7%) occurred with a reported wind of 10 knots or less. Only 30 accidents (2.3%) had a reported wind of 20 knots or greater.

Computed crosswind component values began at zero, directly down the landing runway, and have no maximum amount. For this dataset, the crosswind component ranged from zero to 33.77 (M = 4.58, SD = 4.09) knots with frequencies as shown in Figure 15. The specific numerical amounts are in Appendix C. Eight hundred fifty-nine

landing accidents(66.2%) had a crosswind component of five knots or less. Two hundred seventy-nine of the landing accidents(21.5%) had a direct crosswind component between six to 12 knots.

Figure 15

Frequency of Variable: Crosswind Component

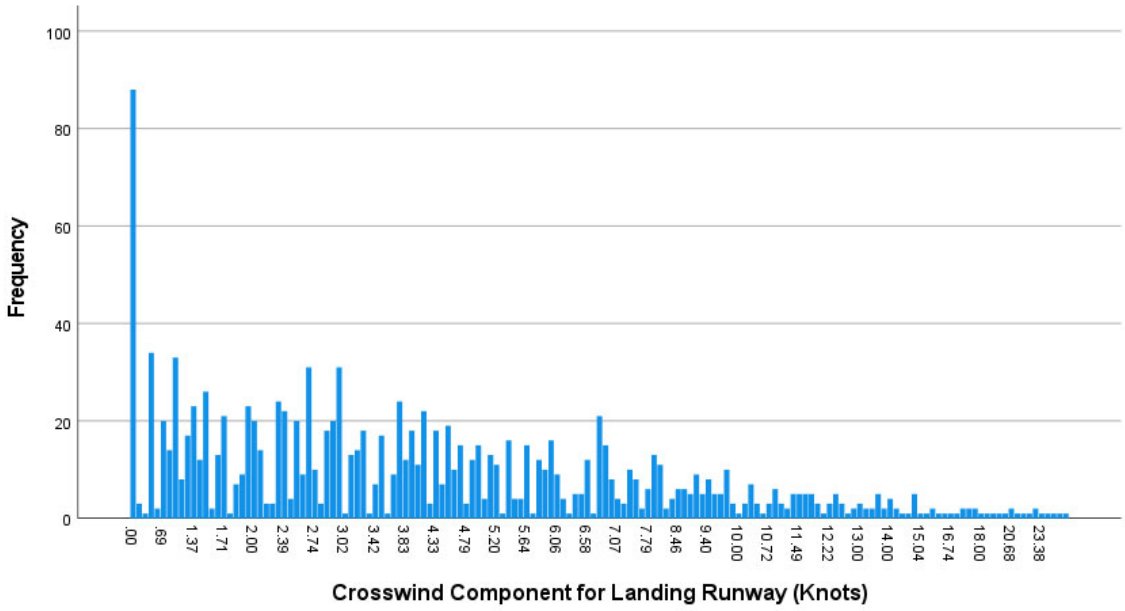

Note. Crosswind component was calculating using the sine of the difference between the wind direction and the landing runway, then multiplied against the wind velocity (FAA, 2014a). There were no missing data for the crosswind component variable.

Variable for aircraft engine type also had no missing values. Table 9 displays the frequency. Reciprocating, propeller aircraft dominated the approach and landing accidents accounting for 92.4%.

Table 9

Numerical Table of Aircraft Engine Type

Type of Engine on the Accident Aircraft	*N*	Percentage
Reciprocating	1199	92.4%
Turbo Fan	39	3.0%
Turbo Jet	5	0.4%
Turbo Prop	54	4.2%
Total	1297	100.0%

Note. There were no missing data for the aircraft engine type variable.

The number of aircraft engines, as shown in Table 10, ranged from zero to three ($M = 1.10$, $SD = 0.31$) engines. These frequencies follow the same trend with the majority of approach and landing accidents occurring in general aviation aircraft with a reciprocating engine.

Table 10

Numerical Table of Number of Aircraft Engines

Number of Aircraft Engines	*N*	Percentage
1	1165	89.8%
2	130	10.0%
3	2	0.2%
Total	1297	100.0%

Note. There were no missing data for the number of aircraft engines variable.

Coordinated Universal Time (UTC) values range from midnight, four zeros, to 2359 ($M = 1634.39$, $SD = 599.08$) hours. All 24 hours were represented in the dataset. The frequencies are displayed in Figure 16 and the specific numerical amounts are in Appendix C. The highest time occurrence of accidents, 44 accidents(3.4%), occurred at

1900 hours. The hours of 1500, 1630, 1700, 1730, 1800, 2000, and 2030 all had accidents counts between 30 and 35. When the variable was transformed into hour groupings, 2000 to 2059 hours had the highest number at 133 accidents(10.3%). The frequency display of this transformed variable is in Appendix C. The time period between 1400 hours and 2359 accounted for 1,069 accidents(82.4%). This confirms previous research on the risks of night landings (FAA, 2016b; Shappell et al., 2007).

Figure 16

Frequency of Variable: UTC Time of Accident

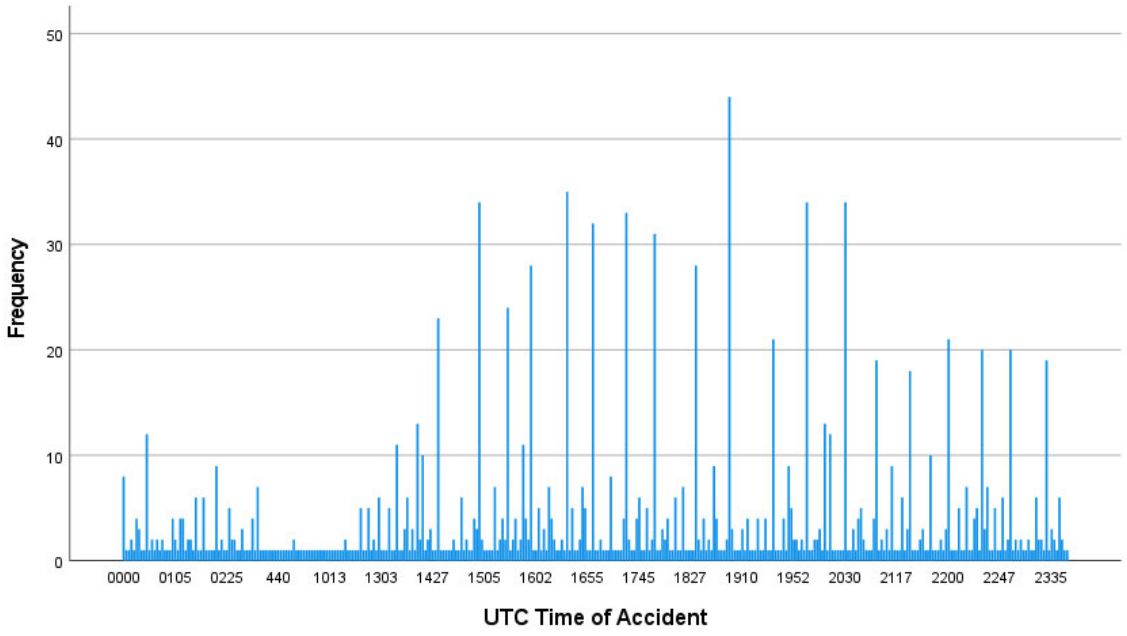

Note. The NTSB accident reports record time in the UTC 24-hour format from four zeros to 2359. There were no missing data for the UTC time of accident variable.

Finally, the two DVs for this study were the severity of aircraft damage and the severity of personal injury. Table 11 and Table 12 display the frequency of the accidents.

Every NTSB accident report included both the severity of aircraft damage and the severity of personal injury.

Table 11

Numerical Table of Severity of Aircraft Damage

Severity of Aircraft Damage	*N*	Percentage
None	2	0.2%
Minor	6	0.5%
Substantial	1251	96.5%
Destroyed	38	2.9%
Total	1297	100.0%

Note. There were no missing data for the severity of aircraft damage variable.

Table 12

Numerical Table of Severity of Personal Injury

Severity of Personal Injury	*N*	Percentage
None	1060	81.7%
Minor	136	10.5%
Serious	45	3.5%
Fatal	56	4.3%
Total	1297	100.0%

Note. There were no missing data for the severity of personal injury variable.

The majority of aircraft were substantially damaged at 1,251 (96.5%) while the majority of accidents had no injuries at 1,060(81.7%). When both DVs are compared to each other, 1,051 accidents(81.0%) had no personal injury and substantial aircraft damage (see Table 13). Understandably, fatal injuries corresponded to either a substantially damaged or destroyed aircraft.

Table 13

Frequency of Severity of Aircraft Damage Compared to Severity of Personal Injury

Severity	Personal Injury: None	Personal Injury: Minor	Personal Injury: Serious	Personal Injury: Fatal
Aircraft Damage: None	1	0	1	0
Aircraft Damage: Minor	5	1	0	0
Aircraft Damage: Substantial	1051	129	39	32
Aircraft Damage: Destroyed	5	6	5	24

Note. There were no missing data for the severity of personal injury or severity of aircraft damage variables.

Missing Data and Outliers

After all of the NTSB aircraft accident reports and websites were manually reviewed and coded, there was no missing data in the dataset. There was one possible outlier where the NTSB accident report stated the pilot's total number of flight hours as 40,000 (NTSB, 2017c). This value was the highest of all total flight hours and 8,294 flight hours more than the second highest total of 31,706 hours. However, the pilot held an air transport pilot with flight instructor certificate. Even though it is possible the accident investigator approximated the pilot's total number of flight hours, it is also possible the accident investigator talked directly to the pilot after the accident since there were no personal injuries. Therefore, this accident remained in the dataset.

Initial SVM Evaluation Results

The completed dataset was loaded into Google Colaboratory (2022) for the development of the severity of personal injury SVM model. The initial python coding using Scikit-learn (2020) evaluated the dataset, variables, and added the three normalized

variables. From there, the dataset was shuffled, since the Excel dataset was in chronological order by date. Then a stratified split was used to ensure both the training and test partitions had the same percentage of each level of personal injury severity. To develop the SVM classification models, the four different kernels were applied separately to the training partition to create four separate SVM models. Finally, a five-fold cross-validation was used on the training partition to develop and fine tune the models to select the best predictive model and then evaluated against the test partition.

The severity of aircraft damage prediction models produced an initial accuracy between 96% and 97%. However, the confusion matrices for the training partitions and the classification reports for the test partitions showed that all of the models were skewed towards substantial aircraft damage (see Table 14 and Table 15). The confusion matrix image shown in Figure 17 reveals that instead of the expected white diagonal from upper left to lower right, the image reveals a model that correctly predicted substantial aircraft damage while incorrectly predicting the other three levels of damage.

Figure 17

Initial Severity of Aircraft Damage Training Confusion Matrix

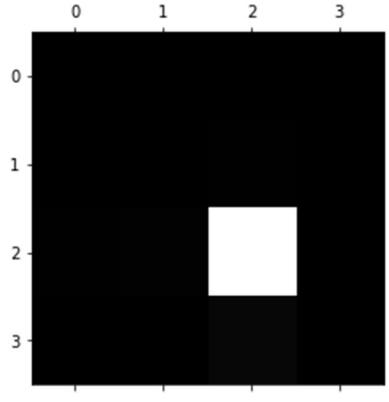

Note. Results shown are with the linear kernel. However, all kernels had similar results.

Table 14

Initial Severity of Aircraft Damage Training – Numerical Confusion Matrix

		Actual Values			
Severity of Aircraft Damage		None	Minor	Substantial	Destroyed
Predicted Values	None	0	0	2	0
	Minor	0	0	5	0
	Substantial	6	9	985	0
	Destroyed	0	1	28	0

Note. Results shown are with the linear kernel. However, all kernels had similar results.

Table 15

Initial Severity of Aircraft Damage Test Classification Report

	Severity of Aircraft Damage	Precision	Sensitivity / Recall	F1-Score	Specificity	Support
Linear	None	0.00	0.00	0.00	1.00	0
	Minor	0.00	0.00	0.00	1.00	1
	Substantial	0.96	0.99	0.98	0.00	250
	Destroyed	0.00	0.00	0.00	0.97	8
	Accuracy			0.96		259
	Macro Average	0.24	0.25	0.25	0.99	259
	Weighted Average	0.93	0.96	0.94	1.00	259

Note. Results shown are with the linear kernel. However, all kernels had similar results.

Similarly, the severity of personal injury SVM models produced a prediction accuracy between 82% and 84%. However, the training confusion matrix (see Figure 18 and Table 16) and the test classification report (see Table 17) showed that the model development and test were skewed towards no personal injury. The lack of a white

diagonal from upper left to lower right reveals a model that correctly predicted no personal injury while incorrectly predicting the other three levels.

Figure 18

Initial Severity of Personal Injury Training Confusion Matrix

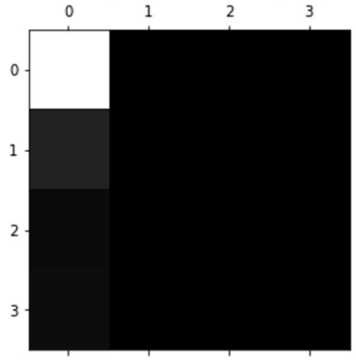

Note. Results shown are with the linear kernel. However, all kernels had similar results.

Table 16

Initial Severity of Personal Injury Training Numerical Confusion Matrix

		Actual Values			
Severity of Personal Injury		None	Minor	Serious	Fatal
Predicted Values	None	840	0	1	0
	Minor	113	0	0	0
	Serious	37	0	0	0
	Fatal	45	0	0	0

Note. Results shown are with the linear kernel. However, all kernels had similar results.

Table 17

Initial Severity of Personal Injury Test Classification Report

Severity of Personal Injury		Precision	Sensitivity / Recall	F1-Score	Specificity	Support
Linear	None	0.84	0.99	0.91	0.00	217
	Minor	0.00	0.00	0.00	0.89	24
	Serious	0.00	0.00	0.00	0.96	8
	Fatal	0.00	0.00	0.00	0.96	10
Accuracy				0.83		259
Macro Average		0.21	0.25	0.23	0.70	259
Weighted Average		0.70	0.83	0.76	0.12	259

Note. Results shown are with the linear kernel. However, all kernels had similar results.

These results showed that the linear kernel SVM model predicted almost all correct for no personal injury and had an accuracy of 83%. However, the model was incorrect for minor, serious, and fatal injuries. Note that the precision, sensitivity/recall, and F1-scores are zero percent for minor, serious, and fatal injuries.

When comparing machine learning models, neither accuracy percentage nor misclassification rate can be the sole basis for validation (Brownlee, 2020a; Geron, 2017; Phy, 2019). The preeminent models have high accuracy, high precision, high sensitivity/recall, and high F1-scores (Kuhn & Johnson, 2016; Geron, 2017; Sofaer et al., 2019). For this study, a model high in all four areas accurately predicted the correct injury level of an accident, true positive, and correctly eliminated the incorrect injury levels, false positives. Unfortunately, imbalanced datasets are subject to false accuracy percentages or misclassification rates as in this initial model development (Branco, et al., 2015; Brownlee, 2020a; Geron, 2017; Kuhn & Johnson, 2016; Sofaer et al., 2019). In

effect, the initial linear model for the severity of personal injury assumed that every accident, except one, resulted in no personal injury and therefore failed validity.

The initial attempt to develop the SVM models was not considered successful. The tilted dataset towards no personal injury(81%), and substantial aircraft damage(97%) at first looked successful because the SVM model's accuracy percentage for the severity of personal injury was in the low 80s and the SVM model's accuracy for aircraft damage was in the low 90s. The results were almost exactly the same no matter which kernel was used in the SVM model.

However, machine learning models should not be evaluated on accuracy or misclassification rates alone but need to be evaluated along with the confusion matrix, precision, sensitivity/recall, and F1-scores (Geron, 2017; Kuhn & Johnson, 2016). When evaluating the confusion matrix and classification reports, it was apparent the SVM models assumed every aviation accident resulted in substantial aircraft damage and no injury (see Figure 17, Figure 18, Table 14, and Table 16). For predicting the severity of aircraft damage, the confusion matrices reveal a model with significant false positives for none, minor, and destroyed aircraft damage. Similarly, on predicting the severity of personal injury, Table 16 and Figure 18 show the classification matrix where the SVM model had significant false positives for minor, serious, and fatal injuries. This was confirmed with values of zero, shown in Table 15, for the none, minor, and destroyed damage, and in Table 17, for the minor, serious, and fatal injury precision, sensitivity/recall, and F1-scores.

Unlike previous aviation accident research, this study desired to use all four levels of the personal injury and aircraft damage variables. However, this lopsided dataset may

be why many previous researchers evaluated the severity of personal injury as a binary variable (Baugh, 2020; Burnett & Si, 2017; Koteeswaran et al., 2019; Kushwaha & Sharma, 2014; Wu et al., 2014). However, to support this study's goal to evaluate severity on a four multi-level scale required the dataset to be augmented.

Database Augmentation Results

To begin the augmented dataset process, the initial SVM workflow (see Figure 5) was stopped and the final SVM workflow (see Figure 6) was initiated. First, the original dataset was shuffled in Microsoft Excel and then 80% of the dataset was separated into a training partition and 20% was moved into a separate Excel file for the test partition. Next, the training partition was augmented using random over-sampling (ROS) because ROS is known to produce better results than random under-sampling and synthetic minority over-sampling technique (SMOTE) (Korstanje, 2021; Leevy et al., 2018). In addition to ROS, the dataset was augmented using the fixed method by duplication of accident data similar to the augmentation of medical research databases for predicting illnesses (Khoshgoftaar et al., 2007; Van Hulse et al., 2007). The augmentation occurred once for the severity of aircraft damage and separately for the severity of personal injury resulting in two separate augmented datasets. This process was followed instead of augmenting the entire dataset and then splitting into two partitions, to avoid sampling bias or overfitting by reducing similar events in both the training and test partitions.

Therefore, the training partitions were augmented differently for each DV to ensure all four levels of severity were equally represented at around 1,000 accident events. For the three categories with the lowest data samples, the accident data were duplicated to approximately 900 to 1,000 events for each level of aircraft damage and

700 to 900 for each level of personal injury. The largest severity percentage was not augmented. Table 18 and Table 19 show data sample size after the augmentation

Table 18

Augmented Numerical Table of Severity of Aircraft Damage

Severity of Aircraft Damage	*N*	Percentage
None	972	25.2%
Minor	972	25.2%
Substantial	1000	25.9%
Destroyed	912	23.7%
Total	3856	100%

Table 19

Augmented Numerical Table of Severity of Personal Injury

Severity of Personal Injury	*N*	Percentage
None	846	24.9%
Minor	959	28.2%
Serious	720	21.2%
Fatal	878	25.8%
Total	3403	100.0%

Reliability and Validity Testing Results

With the augmented datasets, the severity of aircraft damage and severity of personal injury SVM models were developed and tested for reliability and validity. First, each specific kernel was applied to the SVM model. Then, a five-fold cross-validation was used against the training partition to test model reliability (see Table 20 and Table 21). Even though the four kernels performed differently, the low standard deviation between each cross-validation run reveals a consistent performance by the different SVM models against the training partition (Brownlee, 2018; Geron, 2017; Kuhn & Johnson,

2016; Scikit-learn, 2019). Therefore, all of the different SVM models were considered reliable.

Table 20

Severity of Aircraft Damage Cross-Validation

Kernel	Run 1	Run 2	Run 3	Run 4	Run 5	Ave.	*SD*
Linear	88.46%	89.23%	87.42%	86.51%	87.43%	87.83%	0.01
Polynomial	94.42%	90.66%	92.35%	90.27%	92.72%	92.09%	0.02
RBF	97.92%	96.63%	97.92%	98.31%	97.27%	97.61%	0.01
Sigmoid	75.75%	74.58%	74.19%	73.15%	74.55%	74.44%	0.01

Note. RBF = Radial basis function. Ave. = Average.

Table 21

Severity of Personal Injury Cross-Validation

Kernel	Run 1	Run 2	Run 3	Run 4	Run 5	Ave.	*SD*
Linear	45.96%	48.38%	46.76%	45.29%	49.71%	47.22%	0.02
Polynomial	52.57%	59.59%	53.97%	56.18%	58.97%	56.25%	0.03
RBF	78.41%	80.88%	79.41%	80.29%	76.18%	79.03%	0.02
Sigmoid	28.63%	28.09%	29.85%	31.47%	32.65%	30.14%	0.02

Note. RBF = Radial basis function. Ave. = Average.

After the cross-validation was completed, the SVM models were coded for prediction against the test partition and evaluated for validity using confusion matrices and classification reports. For the severity of aircraft damage, the linear, polynomial, and RBF kernel training models showed confident confusion matrices (see Appendix C). However, for the severity of personal injury, only the polynomial and RBF kernel training models displayed an optimistic confusion matrix (see Appendix C). Previous

research analyzing the polynomial and RBF kernels assessed them as great kernels for separating non-linear data (Jiang et al., 2016; Navlani, 2019).

Confusion matrices and classification reports were used to test the validity of the models by displaying the misclassification rates, sensitivity, and specificity for the test partition. For the severity of aircraft damage, the RBF kernel model provided the highest accuracy at 93% while the polynomial was second with 92% (see Table 22). There was no concern of overfitting for any of the models because of the high precision, sensitivity/recall, specificity, and F1-score, meaning the model was able to predict both true and false positives (Geron, 2017; Kuhn & Johnson, 2016; Sofaer et al., 2019).

Table 22

Severity of Aircraft Damage Validity

Kernel	Mis-classification Rate	Accuracy	Precision	Sensitivity / Recall	Specificity	F1-Score
Linear	0.20	0.80	0.71	0.86	0.88	0.76
Polynomial	0.08	0.92	0.94	0.86	0.96	0.88
RBF	0.07	0.93	0.90	0.98	0.95	0.93
Sigmoid	0.53	0.47	0.40	0.56	0.79	0.41

Note. RBF = Radial basis function. Precision, sensitivity/recall, specificity, and F1-score shown are an average across the four levels of severity. Full results are in Appendix C.

For the severity of personal injury, the RBF kernel had the highest accuracy, precision, sensitivity/recall, specificity, and F1-score (see Table 23). The polynomial kernel provided high precision and specificity, but poor accuracy, sensitivity/recall, and F1-score.

Table 23

Severity of Personal Injury Validity

Kernel	Mis-classification Rate	Accuracy	Precision	Sensitivity / Recall	Specificity	F1-Score
Linear	0.47	0.53	0.54	0.54	0.84	0.53
Polynomial	0.43	0.57	0.81	0.56	0.87	0.58
RBF	0.19	0.81	0.81	0.82	0.94	0.81
Sigmoid	0.71	0.29	0.29	0.29	0.76	0.29

Note. RBF = Radial basis function. Precision, sensitivity/recall, specificity, and F1-score shown are an average across the four levels of severity. Full results are in Appendix C.

Prediction Results

Best Prediction Models

The first step in addressing research question one was to develop, fine tune, and evaluate the best models for the severity of aircraft damage and the severity of personal injury. The goal of the selected models was to have a low misclassification rate, high accuracy, high precision, high sensitivity/recall, high specificity, and high F1-score. Although some research, for example medical, prefer a high precision or a high sensitivity/recall, this study desired a predictive model that had both high precision and high sensitivity/recall (Branco et al., 2015; Brownlee, 2020a; Geron, 2017; Kuhn & Johnson, 2016; Leevy, et al., 2018; Sofaer et al., 2019). This way the predictive models would correctly ascertain an accident's specific level of aircraft damage and personal injury, without favoring a true positive or false positive.

For the severity of aircraft damage, the RBF kernel model produced the highest accuracy at 93%, while also producing the correct level of aircraft damage. The linear

model and polynomial model also had an accuracy of 80% and 92% respectively. The polynomial model had the highest recall for the aircraft substantially damaged level, 0.98, however, it was lacking in recall for the destroyed damaged level, at 0.47, as shown in Table 22 and Appendix C. Since both the polynomial and RBF models had above 90% accuracy, Figure 19 shows a side-by-side comparison of their confusion matrix image (Geron, 2017).

Figure 19

Confusion Matrix Image Comparison for Severity of Aircraft Damage: Polynomial Verses RBF

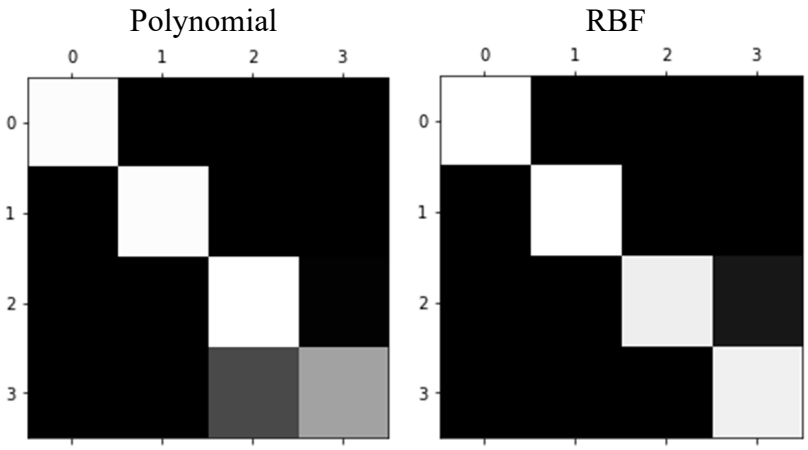

Note. See Appendix D for all four kernel confusion matrix images.

The side-by-side confusion matrix shows that the SVM model with the polynomial kernel was sporadic at predicting the destroyed aircraft damage level, while the SVM model with the RBF kernel cleanly predicted all four levels of severity. Therefore, through all four individual levels, the RBF kernel produced the best holistic model for predicting the severity of aircraft damage. Since the SVM model with the RBF kernel at the default values for σ and C predicted at a 93% for both the training and test

sets, the next step was to optimize the SVM models with the RBF kernels. Once optimized the new models were evaluated against the training and test partitions for improved prediction ability without overfitting. Table 24 shows the different optimized SVM models using the RBF kernels against the default RBF kernel.

Table 24

Optimization of SVM Model with RBF Kernel for Severity of Aircraft Damage (Test)

	σ	C	M. R.	Accuracy	Precision	Sensitivity / Recall	F1-Score
Default	0.03	1	0.07	0.93	0.90	0.98	0.93
Optimization A	0.04	1	0.06	0.94	0.92	0.94	0.93
Optimization B	0.04	5	0.04	0.96	0.94	0.94	0.94
Optimization C	0.04	10	0.05	0.95	0.94	0.94	0.94
Optimization D	0.05	1	0.04	0.96	0.94	0.95	0.94
Optimization E	0.05	5	0.04	0.96	0.94	0.94	0.94
Optimization F	0.05	10	0.04	0.96	0.94	0.94	0.94
Optimization G	0.1	1	0.10	0.90	0.92	0.72	0.78
Optimization H	0.1	5	0.11	0.89	0.92	0.71	0.78
Optimization I	0.1	10	0.10	0.90	0.93	0.71	0.78
Optimization J	10	100	0.26	0.74	0.18	0.25	0.21

Note. M.R. = Misclassification Rate. RBF = Radial basis function. Precision, sensitivity/recall, specificity, and F1-score shown are an average across the four levels of severity.

Initially each optimized SVM model with RBF kernel continued to improve against the training partition with Optimization G through J predicting 100% of the training partition. However, when comparing the same optimized models against the test set, Optimization G through J models were subject to overfitting as shown by the low accuracy, precision, sensitivity/recall, and F1-scores (Geron, 2017; Kuhn & Johnson, 2016; Sofaer et al., 2019). Figure 20 shows how the test accuracy drops even though the training accuracy improves revealing overfit models.

Figure 20

Severity of Aircraft Damage Training Versus Test Optimization

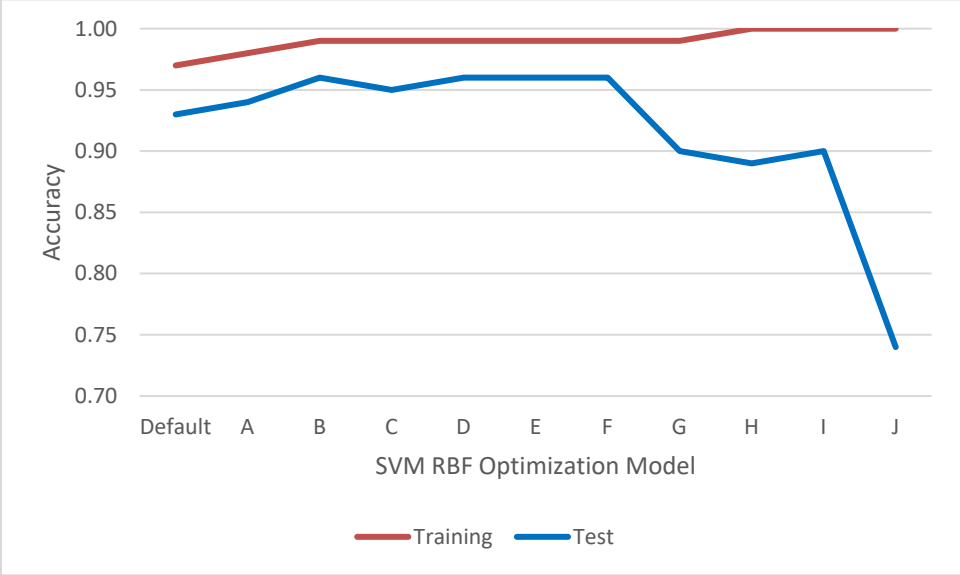

Note. X axis reflects Table 24 Optimized models.

From comparing Table 24 and Figure 20, SVM models with RBF Optimization B, D, E, and F appear identical; however, the Optimization D model has a slightly higher sensitivity/recall of 0.95 compared to 0.94 of the other models. It also had more true positive results for the destroyed level of damage than the other models (see Figure 21,

Table 25, Table 26, and Appendix C). Therefore, the SVM model using the RBF Optimization D kernel had the best predictability for the severity of aircraft damage during approach and landing accidents.

Figure 21

RBF Optimization D Confusion Matrix Image Severity of Aircraft Damage

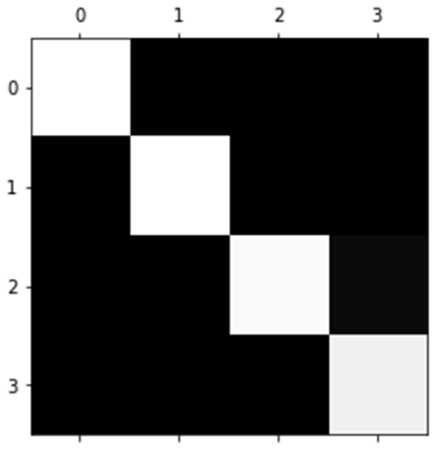

Table 25

Optimization D Model for Aircraft Damage – Numerical Confusion Matrix

		Actual Values			
Severity of Aircraft Damage		None	Minor	Substantial	Destroyed
Predicted Values	None	20	0	0	0
	Minor	0	25	5	0
	Substantial	0	1	241	8
	Destroyed	0	0	0	38

Table 26

Optimization D Model for Aircraft Damage – Classification Report

Severity of Aircraft Damage	Precision	Sensitivity / Recall	F1-Score	Support
None	1.00	1.00	1.00	20
Minor	0.96	0.83	0.89	30
Substantial	0.98	0.96	0.97	250
Destroyed	0.83	1.00	0.90	38
Accuracy			0.96	338
Macro Average	0.94	0.95	0.94	338
Weighted Average	0.96	0.96	0.96	338

The next step in addressing the first research question was to evaluate the best model for predicting the severity of personal injury. All four kernels had much lower accuracy percentages predicting the severity of personal injury than the previous severity of aircraft damage (see Table 23 and Appendix C). The polynomial kernel had the highest precision for the serious and fatal personal injury levels. However, the accuracy, recall, and F1-scores broached concerns. The RBF kernel model had an accuracy significantly better than the other kernels and was the only model with an accuracy above the desired goal of 80%. In addition, the RBF kernel model had high precision, sensitivity/recall, F1-score, and specificity displaying the validity and well roundedness of the model. Figure 22 shows the confusion matrix image of the RBF model.

Figure 22

Default RBF Confusion Matrix Image Severity of Personal Injury

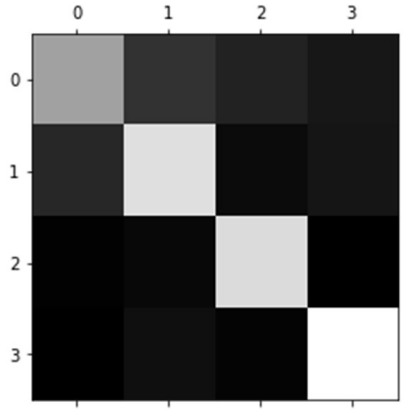

Note. See Appendix D for all four kernel confusion matrix images.

Although the SVM model with the RBF kernel had the highest prediction accuracy at 81%, the next step was to optimize the model by adjusting the default values for σ and C. Table 27 shows the results of some of the optimization models with the complete list of all optimization models in Appendix C.

Table 27

Optimization of SVM Model with RBF Kernel for Severity of Personal Injury (Test)

	σ	C	M. R.	Accuracy	Precision	Sensitivity / Recall	F1-Score
Default	0.03	1	0.19	0.81	0.81	0.82	0.81
Optimization A	0.1	1	0.12	0.88	0.87	0.93	0.89
Optimization B	0.6	10	0.02	0.98	0.99	0.98	0.98
Optimization C	0.65	10	0.02	0.98	0.99	0.98	0.99
Optimization D	0.65	20	0.02	0.98	0.99	0.98	0.99
Optimization E	0.7	10	0.02	0.98	0.99	0.98	0.99
Optimization F	10	1000	0.41	0.59	0.88	0.41	0.44

Note. M.R. = Misclassification Rate. RBF = Radial basis function. Precision, sensitivity/recall, specificity, and F1-score shown are an average across the four levels of severity. This is a sample of the different optimization models. A complete list is in Appendix C.

SVM models using the RBF kernel were developed with σ values between 0.1 and 0.8 and C values between 1 and 100 (see Appendix C). All of these models fell between the 81% defaulted value model and increased up to the 98% of the Optimization B, C, D, and E models. Above the Optimization C model, there was no improvement in accuracy, precision, sensitivity/recall, or F1-scores as shown by Optimization D and E models in Table 27. When comparing all of the optimization models between the training and the test accuracy, Figure 23 shows how the models start to overfit as the accuracy for

the test partition begins to drop even though the training partition accuracy approaches or equals 100%.

Figure 23

Severity of Personal Injury Training Versus Test Optimization

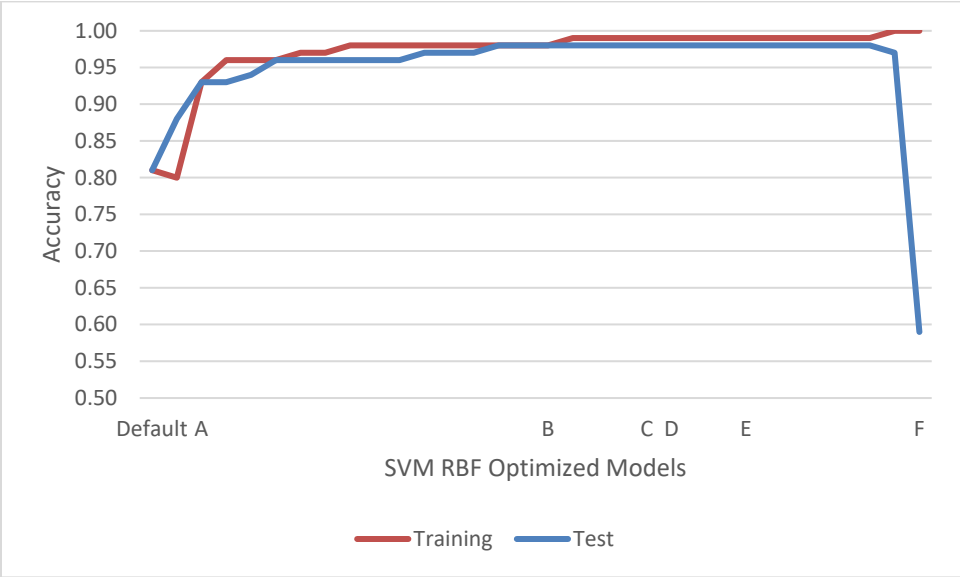

Note. X axis reflects Table 27 optimized models.

The SVM models with parameters σ and C higher than Optimization C model are at risk for overfitting or were subjected to overfitting. Therefore, the Optimization C model achieves the best prediction at the lowest parameter values. Optimization C model's confusion matrix and numerical values are shown in Figure 24 and Table 28. The full classification report for Optimization C is shown in Table 29.

Figure 24

Optimization C Model's Confusion Matrix for Personal Injury

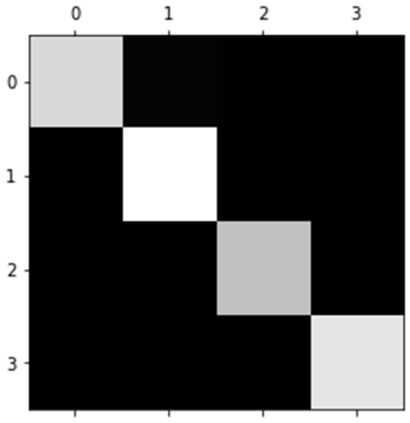

Table 28

Optimization C Model for Personal Injury – Numerical Confusion Matrix

		Actual Values			
Severity of Personal Injury		None	Minor	Serious	Fatal
Predicted Values	None	210	3	0	0
	Minor	5	132	0	0
	Serious	0	0	45	0
	Fatal	1	0	0	53

Table 29

Optimization C Model for Personal Injury – Classification Report

Severity of Personal Injury	Precision	Sensitivity / Recall	F1-Score	Support
None	0.97	0.99	0.98	213
Minor	0.98	0.96	0.97	137
Serious	1.00	1.00	1.00	45
Fatal	1.00	0.98	0.99	54
Accuracy			0.98	449
Macro Average	0.99	0.98	0.99	449
Weighted Average	0.98	0.98	0.98	449

The classification report in Table 29 reveals the optimized model has both a high precision, sensitivity/recall, and F1-score. Therefore, even though this Optimization C SVM model using the RBF kernel has increased the accuracy for predicting the severity of personal injury, there is no concern of overfitting because of the high precision, high sensitivity/recall, and high F1-score confirm the model's ability to predict both true positives and true negatives (Geron, 2017; Kuhn & Johnson, 2016; Sofaer et al., 2019). Therefore, the best model for predicting the severity of personal injury was the Optimization C SVM model using the RBF kernel.

Most Important Factors

The second question was to evaluate each model for the most important factors influencing that model. All of the categorical values had to be coded with dummy variables into subcategories for the SVM. Therefore, the initial model's statistical findings for factor importance had each subcategory separate. The top five factors for the severity of aircraft damage were flight hours, the subcategory single engine certificate, time of day, pilot's age, crosswind component, runway number, and the subcategory of

any obstacle penetration on approach (see Appendix C). For the severity of personal injury, the top factors were the time of day, pilot's flight hours, crosswind component, pilot's age, runway number, and the subcategory of any obstacle penetration on approach (see Appendix C).

However, it was apparent that the interval and ratio variables were at the top of both factor lists. Therefore, to fairly evaluate a factor's importance against an interval or ratio variable, the individual subcategory results were combined. Table 30, Figure 25, and Figure 26 show how each factor influenced the models.

Table 30

Factor Importance

Variable	Importance for Severity of Aircraft Damage	Importance for Severity of Personal Injury	Combined Importance
Status of visual area surface penetrations	0.081	0.057	0.138
Mission C.F.R. category	0.053	0.006	0.059
FAA Visual Area Surface Policy Timeframe	0.096	0.065	0.161
Runway lighting types	0.076	0.099	0.175
Landing runway in use	0.067	0.103	0.17
Crosswind Component	0.078	0.124	0.202
Aircraft engine type	0.043	0.018	0.061
Number of aircraft engines	0.014	0.014	0.028
UTC time of accident	0.114	0.136	0.25
Pilot's certificate	0.157	0.045	0.202
Pilot's rating	0.083	0.052	0.135
Pilot's total number of flight hours	0.122	0.134	0.256
Pilot's age	0.101	0.123	0.224
Number of flight crew	0.022	0.001	0.023

Figure 25

Factor Importance Severity of Aircraft Damage

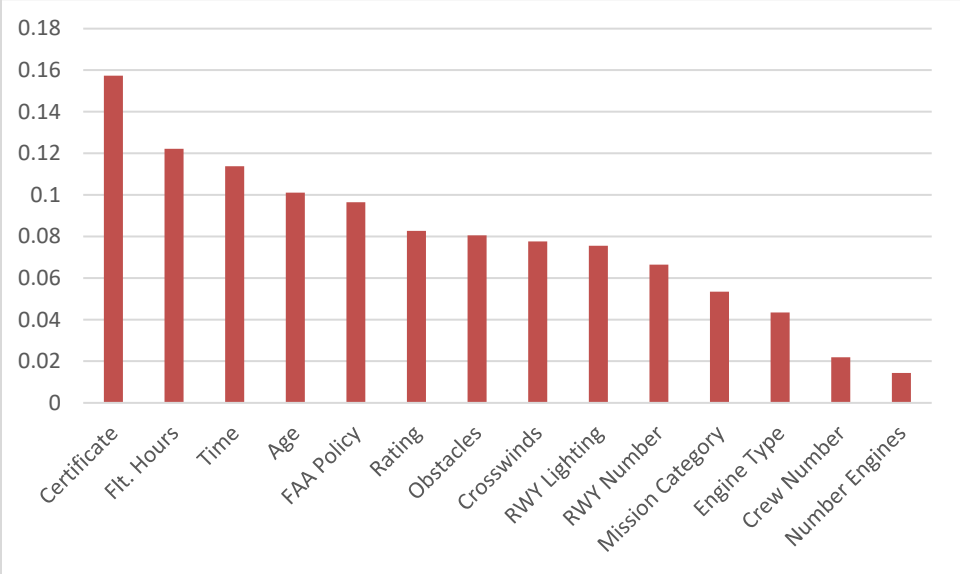

Note. Variables are shown at their categorical level

Figure 26

Factor Importance Severity of Personal Injury

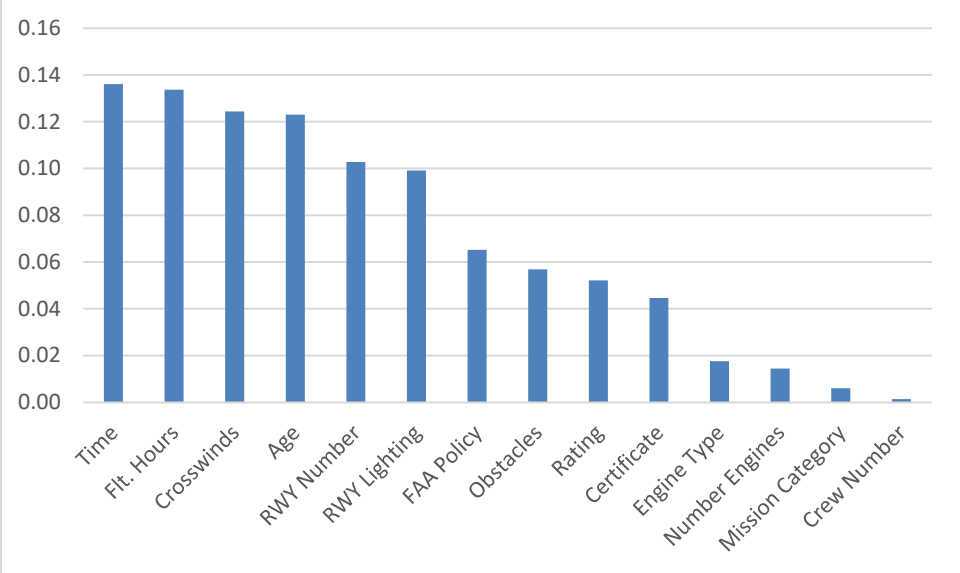

Note. Variables are shown at their categorical level

Therefore, the leading five factors for the severity of aircraft damage were the pilot's certificate, number of flight hours, time of day, pilot's age, and the FAA's obstacle policy. For the severity of personal injury, the top five factors were the time of day, pilot's number of flight hours, crosswind component, pilot's age, and approach runway number.

Evaluating the Three New Variables

The final research question regarded the statistical findings for factor importance of the three new variables: the presence of visual area surface penetrations for a runway, the FAA's visual area surface penetration policy timeframe, and the type of runway approach lighting. Runway lighting type had the highest factor importance at a combined weight of 0.175, followed by the FAA visual area surface policy timeframe at 0.161, and status of visual area surface penetrations at 0.138 (see Table 31). When separated into the sub-category level, the highest of the new variables was any obstacle penetration at 0.097 followed by the FAA policy from 2018 to 2019 at 0.067. Table 32 reveals how these three factors and their sub-categories compared against the remaining variables. Only the FAA policy timeframe was in the top five of the 14 variables for factor influence. However, when evaluating the subcategories, the presence of any obstacle on final approach was the highest subcategory for severity of personal injury and second highest for severity of aircraft damage with a combined importance as second highest (see Table 31, Table 32, and Appendix C).

Table 31

New Variable's Factor Importance

Variable / Sub-Category	Importance for Severity of Aircraft Damage	Importance for Severity of Personal Injury	Combined Importance
Runway lighting types	0.076	0.099	0.175
FAA Visual Area Surface Policy Timeframe	0.096	0.065	0.161
Status of visual area surface penetrations	0.081	0.057	0.138
Any Obstacle Penetration	0.056	0.041	0.097
2018 – 2019 FAA Policy	0.047	0.020	0.067
20:1 Obstacle Penetration Only	0.033	0.025	0.058
2014 – 2015 FAA Policy	0.028	0.023	0.051
PAPI 2	0.026	0.024	0.050
2016 – 2017 FAA Policy	0.022	0.023	0.045
No Obstacle Penetration	0.025	0.016	0.041
34:1 Obstacle Penetration Only	0.023	0.016	0.039
PAPI 4	0.013	0.023	0.036
Approach Lighting System	0.013	0.015	0.028
No Lighting	0.010	0.016	0.026
VASI 2	0.008	0.012	0.020
VASI 4	0.005	0.010	0.015

Note. Appendix C contains all sub-categories.

Table 32

New Variable's Factor Importance Ranking

Variable / Sub-Category	Importance Ranking for Severity of Aircraft Damage	Importance Ranking for Severity of Personal Injury	Combined Ranking
Status of visual area surface penetrations	7 of 14	8 of 14	8 or 14
FAA Visual Area Surface Policy Timeframe	5 of 14	7 of 14	7 of 14
Runway lighting types	9 of 14	6 of 14	6 of 14
Any Obstacle Penetration on Approach	7 of 39 (#2 sub-category)	6 of 39 (#1 sub-category)	7 of 39 (#2 sub-category)

20:1 Obstacle Penetration Only	10 of 39	7 of 39	9 of 39
34:1 Obstacle Penetration Only	16 of 39	18 of 39	16 of 39
No Obstacle Penetration	14 of 39	17 of 39	15 of 39
2014 – 2015 FAA Policy	13 of 39	10 of 39	11 of 39
2016 – 2017 FAA Policy	19 of 39	9 of 39	14 of 39
2018 – 2019 FAA Policy	8 of 39	13 of 39	8 of 39
Approach Lighting System	23 of 39	20 of 39	22 of 39
PAPI 2	14 of 39	8 of 39	12 of 39
PAPI 4	22 of 39	11 of 39	17 of 39
VASI 2	30 of 39	24 of 39	29 of 39
VASI 4	34 of 39	25 of 39	32 of 39
No Lighting	26 of 39	15 of 39	23 if 39

Summary

Chapter IV covered the development of the database per the Chapter III methodology, SEMMA process, data cleaning, organization, and augmentation, and SVM workflow. The chapter also covered the demographic and descriptive statistics, and well as the results of the different SVM models. The last section of the chapter covered the three research questions and provided the results for each question.

For the first research question, the RBF kernel models performed the best for both the severity of aircraft damage and the severity of personal injury. The next question was answered by the top factors for the predicting the severity of aircraft damage. These were the pilot's certificate, pilot's number of flight hours, time of day, pilot's age, and the FAA's obstacle policy. Similarly, the top factors to predict the severity of personal injury were the time of day, pilot's number of flight hours, crosswind component, pilot's age, and approach runway number. Lastly, the final research question specifically evaluated the statistical findings for factor importance of the three new variables. The presence of an obstacle penetration was the first or second subcategory for influencing both SVM models.

Therefore, Chapter IV covers the results from the development of the different SVM models. Chapter V begins with discussing these results, followed by the conclusion and recommendations.

Chapter V: Discussion, Conclusions, and Recommendations

This chapter discusses the results from the development of the different SVM models to predict the severity of personal injury and severity of aircraft damage from an aircraft accident on approach and landing. The first section discusses the development, organization, cleaning, and augmentation of the dataset. The next section discusses the results from Chapter IV, including the three research questions, and is followed by the conclusion and recommendations.

Discussion

This section discusses five general areas: database organization and cleaning, the SVM model development process, and the three research questions.

Dataset Cleaning and Organization

The dataset underwent multiple types of cleaning and organization for this study. Through initial research, it was expected that the database pull from the NTSB would have approximately 2,400 accidents since general aviation alone has roughly 400 approach and landing accidents per year (AOPA, 2018; Boeing, 2019; FSF, 2017; IATA, 2016). However, the initial NTSB download had 6,806 accidents over the six-year period, which was almost triple the expected accidents.

In addition, 3,738 (54.9%) of the accidents occurred at airports without an IAP. These had to be removed because without an IAP the obstacle penetration status could not be verified. The FAA reports that 1,226 of the 5,211 public airports have close in obstacles, or 23.5% (Bureau of Transportation Statistics, 2021; FAA, n.d.-a). Therefore, the researcher considered using those airports either by either assuming all of them had obstacle penetrations or randomly assigning 23.5% of the accidents with obstacle

penetrations. However, both of these assumptions had the potential to skew the results. Therefore, all accidents at airports without an IAP were removed.

Initially, it was not surprising that 1,771 accidents were removed from the dataset because they were not applicable to this research (i.e., an accident was due to an engine failure, a pilot ran out of fuel, collided with wildlife, gear malfunction, etc.). However, there was also a significant number of accidents that had the wrong taxonomy. For example, the NTSB labeled an accident as occurring on landing when in actuality, the aircraft departed the end of the runway because the pilot's door opened during initial takeoff roll and the pilot failed to stop the aircraft on the runway (NTSB, 2015b). The NTSB also classified an accident as occurring on landing when a pilot miscalculated the fuel required resulting in fuel starvation and engine failure on route to the destination airport (NTSB, 2015a). These two accidents, and more, were listed as a taxonomy of accidents on approach and landing. This incorrect taxonomy was a large section of the removed accidents. Had the accidents at the airports that do not have at least one IAP been manually reviewed, the number of incorrect taxonomies would have been higher.

Dataset Augmentation

Data augmentation provides value to machine learning methods when the initial dataset is lopsided by increasing the size of the training partition to provide more events to train the models (Geron, 2017; Khoshgoftaar et al., 2007; Van Hulse et al., 2007). Without the augmentation, the various SVM models were taught to predict the severity of personal injury as no personal injury and the severity of aircraft damage as substantial aircraft damage (see Table 22, Table 23, Figure 17, Figure 18, and Appendix C). These initial SVM models were not realistic for the real world, nor were they generalizable.

Therefore, data augmentation of the training partition provided enough events in all four levels of severity SVM models that could predict the multi-level DV.

However, even with the positive results across the accuracy, precision, sensitivity/recall, specificity, and F1-scores of the data augmented SVM models, there was concern that the augmented dataset may lead to sampling bias, overfitting, or unrealistic SVM models. To avoid sampling bias, the dataset could not be augmented, prior to splitting into a training and test partition. This would have allowed both the training and testing datasets to have significant overlapping events and increased the possibility of overfitting (Ding et al., 2019; Lemley et al., 2017). To eliminate concerns that an augmented dataset would develop an unrealistic model, the ROS fixed method allowed the training partitions to have realistic events similar to previous researchers flipping, cropping, rotating, or blurring images to increase the dataset allowing the trained SVM models to remain generalizable and applicable to the real world (Geron, 2017; Lemley et al., 2017; Lo et al., 2021). The augmented training partition provided an advantage over the non-augmented by developing SVM models with improved accuracy over the original SVM trained models.

Therefore, to avoid developing an SVM model potentially trained and tested against the same data, avoiding sampling bias, overfitting, and an unrealistic model, the machine learning workflow did not follow the normal import of a single dataset to split into the training and test partitions in Google Colaboratory (2022) as shown in Figure 6 (Dibike et al., 2001; Geron, 2017; Jeeva, 2018; Kuhn & Johnson, 2016; Scikit-learn, 2019). Instead, the original dataset was first separated into a training and test partitions using the 80/20 split. From there, the training partition was augmented (see Figure 6).

Finally, the augmented training partition and the test partition were imported into Google Colaboratory (2022) for SVM development, training, and testing.

Using the augmented datasets provided enough training events to forge SVM models that evaluate each level of severity, thus improving the results over the original models, which had assumed the same severity level for each accident. First, the augmented dataset results were not the same for the SVM models with the linear, polynomial, sigmoid, and RBF kernels. Second, the classification reports showed a variety of results for each level of severity. SVM models, with the different kernels, all had multi-level precision, sensitivity/recall, and F1-scores (see Appendix C). Lastly, the confusion matrices showed all four levels of severity were analyzed by the SVM model and varied across the different kernels. Therefore, the augmented dataset results showed a significant improvement in predicting the four levels of severity compared to the initial datasets.

First Research Question

With the augmented dataset, the four SVM models with the different kernels were trained and tested. The SVM model using the RBF kernel performed the best at 93% (see Table 22). However, the SVM model using the polynomial kernel also well exceeded the researcher's goal of 80% accuracy with a test prediction accuracy of 92%. However, when compared side-by-side between the model with the RBF kernel and the model with the polynomial kernel, the confusion matrix shows that the polynomial kernel struggled with the severity levels of substantial and destroyed aircraft damage. Therefore, the SVM model with the RBF kernel was chosen for further optimization.

The SVM model with the Optimization D RBF kernel was selected as the highest predator of the severity of aircraft damage (see Table 24, Figure 21, and Appendix C). Not only did the 96% accuracy well exceed the researcher's threshold of 80%, but the model also had sensitivity/recall scores between 0.83 and 1.00 (see Table 26). Recall measures how well a machine learning model correctly predicts the positive outcome, the and correct level of severity. In addition, the SVM model with the RBF kernel also had precision values between 0.83 and 1.00, which means that when the model predicted a positive return, the model predicted that return correctly. With an average specificity of 0.98, the model correctly predicted when the accident was not a specific level of severity (i.e., false positives). Lastly, the confusion matrix confirms the classification report that the SVM model with the Optimization D RBF kernel accurately predicted all four levels of the severity of aircraft damage (see Figure 21 and Appendix C).

Compared to previous limited research on predicting aircraft damage, this model exceeds the 93% prediction accuracy for aircraft damage due to wildlife strikes or the 78% accuracy for bird strikes (Misra, Toppo, & Mendonca, 2022; Misra & Toppo, n.d.). The SVM model using the Optimization D RBF kernel model accuracy of 96% is also similar to previous general accident prediction modeling with accuracies between 91% and 99% (Koteeswaran et al., 2019). Therefore, the SVM with Optimization D RBF kernel prediction model successfully answered the first part of research question one.

The SVM model using the RBF kernel also had the highest prediction for the severity of personal injury at 81%, just about the researcher's threshold of 80% (see Table 23 and Appendix C). Compared to previous aviation machine learning research, where personal injury was a binary DV, accuracy percentages ranged from 70% up to

90% (Baugh, 2020; Burnett & Si, 2017). Thus, the 81% achieved in this research is between previous binary DV modeling. In addition, the results are similar to other multi-level DV modeling. Li et al. (2008, 2012) achieved an SVM precision accuracy of 83% for their multi-level DV modeling for the severity of personal injury in automobile accidents.

Even though the SVM model with RBF kernel met the threshold of 80%, nonetheless, there was room for optimization. Through adjustments to the C and gamma parameters, different optimized outcomes were examined against the training and test partitions. Each parameter was adjusted separately and then combined and fine-tuned. Table 27 shows a variety of the models that were developed. Optimization C model was chosen as the best performing model because it had the lowest C and gamma parameter values for the models that predicted at a 98% accuracy. Similar to the severity of aircraft damage, the Optimization C model classification report and confusion matrix were evaluated to ensure the model predicted all four levels of severity (see Table 28, Table 29 and Figure 24). Further optimization of the parameters led to an increase in the training accuracy, precision, sensitivity/recall, and F1-scores. However, Figure 23 and Table 27 show that these optimization models were overfitted because the results against the test partition had decreased accuracy, precision, sensitivity/recall, and F1-scores. Therefore, the Optimized C SVM model with the RBF kernel successfully answered the second part of research question one for the severity of personal injury.

Second Research Question

The second research question was to find the most important factors used in the development of the machine learning models to predict the severity of aircraft damage

and the severity of personal injury. The majority of the top five factors for both models, pilot's age, pilot's total flight time, crosswinds, runway number, and time of day, mirrored previous research (Baugh, 2020; Kushwaha & Sharma, 2014; Shappell et al., 2007; Wong et al., 2006; Wu et al., 2014). For personal injury prediction, crosswind component was third, and runway number was fifth, while these two variables were eighth and ninth for predicting aircraft damage. Two remaining factors for the model for the severity of aircraft damage were pilot certificate, which was the top factor in importance, and the FAA obstacle penetration policy, which was the fifth most important.

When reviewing the tables in Appendix C for subcategory factor importance, it is apparent that the non-categorical and non-binary variables are in the top six of both models. This raised concerns that when categorical values are changed into dummy variables, they may lose importance because the subcategories are not linked (i.e., the models do not link obstacle 20:1 penetration, obstacle 34:1 penetration, and no obstacle penetration as part of obstacle penetration status). Therefore, to evaluate a holistic view of the predictive factors, Table 33 depicts the top 10 variables, which consist of five ratio or interval variables and five nominal subcategory variables.

Table 33

Holistic Factor Importance: Top 1 through 10

Variable	Combined Factor Importance for Both Models
Pilot's Total Flight Hours	0.25582
Time of Accident	0.24984
Pilot's Age	0.22406
Crosswind Component	0.20195
Landing Runway Number	0.16916
Single-Engine Land Certificate	0.13338
Any Obstacle Penetration	0.09676
FAA Policy 2018 – 19 (final)	0.06670
FAA Policy 2014 – 15 (interim)	0.06268
20:1 Obstacle Penetration	0.05758

Note. Full results of the individual models are in Appendix C.

Therefore, the top factors for predicting both the severity of aircraft damage and the severity of personal injury are pilot's total flight hours, time of the accident, pilot's age, crosswind component, landing runway number, if the pilot had a single-engine land certificate, if the approach runway had an obstacle penetration, and the FAA visual area surface policy. The factor importance for the single-engine land certificate was similar to Boyd (2019), who stated that accidents in a single-engine aircraft were likely to result in higher injury severity.

Third Research Question

The third research question was to determine the perdition contribution and sensitivity analysis for the three new factors in predicting the severity of aircraft damage and the severity of personal injury due to aviation landing accidents. The three new factors were the presence of visual area surface penetrations for a runway, the FAA's visual area surface penetration policy timeframe, and the type of runway approach

lighting. In Table 31, when viewing the three new variables at a categorical level, the FAA policy had the highest importance among the three. FAA policy was fifth in importance for predicting aircraft damage and seventh for importance for personal injury. Obstacle penetration status was seventh for aircraft damage and eighth for personal injury. Runway lighting was ninth for aircraft damage and sixth for personal injury. However, when looking at Table 31, Table 32, Table 33, and Appendix C, the holistic predictive models, visual area surface obstacle penetration status was the seventh highest overall predictor and the second highest nominal categorical predictor. The FAA visual area surface policy was the third and fourth highest categorical factors and the overall eighth and ninth predictors. The first subcategory for runway lighting, PAPI two, was the seventh highest categorical factor.

The high importance of the visual area surface obstacle penetration aligns with the theory of inattentional blindness – missing an obstacle directly in front of a pilot. Many accident reports indicated that a pilot, from private to airline transport ratings, impacted an obstacle on final (NTSB, 2017a, 2018a, 2018b). For example, on a clear day in Missouri, an experienced commercial pilot collided with power lines half a mile from the runway (NTSB, 2017b). Even if the aircraft did not strike an obstacle, inattentional blindness might be the root of the pilot's late recognition of the obstacle causing a steep, unstable approach, resulting in an accident (NTSB, 2019a). Therefore, the factor importance of the presence of a penetration visual area surface obstacle may be linked to the pilot's inattentional blindness. This also supports AOPA's (2016) concern that any obstacle in the visual area surface was concerning and should not be allowed by FAA policy.

Conclusions

The purpose of this study was to develop a predictive model using SVM algorithms for the severity of aircraft damage and the severity of personal injury, while also evaluating three new variables. The SVM model with RBF kernel function predicted the severity of aircraft damage with 96% accuracy along with precision, sensitivity/recall, and F1-scores in the upper 90s. A second RBF kernel based SVM model predicted the severity of personal injury with 98% accuracy with high precision, sensitivity/recall, and F1-scores. The statistical findings for factor importance were evaluated for each model independently and holistically. This included evaluating three new variables due to inattentional blindness: status of visual area surface penetrations, runway lighting types, and FAA visual area surface policy timeframe.

Theoretical Contributions

This study added three new variables to aviation accident research using the theory of inattentional blindness. Similar to results from inattentional blindness and runway incursion (Kennedy et al., 2014, 2017), these results show that inattentional blindness and the presence of visual area surface penetrations are important factors in predicting the severity of aviation accidents. This study fills the gap in aviation accident literature by incorporating the three new variables with previous important factors to provide a holistic model to predict the severity of aircraft damage and the severity of personal injury in aircraft approach and landing accidents. It is recommended that all three new variables are included in any future aviation accident research.

Practical Contributions

The results of this study show the importance of removing visual area surface obstacles at airports because obstacle penetration was the second highest factor of importance for a categorical variable and the seventh highest overall (see Table 33). This supports the $42 billion dollars the FAA spent at approximately 2,300 airports to remove or lower these obstacle penetrations (FAA, 2020b, 2021a, 2021b). In addition, this study supports AOPA's (2016) claim that any obstacle penetration is unsafe and should not be allowed. Since the presence of an obstacle penetration influences the severity of aircraft damage and personal injury, the FAA should prohibit all public airports from allowing a visual area surface obstacle penetration to exist. This would also support the FAA's goal to reduce general aviation accidents (General Aviation Joint Steering Committee, 2016; Performance.gov, n.d.).

However, the money spent for the installation of runway approach lighting may not significantly reduce the severity of an accident because its importance was outside the top 10. The exact reason is unknown; however, the installation of approach runway lighting may actually increase the severity of aircraft damage and personal injury because the pilot or flight crew may be intently focused on the approach runway lights, especially during poor visibility, and suffer from inattentional blindness missing an obstacle directly in the flight path. In addition, the VGSI may provide a false sense of security to the pilot that there are no obstacle penetrations (AVweb, 2019). The VGSI angle should be adjusted to provide a descent to the runway above any obstacles; however, the presence of a VGSI does not mean that there are no visual area surface obstacle penetrations (IFR Magazine, 2014; NBAA, 2011). Therefore, further study is recommended to determine if

runway approach lighting increases intentional blindness in pilots causing an obstacle to be missed due to a false sense of security.

Another practical contribution of this study to aviation is HFACS research on the risks of final approach and landing accidents. Similar to previous studies, this study confirmed that environmental (i.e., UTC time of accident and crosswind component), and pilot characteristics (i.e., pilot's certificate, pilot's age, and pilot's total number of flight hours) are factors that impact the severity of aviation accidents (Baugh, 2020; Kushwaha & Sharma, 2014; Shappell et al., 2007; Wong et al., 2006; Wu et al., 2014). However, none of the factors that would increase pilot task saturation on final (i.e., mission C.F.R. category, number of aircraft engines, and aircraft engine type) had high sensitivity analysis on the factor contribution. This was different from prior research that indicated that the final approach and landing had the highest task saturation on pilots and flight crews (Ancel et al., 2015; Boyd, 2019; Shappell et al., 2007; Wu, 2018). This study does not disregard a pilot's high task saturation on final approach and landing, nor does it deny the complexity of these phases of flight. Instead, the complexity may be revealed through the pilot's possible inattentional blindness towards obstacle penetrations, which is why the status of the visual area surface penetrations was one of the top categorical variables for predicting the severity of aircraft damage and personal injury.

Lastly, the goal of this study was threefold: to fill a gap in the research through the addition of three new variables, to evaluate and compare the addition of two machine learning kernels, and to evaluate severity of aviation accidents as a multi-level DV. As shown in Table 33, both the new variable of status of visual area surface penetrations and the new variable of FAA visual area surface policy timeframe were within the top 10

important factors importance and within the top five for categorical variables for influencing the prediction of the severity of aircraft damage and personal injury. The first directly contributes to the practicality of spending money to remove visual area surface obstacles and supports any FAA policy to keep these surfaces clear of obstacles. The latter supported previous research on policy and aviation maintenance accidents by showing how policy changes may impact the severity of aviation accidents (Ancel et al., 2015).

The second goal was to evaluate the RBF and sigmoid kernel against the kernels, linear and polynomial, previously used in accident prediction machine learning models (Baugh, 2020; Burnett & Si, 2017; Koteeswaran et al., 2019). Table 22 and Table 23 show how the four kernels compared in predicting the severity of aircraft damage and severity of personal injury. The RBF kernel performed best for both predictions, followed by the polynomial, linear, and sigmoid. Navlani (2019) stated that both the RBF and polynomial kernels perform well with non-linear categorical data. Linear and sigmoid perform better for binary classifications (Geron, 2017; Kuhn & Johnson, 2016; Vapnik, 1999). Therefore, this research concluded that the RBF kernel performed better in aviation accident severity prediction because of the large amount of categorical data.

The last goal of the study was to evaluate the level of severity of aviation accidents on the same multi-level as determined by the FAA (2018b; "Notification and Reporting of Aircraft Accidents or Incidents", 2020). Initially, this was not successful because of the tilted dataset toward an aviation accident culminating in no personal injury and substantial aircraft damage. However, through data augmentation, as discussed, both

SVM models were able to be developed for a multi-level DV. To prevent overfitting, the training and test partitions were separated before augmentation to allow the SVM models to be tested against fresh data and not risk accident redundancies between the two partitions. Therefore, some SVM models using the RBF kernels were subject to overfitting as the C and gamma parameters increased because the models predicted flawlessly within the training partition while undergoing lower accuracies against the training partition. However, the two models selected as the best for predicting the severity of aircraft damage and the severity of personal injury did not risk overfitting because the models had equal training and test misclassification rates, accuracies, precision, sensitivity/recall, and F1-scores (see Table 21, Table 28, Table 29, Figure 25 Figure 26, and Appendix C). Therefore, all three goals of the study were accomplished.

Limitations of the Findings

The primary limitation was that the accident had to occur in the U.S. and at an airport that had at least one IAP. There were no adverse effects by only looking at accidents in the U.S. because the accident information was able to be gathered through the NTSB database (n.d.-a), NTSB accident reports (n.d.-c), FAA's Instrument Flight Procedure Gateway website (n.d.-b), and the AirNav.com (n.d.) website. However, the limitation to airports with at least one IAP resulted in the removal of roughly half of the initial database accidents. Although this was a large amount of raw data, the inability to correctly report and code the status of the visual area surface obstacle penetration supported its removal. Even so, the results that obstacle penetrations could be problematic are still applicable to all airports regardless of whether there was an IAP or not.

Another limitation was to the initial dataset because of the heavily skewed number of aviation accidents that had substantial aircraft damage and no personal injury. Although the data augmentation was successful, it is still a limit that the initial dataset was not balanced for a multi-level DV for severity. The concern for overfitting was removed by comparing the training and test partitions to choose SVM optimized models with no overfitting issues. Therefore, both final SVM models should perform well in predicting future accident data.

Recommendations

Based on the results of this study, the following sections provide recommendations for the aviation community, aviation policymakers, accident prediction research in any industry, and future inattentional blindness and visual area surface obstacle penetration research.

Recommendations for the NTSB

It is recommended that the NTSB improve and standardize its taxonomy for aviation accidents. Almost 50% of the NTSB database had to be removed because of incorrect taxonomy, such as an aircraft accident during a takeoff abort being coded incorrectly as a landing accident (NTSB, 2015b). Incorrect taxonomy may cause problems for other accident research. Accident investigators should receive reoccurring training to standardize accident reporting and taxonomy coding. Lastly, the NTSB should add approach runway lighting type and visual area surface obstacle penetration status to its database to support future aviation accident research.

Recommendations for the FAA

Since the current visual area surface policy by the FAA was the third highest nominal subcategory, it is recommended that the FAA review the current policy and consider revising it for clarity and moving airports towards removing obstacle penetrations. In addition, per AOPA (2016) recommendations, the FAA should work with airport owners and managers to fund the removal of obstacle penetrations since this was the second highest nominal subcategory.

Recommendations for Pilot Training Material and Classes

Pilot training facilities and training manuals should incorporate the risks of inattentional blindness on approach and landing in order to provide pilots with the knowledge of the potential dangers of obstacle penetrations on final approach. Also, training should include information that a pilot must be diligent and not assume an obstacle would be easy to visually acquire.

Recommendations for Future Research Methodology

The RBF kernel outperformed the linear, polynomial, and sigmoid kernels in this study for both the severity of aircraft damage and the severity of personal injury. Previous aviation accident research only evaluated the linear or polynomial kernels (Baugh, 2020; Burnett & Si, 2017; Koteeswaran et al., 2019). However, the results show that even though the RBF kernel has not been used in aviation accident research until now, RBF, along with the polynomial kernel, are considered great kernels for non-linear data because these kernels can separate the non-linear data into a new subsequently higher dimensional space (Navlani, 2019). Jiang et al. (2016) stated that the

RBF kernel had this advantage because it had fewer parameters or numerical restrictions. The RBF equation is as follows (Vapnik, 1999):

$$K(x, x_i) = \exp\left(-\frac{||x - x_i||^2}{2\sigma^2}\right) \quad (32)$$

In Scikit-learn (2022c), the default value of σ is:

$$\sigma = \frac{1}{(\text{n\_features} * \text{X.var}())} \quad (33)$$

where:

$n\_features$ = the number of features derived from the development of the training model (Scikit-learn, 2022d).

For all of the SVM models using the RBF kernel, the defaulted kernel parameter was:

$$\sigma = \frac{1}{(38 * 0.97368)} = 0.027 \quad (34)$$

Also, Scikit-learn (2022c) defaults the value of C, the penalty parameter, at a value of 1.0. Although σ and C parameters have default settings in Scikit-learn coding, the values can be adjusted to impact the support vectors and hyperplane. Both of these parameters can be optimized either through a looping program or by manual input (Kuhn & Johnson, 2016). Therefore, it is recommended for aviation accident prediction modeling to include the RBF kernel as part of the research.

In addition, it is recommended for any accident prediction modeling, regardless of the industry, to include the RBF kernel in the research methodology. Even though this study was focused on aviation accidents, automobile and mining accidents use a similar multi-level severity of personal injury (Aliabadi et al., 2019; Li et al., 2008, 2012). However, with over two million injuries in the workplace each

year, many industries would benefit from incorporating SVM modeling with the RBF kernel in their prevention or accident research (U.S. Bureau of Labor Statistics, 2021). Moreover, the SVM models with the RBF kernel were able to handle multiple categorical variables. Through the inclusion of categorical variables, just as this research added three new categorical variables, the SVM modeling with the RBF kernel may broaden the research to allow more types of variables previously excluded. Therefore, it is recommended for all industries to use the SVM modeling with the RBF kernel because it allows the use of an enhanced multi-level DV and can be used for both predicting the severity of injuries and workplace damage.

Lastly, future aviation accident researchers should be aware of the NTSB taxonomy limitations. It is recommended not to assume that everything pulled from the NTSB database for a specific area of flight, type of accident, etc., are correct. There were numerous times a landing accident taxonomy was used even though the accident occurred while the aircraft was on departure, moving on the taxiway, or due to fuel starvations miles from an airport.

Recommendations for Future Research

Future aviation approach and landing accident research should incorporate the status of visual area surface penetrations and runway lighting types as variables. Future research may not need to incorporate the FAA visual area surface policy. However, because of the importance of this factor, this researcher recommends all industries include a variable for policy, manual, or regulation changes in future research.

It is recommended to continue to study the importance of obstacles in the visual area of an approach through a future aircraft simulator study. This would allow

for a safe environment to analyze why a pilot fails to recognize an obstacle on final approach. That future study could control different variables to examine the impact of inattentional blindness. For example, how does the size, type, color, and height of the obstruction impact pilot inattentional blindness? In addition, the simulator research could track the eye movement of the participants, analogous to previous inattentional blindness studies in radiologists and air traffic controllers (Drew et al., 2013; Imbert et al., 2014). Future simulator research could analyze how runway approach lighting and the depiction of an obstacle on the approach plate impacts the pilot in perceiving the obstacle. Therefore, it is recommended for a future study to practically evaluate the existence of obstacles on final approach and landing based on the findings from this study.

References

Agricultural Aircraft Operations, 14 C.F.R. § 137 (2020),

Airbus S.A.A. (2020). *A statistical analysis of commercial aviation accidents 1958-2019.* https://www.airbus.com/content/dam/corporate-topics/publications/safety-first/Statistical-Analysis-of-Comercial-Aviation-Accidents-1958-2019.pdf

Aircraft Owners and Pilots Association. (2018, November 11). *Accident analysis: Accident database* [Data set]. https://www.aopa.org/asf/ntsb/search_ntsb.cfm

Aircraft Owners and Pilots Association. (2016, June 2). *20 to 1 airport obstructions*. https://www.aopa.org/advocacy/advocacy-briefs/20-to-1-airport-obstructions

Albon, C. (2017, December 20). *SVC Parameters when using RBF Kernel*. https://chrisalbon.com/code/machine_learning/support_vector_machines/svc_parameters_using_rbf_kernel/

Aliabadi, M. M., Aghaei, H., Kalatpuor, O., Soltanian, A. R., & Nikravesh, A. (2019). Analysis of the severity of occupational injuries in the mining industry using a Bayesian network. *Epidemiology and Health*, *41*. https://doi.org/10.4178/epih.e2019017

Anaconda Inc. (2021). *About us.* https://www.anaconda.com/about-us

Ancel, E., Shih, A. T., Jones, S. M., Reveley, M. S., Luxhøj, J. T., & Evans, J. K. (2015). Predictive safety analytics: Inferring aviation accident shaping factors and causation. *Journal of Risk Research, 18*(4), 428-451. https://10.1080/13669877.2014.896402

AirNav.com. (n.d.). *Airport information.* http://airnav.com/airports/

Aviation Impact Reform. (2013, August 17). *UPS flight 1354 crash on approach to BHM, on 8/14/13.* http://aireform.com/ups-flight-1354-crash-on-approach-to-bhm-on-81413/

Aviation Safety Reporting System. (2021, September 20). *ASRS database online – results.* National Aeronautics and Space Administration. https://akama.arc.nasa.gov/ASRSDBOnline/QueryWizard_Results.aspx

AVweb. (2019, June 13). *Danger below MDA?* https://www.avweb.com/flight-safety/technique/danger-below-mda/

Baugh, B. S. (2020). *Predicting general aviation accidents using machine learning algorithms* (Publication No. 545) [Doctoral dissertations, Embry-Riddle

Aeronautical University]. ProQuest Dissertations and Theses Global. https://commons.erau.edu/edt/545

Berwick, R. (2003, October). An idiot's guide to support vector machines (SVMs). *MIT Education.* http://web.mit.edu/6.034/wwwbob/svm-notes-long-08.pdf

Boeing. (2019). *Statistical summary of commercial jet airplane accidents. Worldwide operations 1959–2018.* http://www.boeing.com/resources/boeingdotcom/company/about_bca/pdf/statsum.pdf

Booth, J., Margetts, B., Bryant, W., Issitt, R., Hutchinson, C., Martin, N., & Sebire, N. J. (2021). Machine learning approaches to determine feature importance for predicting infant autopsy outcome. *Pediatric and Developmental Pathology*, *24*(4), 351–360. https://doi.org/10.1177/10935266211001644

Boyd, D. D. (2019). Occupant injury severity in general aviation accidents involving excessive landing airspeed. *Aerospace Medicine and Human Performance, 90*(4), 355-361. https://doi.org/10.3357/AMHP.5249.2019

Branco, P., Torgo, L., & Ribeiro, R. P. (2015). *A Survey of predictive modelling under imbalanced distributions*. https://doi.org/10.48550/arXiv.1505.01658

Brownlee, J. (2018, May 23). A gentle introduction to k-fold cross-validation. *Machine Learning Mastery.* https://machinelearningmastery.com/k-fold-cross-validation/

Brownlee, J. (2020a, January 1). Failure of classification accuracy for imbalanced class distributions. *Machine Learning Mastery.* https://machinelearningmastery.com/failure-of-accuracy-for-imbalanced-class-distributions/

Brownlee, J. (2020b, August 20). How to calculate feature importance with Python. *Machine Learning Mastery.* https://machinelearningmastery.com/calculate-feature-importance-with-python/

Brownlee, J. (2021a, January 5). Random oversampling and undersampling for imbalanced classification. *Machine Learning Mastery.* https://machinelearningmastery.com/random-oversampling-and-undersampling-for-imbalanced-classification/

Brownlee, J. (2021b, June 2). Why optimization is important in machine learning. *Machine Learning Mastery.* https://machinelearningmastery.com/why-optimization-is-important-in-machine-learning/

Bruggers, J. (2016, November 7). Federal agency faults Bowman Field tree plan. *Courier Journal.* https://www.courier-

journal.com/story/tech/science/environment/2016/11/07/federal-agency-faults-bowman-field-tree-plan/93416316/

Bureau of Transportation Statistics (2021). *Number of U.S. airports.* United States Department of Transportation. https://www.bts.gov/content/number-us-airportsa

Burnett, R., & Si, D. (2017). Prediction of injuries and fatalities in aviation accidents through machine learning. *Proceedings of the International Conference on Compute and Data Analysis*, 60-68. https://doi.org/10.1145/3093241.3093288

Byrne, B. M. (2016). *Structural equation modeling with AMOS: Basic concepts, applications, and programming*. Routledge. https://doi.org/10.4324/9781410600219

Carpenter, S. (2001, April). Sights unseen. *American Psychological Association, 32*(4), 54. https://www.apa.org/monitor/apr01/blindness

Certification: Pilots, Flight Instructors, and Ground Instructors, 14 C.F.R. § 61 (2020).

Chen, P., & Pai, C. (2018). Pedestrian smartphone overuse and inattentional blindness: An observational study in Taipei, Taiwan. *BMC Public Health, 18*(1), 1342. https://doi.org/10.1186/s12889-018-6163-5

Dattel, A. R., Battle, A. N., Stefonetti, M. C., Bifano, M., & Majdic, K. (2015). The relationship between inattentional blindness, inattentional insensitivity, situation awareness, and performance in a driving simulator. *Proceedings of the Human Factors and Ergonomics Society Annual Meeting, 59*(1), 1356-1360. https://doi.org/10.1177/1541931215591225

Deener, S. (2013, November 26). *FAA addresses obstacles in descent paths: New guidance preserves instrument approaches*. AOPA. https://www.aopa.org/news-and-media/all-news/2013/november/26/approach-obstacle-guidance

De Luca, G. (2020, September 9). *SVM vs neural network*. Baeldung. https://www.baeldung.com/cs/svm-vs-neural-network

Dibike, Y. B., Velickov, S., Solomatine, D., & Abbott, M. B. (2001). Model induction with support vector machines: Introduction and applications. *Journal of Computing in Civil Engineering, 15*(3), 208-216. https://doi.org/10.1061/(asce)0887-3801(2001)15:3(208)

Ding, J., Li, X., Kang, X., & Gudivada, V. N. (2019). A case study of the augmentation and evaluation of training data for deep learning. *ACM Journal of Data and Information Quality, 11*(4), 1–22. https://doi.org/10.1145/3317573

Dinov, I. D. (2018). *Data science and predictive analytics.* Springer Publishing. https://doi.org/10.1007/978-3-319-72347-1

Draelos, R. (2020). *Best use of train/val/test splits.* https://glassboxmedicine.com/2019/09/15/best-use-of-train-val-test-splits-with-tips-for-medical-data/

Drew, T., Võ, M. L., & Wolfe, J. M. (2013). The invisible gorilla strikes again: Sustained inattentional blindness in expert observers. *Psychological Science, 24*(9), 1848-1853. https://doi.org/10.1177/0956797613479386

Durantin, G., Dehais, F., Gonthier, N., Terzibas, C., & Callan, D. E. (2017). Neural signature of inattentional deafness. *Human Brain Mapping, 38*(11), 5440-5455. https://doi.org/10.1002/hbm.23735

Edmonds, W. A., & Kennedy, T. D. (2017). *An applied guide to research designs: Quantitative, qualitative, and mixed methods.* Sage Publishing. https://dx.doi.org/10.4135/9781071802779.n5

Erdem, M., Boran, F. E., & Akay, D. (2016). Classification of risks of occupational low back disorders with support vector machines. *Human Factors and Ergonomics in Manufacturing & Service Industries, 26*(5), 550-558. https://doi.org/10.1002/hfm.20671

Fan, S. (2018, May 7). *Understanding the mathematics behind support vector machines.* https://shuzhanfan.github.io/2018/05/understanding-mathematics-behind-support-vector-machines/

Federal Aviation Administration. (n.d.-a). *Airport data and information portal.* https://adip.faa.gov/agis/public/#/public

Federal Aviation Administration. (n.d.-b). *Instrument flight procedures information gateway.* https://www.faa.gov/air_traffic/flight_info/aeronav/procedures/

Federal Aviation Administration. (2012). *Instrument flying handbook.* G.P.O.

Federal Aviation Administration. (2013a). *FAA tasking letter to RTCA.* https://www.rtca.org/sites/default/files/mitigation_of_obstructions_within_the_201_visual_area_surface_apprvd.pdf

Federal Aviation Administration. (2013b). *Interim policy guidance for mitigation of penetrations to the 20:1 visual area surface.* https://www.rtca.org/sites/default/files/mitigation_of_obstructions_within_the_201_visual_area_surface_apprvd.pdf

Federal Aviation Administration. (2014). *Airport design* (Advisory Circular 150/5300-13A Change 1). http://www.faa.gov/documentLibrary/media/Advisory_Circular/150-5300-13A-chg1-interactive-201907.pdf

Federal Aviation Administration. (2015). *Reminder of responsibilities for FAA personnel and airport sponsors for protecting approach and departure surfaces.* https://www.faa.gov/airports/engineering/media/policy-reminder-protecting-approach-and-departure-surfaces.pdf

Federal Aviation Administration. (2016a). *Aeronautical charting forum 16-01.* https://www.faa.gov/about/office_org/headquarters_offices/avs/offices/afx/afs/afs400/afs420/acfipg/media/booklets/ACF_16-01_Booklet.pdf

Federal Aviation Administration. (2016b). *Aircraft flying handbook* (FAA-H-8083-3B). G.P.O.

Federal Aviation Administration. (2016c). *Pilot's handbook of aeronautical knowledge.* G.P.O.

Federal Aviation Administration. (2017). *Instrument procedures handbook* (FAA-H-8083-16B). G.P.O

Federal Aviation Administration. (2018a). *Aircraft accident and incident notification, investigation, and reporting* (8020.11D). G.P.O.

Federal Aviation Administration. (2018b). *Flight procedures and airspace* (8260.19H Change 1). G.P.O.

Federal Aviation Administration. (2018c). *United States standard for terminal instrument procedures (TERPS)* (8260.3D). G.P.O.

Federal Aviation Administration. (2020a, July 16). *Aeronautical information manual.* https://www.faa.gov/air_traffic/publications/atpubs/aim_html/index.html

Federal Aviation Administration. (2020b, September 24). *U.S. Transportation Secretary Elaine L. Chao announces $335 million in infrastructure grants to America's airports.* https://www.faa.gov/newsroom/us-transportation-secretary-elaine-l-chao-announces-335-million-infrastructure-grants?newsId=25340

Federal Aviation Administration. (2021a, July 15). *Airport Improvement Program (AIP) grant histories.* https://www.faa.gov/airports/aip/grant_histories/

Federal Aviation Administration. (2021b, August 19). *Airport rescue grants.* https://www.faa.gov/airports/airport_rescue_grants/

Federal Aviation Administration. (2021c, September). *Federal Aviation Administration: FY 2022 portfolio of goals.* https://www.faa.gov/sites/faa.gov/files/2022-04/fy22_portfolio_goals.pdf

Federal Funding of Visual Glideslope Indicators, 50 Feb. Reg. 34574 (August 26, 1985).

Flight Safety Foundation. (2017). *Go-around decision-making and execution project*. https://flightsafety.org/toolkits-resources/go-around-project-final-report/

Franchitti, J. (n.d.). *Cloud-Based machine and deep learning, Session 5: Supervised machine learning algorithms* [PowerPoint slides]. New York University. http://www.nyu.edu/classes/jcf/CSCI-GA.3033-010_sp19/slides/session5/SupervisedMachineLearningAlgorithms.pdf

Gandhi, R. (2018, June 7). *Support vector machine – Instruction to machine learning algorithms.* https://towardsdatascience.com/support-vector-machine-introduction-to-machine-learning-algorithms-934a444fca47

Gannon, P. (2009, July 2). FAA rules mean family's trees must come down. *Star News*. https://www.starnewsonline.com/article/NC/20090702/News/605058599/WM

General Aviation Joint Steering Committee. (2016, March). *Charter.* https://www.gajsc.org/wordpress/wp-content/uploads/2016/03/GAJSC-Charter-3.10.16.pdf

General Definitions, 14 C.F.R. § 1.1. (2020).

General Operating and Flight Rules, 14 C.F.R. § 91 (2017).

Geron, A. (2017). *Hands-on machine learning with Scikit-learn, keras, and tensorflow: Concepts, tools, and techniques to build intelligent systems*. O`Reilly.

Google. (2022). *Google Colaboratory* [Computer software]. https://colab.research.google.com/?utm_source=scs-index

Gupta, P., & Sehgal, N. K. (2021). *Introduction to machine learning in the cloud with Python: Concepts and practices*. Springer.

Hair, J. F., Black, W. C., Babin, B. J., & Anderson, R. E. (2010). *Multivariate data analysis* (7th ed.). Prentice-Hall.

Harris, D. (2011). *Human performance on the flight deck.* Ashgate.

Hart, G. (2018, April 28). Airport has tree problem. *Adirondack Daily Enterprise.* https://www.adirondackdailyenterprise.com/news/local-news/2018/04/airport-has-tree-problem/

Hastie, T., Tibshirani, R., & Friedman, J. (2008). *The elements of statistical learning.* Springer. https://doi.org/10.1007/b94608

Hayati, M., Muthmainah, S., & Ghufran, S. (2021). Random and synthetic over-sampling approach to resolve data imbalance in classification. *International Journal of Artificial Intelligence Research. 4*(2), 86. http://dx.doi.org/10.29099/ijair.v4i2.152

Horstmann, G., & Ansorge, U. (2016). Surprise capture and inattentional blindness. *Cognition, 157*, 237-249. https://doi.org/10.1016/j.cognition.2016.09.005

Huddleston, J. (2012, August 1). Fly the plate and you won't get hurt. *AINonline.* https://www.ainonline.com/aviation-news/aviation-international-news/2012-08-01/fly-plate-and-you-wont-get-hurt

IBM. (n.d.). *SPSS statistics software* [Computer software]. https://www.ibm.com/SPSS/Software

IBM. (2020). *Machine learning with Python* [Computer software]. https://www.coursera.org/learn/machine-learning-with-python

IFR Magazine. (2014, July 30). *Visual Area Protection.* https://www.ifr-magazine.com/system/visual-area-protection/

Igel, C., Heidrich-Meisner, V., & Glasmachers, T. (2008). Shark. *Journal of Machine Learning Research*, 9, 993-996. http://image.diku.dk/shark/sphinx_pages/build/html/rest_sources/tutorials/algorithms/svmModelSelection.html

Imbert, J., Hodgetts, H. M., Parise, R., Vachon, F., Dehais, F., & Tremblay, S. (2014). Attentional costs and failures in air traffic control notifications. *Ergonomics, 57*(12), 1817-1832. https://doi.org/10.1080/00140139.2014.952680

International Air Transportation Association. (2016). *Unstable approaches: Risk mitigation policies, procedures and best practices*.

International Civil Aviation Organization. (2018). *Aerodrome design and operations.* (Annex 14, Vol 1).

Jeeva, M. (2018, September 15). *The scuffle between two algorithms – Neural networks vs. support vector machine.* https://medium.com/analytics-vidhya/the-scuffle-between-two-algorithms-neural-network-vs-support-vector-machine-16abe0eb4181

Jiang, M., Luo, J., Jiang, D., Xiong, J., Song, H., & Shen, J. (2016). A cuckoo search-support vector machine model for predicting dynamic measurement errors of sensors. *IEEE Access, 4*, 5030-5037. https://doi.org/10.1109/access.2016.2605041

Jiang, Y., Liu, Y., Liu, D., & Song, H. (2020). Applying machine learning to aviation big data for flight delay prediction. *IEEE International Conference on Cloud and Big Data Computing,* 665-672. https://doi.org/10.1109/dasc-picom-cbdcom-cyberscitech49142.2020.00114

Kennedy, Q., Taylor, J. L., Reade, G., & Yesavage, J. A. (2010). Age and expertise effects in aviation decision-making and flight control in a flight simulator. *Aviation, Space, and Environmental Medicine, 81*(5), 489–497. https://doi.org/10.3357/ASEM.2684.2010

Kennedy, K. D., Stephens, C. L., Williams, R. A., & Schutte, P. C. (2014). Automation and inattentional blindness in a simulated flight task. *Proceedings of the Human Factors and Ergonomics Society Annual Meeting, 58*(1), 2058-2062. https://doi.org/10.1177/1541931214581433

Kennedy, K. D., Stephens, C. L., Williams, R. A., & Schutte, P. C. (2017). Repeated induction of inattentional blindness in a simulated aviation environment. *Proceedings of the Human Factors and Ergonomics Society Annual Meeting, 61*(1), 1959-1963. https://doi.org/10.1177/1541931213601969

Khoshgoftaar, T. M., Seiffert, C., Van Hulse, J., Napolitano, A., & Folleco, A. (2007). Learning with limited minority class data. *Sixth International Conference on Machine Learning and Applications (ICMLA 2007)*, 348–353. https://doi.org/10.1109/ICMLA.2007.76

Kohli, S. (2019, November 17). *Understanding a classification report for your machine learning model.* https://medium.com/@kohlishivam5522/understanding-a-classification-report-for-your-machine-learning-model-88815e2ce397

Korstanje, J. (2021, August 29). SMOTE. *Towards Data Science.* https://towardsdatascience.com/smote-fdce2f605729

Koteeswaran, S., Malarvizhi, N., Kannan, E., Sasikala, S., & Geetha, S. (2019). Data mining application on aviation accident data for predicting topmost causes for accidents. *Cluster Computing, 22*(S5), 11379-11399. https://10.1007/s10586-017-1394-2

Kreitz, C., Furley, P., Memmert, D., & Simons, D. J. (2015). Inattentional blindness and individual differences in cognitive abilities. *PloS One, 10*(8), e0134675. https://doi.org/10.1371/journal.pone.0134675

Kreitz, C., Hüttermann, S., & Memmert, D. (2020). Distance is relative: Inattentional blindness critically depends on the breadth of the attentional focus. *Consciousness and Cognition, 78*. https://doi.org/10.1016/j.concog.2020.102878

Kreitz, C., Schnuerch, R., Gibbons, H., & Memmert, D. (2015). Some see it, some don't: Exploring the relation between inattentional blindness and personality factors. *PloS One, 10*(5), e0128158. https://doi.org/10.1371/journal.pone.0128158

Kuhn, M., & Johnson, K. (2016). *Applied predictive modeling*. Springer. https://doi.org/10.1007/978-1-4614-6849-3

Kuhn, G., Tatler, B. W., Findlay, J. M., & Cole, G. G. (2008). Misdirection in magic: Implications for the relationship between eye gaze and attention. *Visual Cognition*, *16*(2-3), 391–405. https://doi.org/10.1080/13506280701479750

Kuhn, G., & Tatler, B. W. (2005). Magic and fixation: Now you don't see it, now you do. *Perception*, *34*(9), 1155-1161. https://doi.org/10.1068/p3409bn1

Kuhn, G., & Tatler, B. W. (2011). Misdirected by the gap: The relationship between inattentional blindness and attentional misdirection. *Consciousness and Cognition, 20*(2), 432-436. https://doi.org/10.1016/j.concog.2010.09.013

Kumar, A. (2018, December 17). *C and gamma in SVM*. https://medium.com/@myselfaman12345/c-and-gamma-in-svm-e6cee48626be

Kushwaha, M., & Sharma, S. K. (2014). Impact of environmental factors on aviation safety. *Advances in Aerospace Science and Applications, 4*(1), 73-78. https://www.ripublication.com/aasa-spl/aasav4n1spl_12.pdf

Lebar, G. G. (2016, June 17). *2016 Maryland aviation conference* [PowerPoint slides]. https://www.marylandairportmanagers.org/wp-content/uploads/2016/06/2016-Maryland-Aviation-Conference-20-1-for-Industry.pptx

Leevy, J. L., Khoshgoftaar, T. M., Bauder, R. A., & Seliya, N. (2018). A survey on addressing high-class imbalance in big data. *Journal of Big Data*, *5*(1), 1–30. https://doi.org/10.1186/s40537-018-0151-6

Lemley, J., Bazrafkan, S., & Corcoran, P. (2017). Smart Augmentation - Learning an optimal data augmentation strategy. arXiv.org. https://doi.org/10.1109/ACCESS.2017.2696121

Li, X., Lord, D., Zhang, Y., & Xie, Y. (2008). Predicting motor vehicle crashes using support vector machine models. *Accident Analysis and Prevention, 40*(4), 1611-1618. https://doi.org/10.1016/j.aap.2008.04.010

Li, Z., Liu, P., Wang, W., & Xu, C. (2012). Using support vector machine models for crash injury severity analysis. *Accident Analysis and Prevention, 45*, 478-486. https://doi.org/10.1016/j.aap.2011.08.016

Liu, D., Nickens, T., Hardy, L., & Boquet, A. (2013). Effect of HFACS and non-HFACS-related factors on fatalities in general aviation accidents using neural networks. *The International Journal of Aviation Psychology, 23*(2), 153-168. https://doi.org/10.1080/10508414.2013.772831

Lin, H. T., & Lin, C. J. (2003). *A study on sigmoid kernels for SVM and the training of non-PSD kernels by SMO-type methods.* http://www.kernel-machines.org/papers/upload_28756_tanh.pdf

Lo, J., Cardinell, J., Costanzo, A., & Sussman, D. (2021). Medical augmentation (med-a) for optimal data augmentation in medical deep learning networks. *Sensors* (Basel, Switzerland), *21*(21). https://doi.org/10.3390/s21217018

Lyte, B. (2014, April 12). Trees return as Westchester airport issue. *Stamford Advocate.* https://www.stamfordadvocate.com/local/article/Trees-return-as-Westchester-airport-issue-5398369.php

Mack, A., & Rock, I. (1998). *Inattentional blindness*. MIT Press. https://doi.org/10.7551/mitpress/3707.001.0001

Malik, U. (2022). Random forest algorithm with python and Scikit-learn. *Stack Abuse.* https://stackabuse.com/random-forest-algorithm-with-python-and-scikit-learn/

Marius, H. (2020, June 9). Multiclass classification with support vector machines (SVM), dual problem and kernel functions. *Towards Data Science.* https://towardsdatascience.com/multiclass-classification-with-support-vector-machines-svm-kernel-trick-kernel-functions-f9d5377d6f02

Martin, S. (2020, November 17). The incorrect short field landing technique resulted in a runway overrun. *Boldmethod.* https://www.boldmethod.com/learn-to-fly/maneuvers/incorrect-short-field-landing-runway-overrun-on-landing/

Melgani, F., & Bruzzone, L. (2004). Classification of hyperspectral remote sensing images with support vector machines. *IEEE Transactions on Geoscience and Remote Sensing, 42*(8), 1778-1790. https://doi.org/10.1109/igarss.2002.1025088

Memmert, D. (2010). The gap between inattentional blindness and attentional misdirection. *Consciousness and Cognition, 19*(4), 1097-1101. https://doi.org/10.1016/j.concog.2010.01.001

Microsoft. (2021, November 4). *Normalize data component.* https://docs.microsoft.com/en-us/azure/machine-learning/component-reference/normalize-data

Misra, S., Toppo, I., & Mendonca, F. A. C. (2022). Assessment of aircraft damage due to bird strikes: A machine learning approach. *International Journal of Sustainable Aviation*, *8*(2), 136–151. https://doi.org/10.1504/IJSA.2022.122328

Misra, S., & Toppo, I. (n.d.). *Data mining techniques to predict aircraft damage levels for wildstrikes in United States* [Poster]. https://commons.erau.edu/discovery-day/db-discovery-day-2021/poster-session-grad/16/

Mohajon, J. (2020, May 28). Confusion matrix for your multi-class machine learning model. *Towards Data Science.* https://towardsdatascience.com/confusion-matrix-for-your-multi-class-machine-learning-model-ff9aa3bf7826

Moriarty, D., & Jarvis, S. (2014). A systems perspective on the unstable approach in commercial aviation. *Reliability Engineering & System Safety, 131*, 197-202. https://10.1016/j.ress.2014.06.019

Morin, D. (2007). *Chapter 6: The Lagrangian method*. Harvard University. https://scholar.harvard.edu/files/david-morin/files/cmchap6.pdf

Most, S. B. (2010). What's "inattentional" about inattentional blindness? *Consciousness and Cognition, 19*(4), 1102. https://doi.org/10.1016/j.concog.2010.01.011

Most, S. B. (2013). Setting sights higher: Category-level attentional set modulates sustained inattentional blindness. *Psychological Research, 77*(2), 139-146. https://doi.org/10.1007/s00426-011-0379-7

Most, S. B., & Astur, R. S. (2007). Feature-based attentional set as a cause of traffic accidents. *Visual Cognition, 15*(2), 125-132. https://doi.org/10.1080/13506280600959316

Most, S. B., Simons, D. J., Scholl, B. J., Jimenez, R., Clifford, E., & Chabris, C. F. (2001). How not to be seen: The contribution of similarity and selective ignoring to sustained inattentional blindness. *Psychological Science, 12*(1), 9-17. https://doi.org/10.1111/1467-9280.00303

Murphy, G., & Greene, C. M. (2015). High perceptual load causes inattentional blindness and deafness in drivers. *Visual Cognition, 23*(7), 810-814. https://doi.org/10.1080/13506285.2015.1093245

Murphy, G., & Greene, C. M. (2016). Perceptual load induces inattentional blindness in drivers. *Applied Cognitive Psychology, 30*(3), 479-483. https://doi.org/10.1002/acp.3216

Namowitz, D. (2016, June 20). *'Not authorized at night' new AOPA fact sheet explains instrument approach restriction policy.* AOPA. https://www.aopa.org/news-and-media/all-news/2016/june/20/not-authorized-at-night

Nalepa, J., & Kawulok, M. (2018, January 3). Selecting training sets for support vector machines: A review. *Artificial Intelligence Review.* https://doi.org/10.1007/s10462-017-9611-1

National Business Aviation Association. (2011, April 8). *Enhanced flight visual systems, visual glide slope indicators and approach charts.* https://nbaa.org/aircraft-operations/airspace/enhanced-flight-visual-systems-visual-glide-slope-indicators-and-approach-charts/

National Business Aviation Association. (2013, September 5). *New York LaGuardia (LGA) runway 4 ILS glideslope not available until further notice.* https://nbaa.org/aircraft-operations/airspace/regional/northeast/new-york-laguardia-lga-runway-4-ils-glideslope-not-available-until-further-notice/

National Transportation Safety Board. (n.d.-a). *Aviation accident database & synopses.* https://www.ntsb.gov/_layouts/ntsb.aviation/index.aspx

National Transportation Safety Board. (n.d.-b). *Aviation data dictionary.* https://www.ntsb.gov/_layouts/ntsb.aviation/AviationDownloadDataDictionary.aspx

National Transportation Safety Board. (n.d.-c). *Carol query.* https://data.ntsb.gov/carol-main-public/basic-search

National Transportation Safety Board. (n.d.-d). *The investigative process.* https://www.ntsb.gov/investigations/process/Pages/default.aspx

National Transportation Safety Board. (1995). *National Transportation Safety Board aircraft accident report: DCA96MA008.* http://libraryonline.erau.edu/online-full-text/ntsb/aircraft-accident-reports/AAR96-05.pdf

National Transportation Safety Board. (2015a). *National Transportation Safety Board aircraft accident report: ERA16LA007.* https://data.ntsb.gov/carol-repgen/api/Aviation/ReportMain/GenerateNewestReport/92149/pdf

National Transportation Safety Board. (2015b). *National Transportation Safety Board aircraft accident report: GAA15CA295.* https://data.ntsb.gov/carol-repgen/api/Aviation/ReportMain/GenerateNewestReport/92132/pdf

National Transportation Safety Board. (2017a). *National Transportation Safety Board aircraft accident report: CEN17FA164.* https://data.ntsb.gov/carol-repgen/api/Aviation/ReportMain/GenerateNewestReport/95050/pdf

National Transportation Safety Board. (2017b). *National Transportation Safety Board aircraft accident report: GAA17CA412.* https://data.ntsb.gov/carol-repgen/api/Aviation/ReportMain/GenerateNewestReport/95591/pdf

National Transportation Safety Board. (2017c). *National Transportation Safety Board aircraft accident report: GAA17CA484.* https://data.ntsb.gov/carol-repgen/api/Aviation/ReportMain/GenerateNewestReport/95800/pdf

National Transportation Safety Board. (2017d). *National Transportation Safety Board aircraft accident report: GAA18CA007.* https://data.ntsb.gov/carol-repgen/api/Aviation/ReportMain/GenerateNewestReport/96164/pdf

National Transportation Safety Board. (2018a). *National Transportation Safety Board aircraft accident report: GAA18CA007.* https://data.ntsb.gov/carol-repgen/api/Aviation/ReportMain/GenerateNewestReport/96164/pdf

National Transportation Safety Board. (2018b). *National Transportation Safety Board aircraft accident report: GAA18CA243.* https://data.ntsb.gov/carol-repgen/api/Aviation/ReportMain/GenerateNewestReport/97139/pdf

National Transportation Safety Board. (2019a). *National Transportation Safety Board aircraft accident report: ERA18LA096.* https://data.ntsb.gov/carol-repgen/api/Aviation/ReportMain/GenerateNewestReport/96826/pdf

National Transportation Safety Board. (2019b, September 19). *National Transportation Safety Board aviation accident preliminary report: CEN19MA312.* https://app.ntsb.gov/pdfgenerator/ReportGeneratorFile.ashx?EventID=20190911X54810&AKey=1&RType=Prelim&IType=MA

Navlani, A. (2019, December 27). *Support vector machines with Scikit-learn.* https://www.datacamp.com/community/tutorials/svm-classification-scikit-learn-python

Neisser, U. (1979). *The control of information pickup in selective looking in perception and its development: A tribute to Eleanor J. Gibson*. Erlbaum.

New, J. J., & German, T. C. (2015). Spiders at the cocktail party: An ancestral threat that surmounts inattentional blindness. *Evolution and Human Behavior, 36*(3), 165-173. https://doi.org/10.1016/j.evolhumbehav.2014.08.004

Notification and reporting of aircraft accidents or incidents and overdue aircraft, and preservation of aircraft wreckage, mail, cargo, and records, 49 C.F.R. § 830 (2020).

Oktay, B., & Cangöz, B. (2018). I thought I saw "Zorro": An inattentional blindness study. *Noro Psikiyatri Arsivi, 55*(1), 59-66. https://doi.org/10.29399/npa.19227

Olsen, N. S., & Shorrock, S. T. (2010). Evaluation of the HFACS-ADF safety classification system: Inter-coder consensus and intra-coder consistency. *Accident Analysis & Prevention, 42*(2), 437-44. https://doi.org/10.1016/j.aap.2009.09.005

Operations: Foreign Air Carriers and Foreign Operators of U.S. Registered Aircraft Engaged in Common Carriage, 14 C.F.R. § 129 (2020).

Operating Requirements: Commuter and On Demand Operations and Rules Governing Persons On Board Such Aircraft, 14 C.F.R. § 135 (2020).

Operating Requirements: Domestic, Flag, and Supplemental Operations, 14 C.F.R. § 121 (2020).

Pai, C. (2016). Texting and walking: A controlled field study of crossing behaviours and inattentional blindness in Taiwan. *Injury Prevention, 22*. https://doi.org/10.1136/injuryprev-2016-042156.751

Pammer, K., Sabadas, S., & Lentern, S. (2018). Allocating attention to detect motorcycles: The role of inattentional blindness. *Human Factors: The Journal of Human Factors and Ergonomics Society, 60*(1), 5-19. https://doi.org/10.1177/0018720817733901

Parikh, R., Parikh, S., Arun, E., & Thomas, R. (2009). Likelihood ratios: clinical application in day-to-day practice. *Indian Journal of Ophthalmology*, *57*(3), 217–221. https://doi.org/10.4103/0301-4738.49397

Pedregosa, F., Varoquaux, G., Gramfort, A., Michel, V., Thirion, B., Grisel, O., Blondel, M., Prettenhofer, P., Weiss, R., Dubourg, V., Vanderplas, J., Passos, A., Cournapeau, D., Brucher, M., Perrot, M., & Duchesnay, E. (2011). Scikit-learn: Machine learning in Python. *Journal of Machine Learning Research*, *12*(10), 2825–2830. https://www.jmlr.org/papers/volume12/pedregosa11a/pedregosa11a.pdf

Performance.gov. (n.d.). *Reduce the rate of aviation accidents.* https://obamaadministration.archives.performance.gov/content/reduce-rate-aviation-accidents-0.html#progressUpdate

Phy, V. (2019, December 9). Accuracy is not enough for classification tasks. *Towards Data Science.* https://towardsdatascience.com/accuracy-is-not-enough-for-classification-task-47fca7d6a8ec

Prem. (2021, February 15). Which is better – Random forest vs support vector machine vs neural network. *Iunera.* https://www.iunera.com/kraken/fabric/random-forest-vs-support-vector-machine-vs-neural-network/

Pugnaghi, G., Memmert, D., & Kreitz, C. (2019). Examining effects of preconscious mere exposure: An inattentional blindness approach. *Consciousness and Cognition, 75*. https://doi.org/10.1016/j.concog.2019.102825

Pugnaghi, G., Memmert, D., & Kreitz, C. (2020). Loads of unconscious processing: The role of perceptual load in processing unattended stimuli during inattentional blindness. *Attention, Perception & Psychophysics.* https://doi.org/10.3758/s13414-020-01982-8

Roelfsema, P. R., Lamme, V. A. F., & Spekreijse, H. (2000). The implementation of visual routines. *Vision Research, 40*(10), 1385-1411. https://doi.org/10.1016/s0042-6989(00)00004-3

Ronaghan, S. (2018, May 11). The mathematics of decision trees, random forest and feature importance in scikit-learn and spark. *Towards Data Science.* https://towardsdatascience.com/the-mathematics-of-decision-trees-random-forest-and-feature-importance-in-scikit-learn-and-spark-f2861df67e3#:~:text=Feature%20importance%20is%20calculated%20as,the%20more%20important%20the%20feature.

Radio Technical Commission for Aeronautics. (2014). *Mitigation of obstructions within the 20:1 visual area surface.* https://www.rtca.org/wp-content/uploads/2021/08/TOC-Final-Reports-1.zip

Radio Technical Commission for Aeronautics. (2016). *Meeting summary to the Tactical Operations Committee (TOC).* https://www.rtca.org/wp-content/uploads/2020/08/toc_march_2016_summary.pdf

Ryser, R. (2016, July 26). Tree removal on private lots near Danbury Airport to cost $1 million. *News-Times*. https://www.newstimes.com/local/article/Tree-removal-on-private-lots-near-Danbury-Airport-8425159.php

Saini, A. (2021, October 19). An introduction to random forest algorithm for beginners. *Analytics Vidhya.* https://www.analyticsvidhya.com/blog/2021/10/an-introduction-to-random-forest-algorithm-for-beginners/

Sánchez-González, B., Barja, I., Piñeiro, A., Hernández-González, M. C., Silván, G., Illera, J. C., & Latorre, R. (2018). Support vector machines for explaining

physiological stress response in wood mice (apodemus sylvaticus). *Scientific Reports, 8*(1). https://doi.org/10.1038/s41598-018-20646-0

Saryazdi, R., Bak, K., & Campos, J. L. (2019). Inattentional blindness during driving in younger and older adults. *Frontiers in Psychology, 10*. https://doi.org/10.3389/fpsyg.2019.00880

Safe, efficient se, and preservation of the navigable airspace, 14 C.F.R. § 77 (2020).

SAS Institute. (n.d.). *Measuring prediction error.* https://documentation.sas.com/?docsetId=emhpprcref&docsetVersion=14.2&docsetTarget=emhpprcref_hpforest_details16.htm&locale=en

SAS Institute. (2013). *Data mining from A to Z: Better insights, new opportunities.* http://www.datascienceassn.org/sites/default/files/Data%20Mining%20from%20A%20to%20Z.pdf

SAS Institute. (2020, February 5). *Data mining and SEMMA.* http://support.sas.com/documentation/cdl/en/emcs/66392/HTML/default/viewer.htm#n0pejm83csbja4n1xueveo2uoujy.htm

Schott, M. (2019, April 25). Random forest algorithm for machine learning. *Capital One Tech.* https://medium.com/capital-one-tech/random-forest-algorithm-for-machine-learning-c4b2c8cc9feb

Scikit-learn. (2019). *3.1. Cross-validation: Evaluating estimator performance*. https://scikit-learn.org/stable/modules/cross_validation.html

Scikit-learn. (2020). *1.4. Support vector machines.* https://scikit-learn.org/stable/modules/svm.html

Scikit-learn. (2021, March 7). *Confusion matrix.* https://scikit-learn.org/stable/modules/generated/sklearn.metrics.confusion_matrix.html

Scikit-learn. (2022a, May 27). *Classification report.* https://scikit-learn.org/stable/modules/generated/sklearn.metrics.classification_report.html

Scikit-learn. (2022b, June 15). *Feature importances with a forest of trees.* https://scikit-learn.org/stable/auto_examples/ensemble/plot_forest_importances.html

Scikit-learn. (2022c, June 2). *Sklearn.svm.SVC.* https://scikit-learn.org/stable/modules/generated/sklearn.svm.SVC.html

Scikit-learn. (2022d, June 2). *RBF SVM parameters.* https://scikit-learn.org/stable/auto_examples/svm/plot_rbf_parameters.html

Shappell, S., Detwiler, C., Holcomb, K., Hackworth, C., Boquet, A., & Wiegmann, D. A. (2007). Human error and commercial aviation accidents: An analysis using the human factors analysis and classification system. *Human Factors, 49*(2), 227-242. https://10.1518/001872007X312469

Shen, K. Q., Ong, C. J., Li, X. P., & Wilder-Smith, E. P. V. (2007). Feature selection via sensitivity analysis of SVM probabilistic outputs. *Machine Learning*, *70*(1), 1–20. https://doi.org/10.1007/s10994-007-5025-7

Shen, Z., Pan, G., & Yan, Y. (2020). A high-precision fatigue detecting method for air traffic controllers based on revised fractal dimension feature. *Mathematical Problems in Engineering.* https://10.1155/2020/4563962

Shmueli, G., Bruce, P. C., & Patel, N. R. (2016). *Data mining for business analytics: Concepts, techniques, and applications with XLMiner.* John Wiley & Sons, Inc.

Simons, D. J., & Chabris, C. F. (1999). Gorillas in our midst: Sustained inattentional blindness for dynamic events. *Perception, 28*(9), 1059-1074. https://doi.org/10.1068/p281059

Sofaer, H. R., Hoeting, J. A., & Jarnevich, C. S. (2019). The area under the precision-recall curve as a performance metric for rare binary events. *Methods in Ecology and Evolution*, *10*(4), 565–577. https://doi.org/10.1111/2041-210X.13140

Stecanella, B. (2017, June 22). An introduction to support vector machines (SVM). *MonkeyLearn*. https://monkeylearn.com/blog/introduction-to-support-vector-machines-svm/#:~:text=A%20support%20vector%20machine%20(SVM,on%20a%20text%20classification%20problem

Stothart, C. R., Wright, T. J., Simons, D. J., & Boot, W. R. (2017). The costs (or benefits) associated with attended objects do little to influence inattentional blindness. *Acta Psychologica, 173*, 101-105. https://doi.org/10.1016/j.actpsy.2016.12.012

Strobl, C., Boulesteix, A. L., Zeileis, A., & Hothorn, T. (2007). Bias in random forest variable importance measures: Illustrations, sources and a solution. *BMC Bioinformatics, 8*(25). https://doi.org/10.1186/1471-2105-8-25

Tatler, B. W., & Kuhn, G. (2007). Chapter 33 - Don't look now: The magic of misdirection. In R. P.G. Van Gompel, M. H. Fischer, ... R. L. Hill (Eds.) *Eye movement research: Insights into mind and brain* (pp. 697-714). Elsevier. https://doi.org/10.1016/b978-008044980-7/50035-5

Ullman, S. (1996). *High-level vision: Object recognition and visual cognition*. MIT Press. https://doi.org/10.7551/mitpress/3496.001.0001

U.S. Bureau of Labor Statistics. (2021, November 03). *Employer-Reported workplace injuries and illnesses, 2020.* United States Department of Labor. https://www.bls.gov/news.release/osh.nr0.htm

Valdés, R. A., Comendador, F. G., Gordún, L. M., & Sáez Nieto, F. J. (2011). The development of probabilistic models to estimate accident risk (due to runway overrun and landing undershoot) applicable to the design and construction of runway safety areas. *Safety Science, 49*(5), 633-650. https://doi.org/10.1016/j.ssci.2010.09.020

Van Hulse, J., Khoshgoftaar, T. M., & Napolitano, A. (2007). Experimental perspectives on learning from imbalanced data. *ACM International Conference Proceeding Series; Vol. 227: Proceedings of the 24th International Conference on Machine Learning; 20-24 June 2007*, 935–942. https://doi.org/10.1145/1273496.1273614

Vapnik, V. N. (1999, September 5). An overview of statistical learning theory. *IEEE Transaction on Neural Networks, 10*(5), 988-999. https://doi.org/10.1109/72.788640

Varghese, D. (2018, December 6). Comparative study on classic machine learning algorithms. *Towards Data Science.* https://towardsdatascience.com/comparative-study-on-classic-machine-learning-algorithms-24f9ff6ab222

Wang, C. (2014). Optimization of SVM Method with RBF kernel. *Applied Mechanics and Materials,496-500*, 2306–2310. https://doi.org/10.4028/www.scientific.net/AMM.496-500.2306

Wang, L., Ren, Y., & Wu, C. (2018). Effects of flare operation on landing safety: A study based on ANOVA of real flight data. *Safety Science, 102*, 14-25. https://doi.org/10.1016/j.ssci.2017.09.027

Webster, K., Clarke, J., Mack, A., & Ro, T. (2018). Effects of canonical color, luminance, and orientation on sustained inattentional blindness for scenes. *Attention, Perception, & Psychophysics, 80*(7), 1833-1846. https://doi.org/10.3758/s13414-018-1558-z

Wood, K., & Simons, D. J. (2019). Now or never: Noticing occurs early in sustained inattentional blindness. *Royal Society Open Science, 6*(11). https://doi.org/10.1098/rsos.191333

Wong, D. K. Y., Pitfield, D. E., Caves, R. E., & Appleyard, A. J. (2006). Quantifying and characterizing aviation accident risk factors. *Journal of Air Transport Management, 12*(6), 352-357. https://10.1016/j.jairtraman.2006.09.002

Wright, T. J., Roque, N. A., Boot, W. R., & Stothart, C. (2018). Attention capture, processing speed, and inattentional blindness. *Acta Psychologica, 190*, 72-77. https://doi.org/10.1016/j.actpsy.2018.07.005

Wu, Y. R., Xu, J. H., Ren, X. H., & Duanmu, J. S. (2014). Aviation human factors accident causation model based on structure entropy. *Applied Mechanics and Materials, 488-489*, 1354-1357. https://10.4028/www.scientific.net/AMM.488-489.1354

Yang, J., Liu, L., Zhang, L., Li, G., Sun, Z., & Song, H. (2019). Prediction of marine pycnocline based on kernel support vector machine and convex optimization technology. *Sensors (Basel, Switzerland), 19*(7), 1562. https://doi.org/10.3390/s19071562

Yildirim, S. (2020, February 11). Decision trees and random forests – Explained. *Towards Data Science.* https://towardsdatascience.com/decision-tree-and-random-forest-explained-8d20ddabc9dd

Zhang, H., Yan, C., Zhang, X., & Fang, J. (2018). Sustained inattentional blindness does not always decrease with age. *Frontiers in Psychology, 9*. https://doi.org/10.3389/fpsyg.2018.01390

Zhao, Z. W., Wei, P., Fang, P., Zhang, X., Yan, N., Liu, W., Zhao, H., & Wu, Q. (2022). Classification of Zambian grasslands using random forest feature importance selection during the optimal phenological period. *Ecological Indicators*, *135*. https://doi.org/10.1016/j.ecolind.2021.108529

Zhou, D., Zhuang, X., Zuo, H., Wang, H., & Yan, H. (2020). Deep learning-based approach for civil aircraft hazard identification and prediction. *IEEE Access, 8*, 103665-103683. https://10.1109/ACCESS.2020.2997371

Appendix A

Data Collection Device - Instrument Approach Procedure Forms and Chart

Example IAP Forms and chart at KMBY, Omar N Bradley Airport, Missouri.

Arrows point to the information used to help collect the dataset (FAA, n.d.-b).

FEDERAL AVIATION ADMINISTRATION

FLIGHT STANDARDS SERVICE

RNAV (GPS) STANDARD INSTRUMENT APPROACH PROCEDURE

TITLE 14 CFR PART 97.33

Bearings, headings, courses, tracks and radials are magnetic. Elevations and altitudes are in feet, MSL, except HAT, HAA, TCH, and RA. Altitudes are minimum altitudes unless otherwise indicated. Ceilings are in feet above airport elevation. Distances are in nautical miles unless otherwise indicated, except visibilities which are in statute miles or feet RVR.

AIRPORT	AIRPORT ID	PROCEDURE NAME	ORIGINAL/AMENDMENT	CITY	STATE
OMAR N BRADLEY	KMBY	RNAV (GPS) RWY 31	ORIG-B	MOBERLY	MO

AIRPORT ELEVATION	TDZE	SUPERSEDED	ORIGINAL/AMENDMENT	DATED	MAG VAR	EPOCH YEAR
867	867	RNAV (GPS) RWY 31	ORIG-A	05/28/2015	1E	2010

FACILITY	COORDINATES OF FACILITIES	ACTUAL EFFECTIVE DATE	REQUIRED EFFECTIVE DATE	CANCEL/SUSPEND
RNAV		15 AUGUST 2019	ROUTINE	

TERMINAL ROUTES

FROM	FIX TYPE	TO	FIX TYPE	LEG TYPE	FO/FB	RNP	COURSE	DISTANCE	ALTITUDE
ALHAH	IAF	VETTS	NOPT	TF	FB	1.00	253.04	23.98	3100
HLV VORTAC	IAF	VETTS	NOPT	TF	FB	1.00	338.73	14.49	3100
VETTS	IF/IAF	REWAK		TF	FB	1.00	308.84	6.02	2500
REWAK	FAF	CASAS/1.70 NM TO RW31		TF	FB	0.30	308.77	3.33	
CASAS/1.70 NM TO RW31		RW31	MAP	TF	FO	0.30	308.77	1.70	
RW31	MAP	1117 MSL		CA			308.77		
1117 MSL		DRADE		DF	FO	1.00			2900

MISSED APPROACH

MAP:
LPV: DA
LNAV/VNAV: DA
LNAV: RW31

MISSED APPROACH INSTRUCTIONS:
CLIMB TO 2900 DIRECT DRADE AND HOLD.

ALTERNATE MISSED APPROACH INSTRUCTIONS:

QUALITY 6 CHECKED

AIRPORT	AIRPORT ID	PROCEDURE NAME	ORIGINAL/AMENDMENT	CITY	STATE
OMAR N BRADLEY	KMBY	RNAV (GPS) RWY 31	ORIG-B	MOBERLY	MO

PROFILE:

1. PT **SIDE OF COURSE** **OUTBOUND** **FT WITHIN** **MILES OF** (IAF)

2. HOLD SE VETTS, RT, 308.84 INBOUND, 3100 FT. IN LIEU OF PT (IAF), MAX 6000.

3. FAC: 308.77 **FAF:** REWAK **DIST FAF TO MAP:** 5.03 **DIST FAF TO THLD:** 5.03

4. MIN ALT: VETTS 3100, REWAK 2500, CASAS/1.70 NM TO RW31 1420*

5. DIST TO THLD FROM OM: **MM:** **IM:** **150 HAT:** **250 HAT:** 0.69 **GS ANT:**

6. MIN GP INCPT: 2500 **GP ALT AT FAF :** REWAK 2500 **OM:** **MM:** **IM:**

7. GP ANGLE: 3.00 **34:1:** IS NOT CLEAR **20:1:** IS CLEAR **TCH:** 37.0

8. MSA FROM: RW31 3100

PBN REQUIREMENTS NOTE:

RNP APCH.

NOTES:

CHART NOTE: CIRCLING TO RWY 5, 23 NA AT NIGHT.
CHART NOTE: RWY 31 HELICOPTER VISIBILITY REDUCTION BELOW 3/4 SM NOT AUTHORIZED.
CHART NOTE: BARO-VNAV NA WHEN USING COLUMBIA ALTIMETER SETTING.
CHART NOTE: FOR UNCOMPENSATED BARO-VNAV SYSTEMS, LNAV/VNAV NA BELOW -16°C OR ABOVE 54°C.
CHART NOTE: VDP NA WHEN USING COLUMBIA ALTIMETER SETTING.
CHART PLANVIEW NOTE: PROCEDURE NA FOR ARRIVAL ON HLV VORTAC AIRWAY RADIALS 270 CW 036.
CHART NOTE: WHEN LOCAL ALTIMETER SETTING NOT RECEIVED, USE COLUMBIA ALTIMETER SETTING: INCREASE LPV DA TO 1212 FEET AND ALL VISIBILITIES 1/8 SM; INCREASE LNAV/VNAV DA TO 1278 FEET AND ALL VISIBILITIES 1/4 SM; INCREASE ALL MDA 100 FEET AND VISIBILITY CAT C 1/4 SM.

ADDITIONAL FLIGHT DATA:

CHART VDP AT 1.20 NM TO RW31*
*LNAV ONLY
WAAS CHANNEL #61321
REFERENCE PATH ID: W31A
CHART FAS OBST: 1013 TOWER 392649N/0922450W.
HOLD NW, RT, 128.59 INBOUND
LTP HAE: 230.3 M

MINIMUMS:
TAKEOFF: SEE FAA FORM 8260-15A FOR THIS AIRPORT

ALTERNATE: NA [X]

CATEGORY:	A			B			C			D			E		
FINAL TYPE	DA/MDA	VIS	HAT/HAA	DA/MDA	VIS	HAT/HAA	DA/MDA	VIS	HAT/HAA	DA/MDA	VIS	HAT/HAA	DA/MDA	VIS	HAT/HAA
LPV DA	1117	7/8	250	1117	7/8	250	1117	7/8	250		NA				
LNAV/VNAV DA	1183	7/8	316	1183	7/8	316	1183	7/8	316		NA				
LNAV MDA	1280	1	413	1280	1	413	1280	1 1/8	413		NA				
CIRCLING	1420	1	553	1420	1	553	1480	1 3/4	613		NA				

QUALITY 6 CHECKED

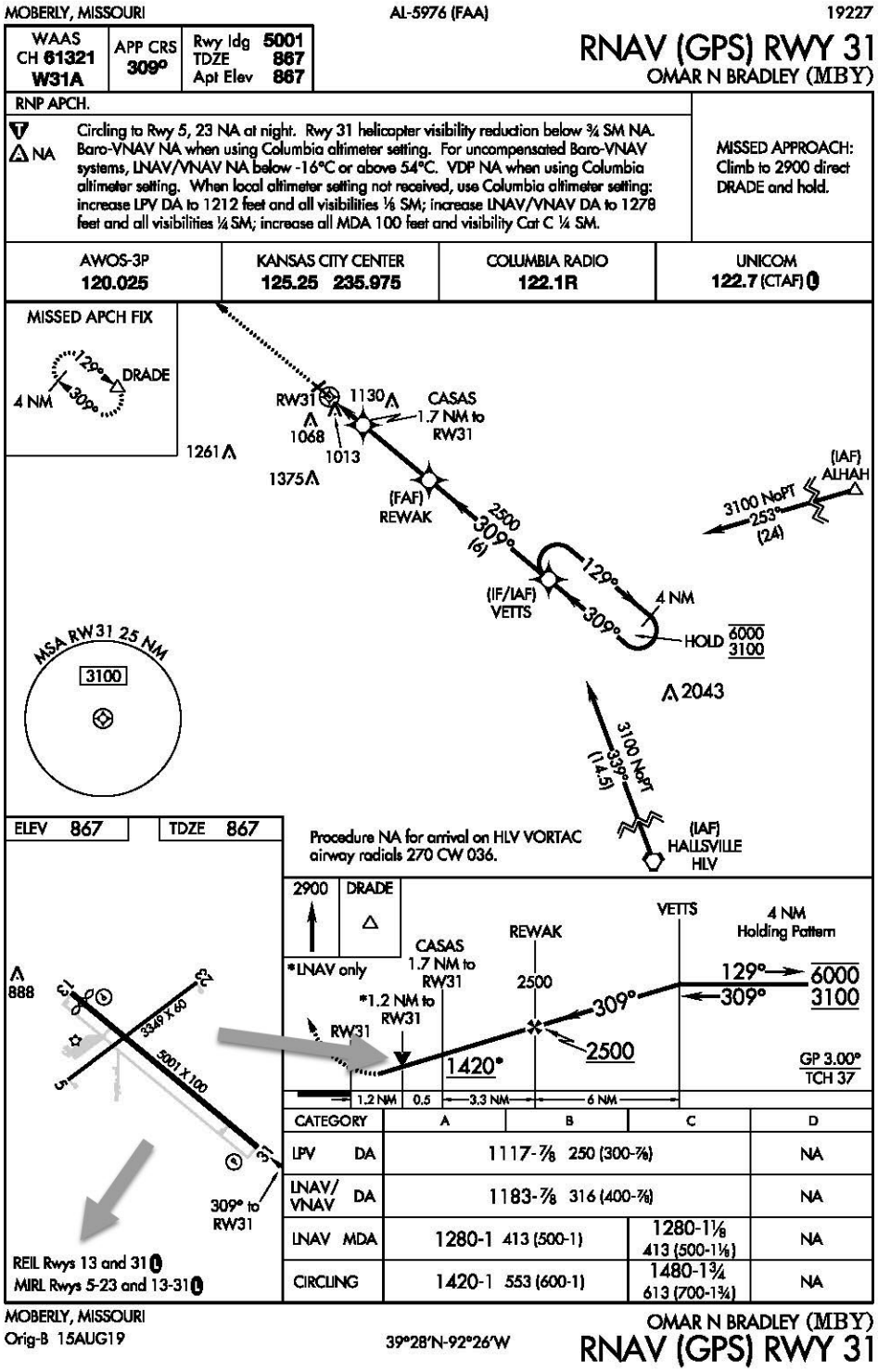
MOBERLY, MISSOURI
AL-5976 (FAA)
19227
WAAS CH 61321 W31A
APP CRS 309°
Rwy Idg 5001
TDZE 867
Apt Elev 867
RNAV (GPS) RWY 31
OMAR N BRADLEY (MBY)
RNP APCH.
Circling to Rwy 5, 23 NA at night. Rwy 31 helicopter visibility reduction below ¾ SM NA. Baro-VNAV NA when using Columbia altimeter setting. For uncompensated Baro-VNAV systems, LNAV/VNAV NA below -16°C or above 54°C. VDP NA when using Columbia altimeter setting. When local altimeter setting not received, use Columbia altimeter setting: increase LPV DA to 1212 feet and all visibilities ⅛ SM; increase LNAV/VNAV DA to 1278 feet and all visibilities ¼ SM; increase all MDA 100 feet and visibility Cat C ¼ SM.
NA
MISSED APPROACH: Climb to 2900 direct DRADE and hold.
AWOS-3P 120.025
KANSAS CITY CENTER 125.25 235.975
COLUMBIA RADIO 122.1R
UNICOM 122.7 (CTAF)
MISSED APCH FIX
DRADE
4 NM
129°
309°
RW31
1130
CASAS
1.7 NM to RW31
1068
1013
1261
1375
(FAF)
REWAK
2500
309°
(6)
(IAF)
ALHAH
3100 NoPT
253°
(24)
(IF/IAF)
VETTS
129°
309°
4 NM
HOLD
6000
3100
MSA RW31 25 NM
3100
2043
3100 NoPT
339°
(14.5)
(IAF)
HALLSVILLE
HLV
ELEV 867
TDZE 867
Procedure NA for arrival on HLV VORTAC airway radials 270 CW 036.
2900
DRADE
*LNAV only
CASAS
1.7 NM to RW31
REWAK
2500
*1.2 NM to RW31
RW31
1420
2500
VETTS
4 NM
Holding Pattern
129°
309°
6000
3100
GP 3.00°
TCH 37
1.2 NM
0.5
3.3 NM
6 NM
888
3349 X 60
5001 X 100
309° to RW31
REIL Rwys 13 and 31
MIRL Rwys 5-23 and 13-31
CATEGORY
A
B
C
D
LPV DA
1117-⅞ 250 (300-⅞)
NA
LNAV/VNAV DA
1183-⅞ 316 (400-⅞)
NA
LNAV MDA
1280-1 413 (500-1)
1280-1⅛ 413 (500-1⅛)
NA
CIRCLING
1420-1 553 (600-1)
1480-1¾ 613 (700-1¾)
NA
MOBERLY, MISSOURI
Orig-B 15AUG19
39°28'N-92°26'W
OMAR N BRADLEY (MBY)
RNAV (GPS) RWY 31
NC-3, 12 SEP 2019 to 10 OCT 2019
NC-3, 12 SEP 2019 to 10 OCT 2019

Appendix B

NTSB Accident Report

Example NTSB accident report at KPTK, Oakland County International, Michigan (NTSB, 2017d). The analysis section was used to determine if the accident qualified for the study. The factual data were used to code the pilot's hours into the dataset. Finally, the factual data were compared to the pull from the NTSB database to ensure accuracy.

National Transportation Safety Board
Aviation Accident Final Report

Location:	Waterford, Michigan	Accident Number:	GAA18CA007
Date & Time:	October 6, 2017, 23:55 Local	Registration:	N5EC
Aircraft:	Cessna T210	Aircraft Damage:	Substantial
Defining Event:	Collision during takeoff/land	Injuries:	1 None
Flight Conducted Under:	Part 91: General aviation - Personal		

Analysis

The pilot of the airplane reported that, while on an instrument flight rules approach to land in instrument meteorological conditions at night, he was "a little late descending" on the glideslope. He added that, during the approach, he increased the descent rate and became "a little right of course." He noticed approach lights but became "fixated" on the instruments while attempting to correct for being off course. Subsequently, the airplane struck the tops of trees, and he immediately pulled up. He landed without further incident.

The airplane sustained substantial damage to the right wing, empennage, and fuselage.

The pilot reported that there were no preaccident mechanical failures or malfunctions with the airplane that would have precluded normal operation.

The automated weather observation system at the accident airport reported, about the time of the accident, that the wind was from 140° at 5 knots, visibility 3/4 statute mile, light rain, and clouds overcast at 200 ft. The pilot landed on runway 9 and flew the RNAV GPS runway 9 approach.

Probable Cause and Findings

The National Transportation Safety Board determines the probable cause(s) of this accident to be:

The pilot's unstabilized approach at night, which resulted in collision with trees.

Findings

Aircraft	Descent/approach/glide path - Not attained/maintained
Personnel issues	Aircraft control - Pilot
Environmental issues	Tree(s) - Effect on operation
Environmental issues	Dark - Effect on personnel

Factual Information

History of Flight

Approach-IFR final approach	Course deviation
Approach-IFR final approach	Altitude deviation
Approach-IFR final approach	Collision during takeoff/land (Defining event)
Approach-IFR final approach	Collision with terr/obj (non-CFIT)

Pilot Information

Certificate:	Private	Age:	74,Male
Airplane Rating(s):	Single-engine land; Multi-engine land	Seat Occupied:	Left
Other Aircraft Rating(s):	None	Restraint Used:	3-point
Instrument Rating(s):	Airplane	Second Pilot Present:	No
Instructor Rating(s):	None	Toxicology Performed:	No
Medical Certification:	Class 3 Without waivers/limitations	Last FAA Medical Exam:	June 9, 2017
Occupational Pilot:	No	Last Flight Review or Equivalent:	April 28, 2017
Flight Time:	(Estimated) 3611 hours (Pilot In Command, all aircraft)		

Aircraft and Owner/Operator Information

Aircraft Make:	Cessna	Registration:	N5EC
Model/Series:	T210 M	Aircraft Category:	Airplane
Year of Manufacture:	1977	Amateur Built:	
Airworthiness Certificate:	Normal	Serial Number:	62373
Landing Gear Type:	Retractable - Tricycle	Seats:	6
Date/Type of Last Inspection:	November 10, 2016 Annual	Certified Max Gross Wt.:	3800 lbs
Time Since Last Inspection:		Engines:	1 Reciprocating
Airframe Total Time:	4386.7 Hrs as of last inspection	Engine Manufacturer:	CONT MOTOR
ELT:	C91 installed, not activated	Engine Model/Series:	TSIO-520-R11B
Registered Owner:		Rated Power:	310 Horsepower
Operator:	On file	Operating Certificate(s) Held:	None

Meteorological Information and Flight Plan

Conditions at Accident Site:	Instrument (IMC)	**Condition of Light:**	Night/dark
Observation Facility, Elevation:	KPTK,976 ft msl	**Distance from Accident Site:**	0 Nautical Miles
Observation Time:	02:53 Local	**Direction from Accident Site:**	86°
Lowest Cloud Condition:		**Visibility**	
Lowest Ceiling:	Overcast / 200 ft AGL	**Visibility (RVR):**	
Wind Speed/Gusts:	5 knots /	**Turbulence Type Forecast/Actual:**	/ None
Wind Direction:	140°	**Turbulence Severity Forecast/Actual:**	/ N/A
Altimeter Setting:	29.95 inches Hg	**Temperature/Dew Point:**	16°C / 16°C
Precipitation and Obscuration:	Moderate - None - Mist		
Departure Point:	WINCHESTER, IN (I22)	**Type of Flight Plan Filed:**	IFR
Destination:	Waterford, MI (PTK)	**Type of Clearance:**	IFR
Departure Time:	22:30 Local	**Type of Airspace:**	Class D

Airport Information

Airport:	OAKLAND COUNTY INTL PTK	**Runway Surface Type:**	Asphalt
Airport Elevation:	980 ft msl	**Runway Surface Condition:**	Dry
Runway Used:	09R	**IFR Approach:**	Global positioning system;RNAV
Runway Length/Width:	6521 ft / 150 ft	**VFR Approach/Landing:**	Full stop

Wreckage and Impact Information

Crew Injuries:	1 None	**Aircraft Damage:**	Substantial
Passenger Injuries:		**Aircraft Fire:**	None
Ground Injuries:	N/A	**Aircraft Explosion:**	None
Total Injuries:	1 None	**Latitude, Longitude:**	42.664722,-83.423057(est)

Appendix C

Tables

Table C1

Numerical Table of Pilot's Certificate Frequencies

Type of Certificate	*N*	Percentage
Airline Transport Pilot	93	7.2%
Airline Transport Pilot plus Flight Instructor	81	6.2%
Commercial	150	11.6%
Commercial plus Flight instructor	122	9.4%
Private	602	46.4%
Private plus Flight Instructor	3	0.2%
Recreational	1	0.1%
Sport	25	1.9%
Sport plus Flight Instructor	2	0.2%
Student	218	16.8%
Total	1297	100.0%

Note. Pilots with a student certificate cannot also hold flight instructor certificate (Certification: Pilots, Flight Instructors, and Ground Instructors, 2020). There were no reported accidents with pilots who held a recreational certificate plus flight instructor. There were no missing data for the pilot's certificate variable.

Table C2

Numerical Table of Pilot's Rating Frequencies

Type of Rating	*N*	Percentage
Multiengine	240	18.5%
Multiengine with Flight Instructor	352	27.1%
Single-engine	436	33.6%
Single-engine with Flight Instructor	269	20.7%
Total	1297	100.0%

Note. There were no missing data for the pilot's rating variable.

Table C3

Numerical Table of Runway Lighting Types Frequencies

Type of Runway Lighting	*N*	Percentage
Approach Lighting System	19	1.5%
Approach Lighting System plus PAPI 2	21	1.6%
Approach Lighting System plus PAPI 4	171	13.2%
Approach Lighting System plus VASI 2	1	0.1%
Approach Lighting System plus VASI 4	34	2.6%
None	178	13.7%
PAPI 2	345	26.6%
PAPI 4	367	28.3%
VASI 2	76	5.9%
VASI 4	85	6.6%
Total	1297	100.0%

Note. There were no missing data for the runway lighting types variable.

Table C4

Numerical Table of FAA Visual Area Surface Policy Timeframe Frequencies

FAA Policy Two - Year Periods	*N*	Percentage
Interim Policy Period from 2014 – 2015	393	30.3%
Assessment Policy Period from 2016 - 2017	486	37.5%
Final Policy Period from 2018 – 2019	418	32.2%
Total	1297	100.0%

Note. Each two-year policy timeframe began on January 1st of the listed year and ended on December 31st of the following year. There were no missing data for the FAA visual area surface policy timeframe variable.

Table C5

Numerical Frequencies of Landing Accidents by State

Two-Letter State Abbreviations	*N*	Percentage
AK	33	2.5%
AL	14	1.1%
AR	12	0.9%
AZ	62	4.8%
CA	144	11.1%
CO	34	2.6%
CT	13	1.0%
FL	113	8.7%
GA	38	2.9%
HI	8	0.6%
IA	12	0.9%
ID	26	2.0%
IL	20	1.5%
IN	23	1.8%
KS	19	1.5%
KY	10	0.8%
LA	10	0.8%
MA	13	1.0%
MD	30	2.3%
ME	3	0.2%
MI	31	2.4%
MN	26	2.0%
MO	31	2.4%
MS	4	0.3%
MT	17	1.3%
NC	30	2.3%
ND	5	0.4%
NE	7	0.5%
NH	8	0.6%
NJ	27	2.1%
NM	22	1.7%
NV	23	1.8%
NY	20	1.5%
OH	48	3.7%
OK	15	1.2%
OR	30	2.3%

PA	36	2.8%
RI	6	0.5%
SC	16	1.2%
SD	5	0.4%
TN	24	1.9%
TX	82	6.3%
UT	19	1.5%
VA	39	3.0%
VT	6	0.5%
WA	35	2.7%
WI	22	1.7%
WV	7	0.5%
WY	19	1.5%
Total	1297	100.0%

Note. Every state is listed except for Delaware. There were no missing data for the state of the landing runway accident.

Table C6

Numerical Table of Landing Runway in Use

Runway Number of Landing Runway	*N*	Percentage
01	25	1.9%
02	18	1.4%
03	26	2.0%
04	35	2.7%
05	36	2.8%
06	16	1.2%
07	25	1.9%
08	21	1.6%
09	33	2.5%
10	27	2.1%
11	22	1.7%
12	29	2.2%
13	38	2.9%
14	22	1.7%
15	20	1.5%
16	45	3.5%
17	56	4.3%
18	64	4.9%
19	34	2.6%
20	35	2.7%
21	33	2.5%
22	40	3.1%
23	35	2.7%
24	47	3.6%
25	55	4.2%
26	47	3.6%
27	52	4.0%
28	52	4.0%
29	29	2.2%
30	39	3.0%
31	44	3.4%
32	31	2.4%
33	31	2.4%
34	45	3.5%

35	42	3.2%
36	48	3.7%
Total	1297	100.0%

Note. Runway numbers were recorded using the two number designation (34 vice 340).

There were no missing data for the landing runway in use variable.

Table C7

Numerical Table of Crosswind Component

Computed Crosswind Component (Knots)	*N*	Percentage
.00	88	6.8%
.35	3	0.2%
.44	1	0.1%
.52	34	2.6%
.68	2	0.2%
.69	20	1.5%
.87	14	1.1%
1.03	33	2.5%
1.04	8	0.6%
1.22	17	1.3%
1.37	23	1.8%
1.39	12	0.9%
1.50	26	2.0%
1.53	2	0.2%
1.56	13	1.0%
1.71	21	1.6%
1.72	1	0.1%
1.74	7	0.5%
1.91	9	0.7%
1.93	23	1.8%
2.00	20	1.5%
2.05	14	1.1%
2.08	3	0.2%
2.26	3	0.2%
2.30	24	1.9%
2.39	22	1.7%
2.43	4	0.3%
2.50	20	1.5%
2.57	9	0.7%
2.60	31	2.4%
2.74	10	0.8%
2.78	3	0.2%
2.82	18	1.4%
2.95	20	1.5%
3.00	31	2.4%
3.02	1	0.1%

3.06	13	1.0%
3.08	14	1.1%
3.21	18	1.4%
3.35	1	0.1%
3.42	7	0.5%
3.46	17	1.3%
3.47	1	0.1%
3.50	9	0.7%
3.76	24	1.9%
3.83	12	0.9%
3.86	18	1.4%
3.94	11	0.8%
4.00	22	1.7%
4.10	3	0.2%
4.33	18	1.4%
4.45	7	0.5%
4.50	19	1.5%
4.60	10	0.8%
4.70	15	1.2%
4.79	3	0.2%
4.92	12	0.9%
5.00	15	1.2%
5.13	4	0.3%
5.14	13	1.0%
5.20	11	0.8%
5.21	1	0.1%
5.36	16	1.2%
5.47	4	0.3%
5.50	4	0.3%
5.64	15	1.2%
5.74	1	0.1%
5.79	12	0.9%
5.91	10	0.8%
6.00	16	1.2%
6.06	9	0.7%
6.13	4	0.3%
6.16	1	0.1%
6.43	5	0.4%
6.50	5	0.4%
6.58	12	0.9%
6.84	1	0.1%
6.89	21	1.6%
6.93	15	1.2%

7.00	8	0.6%
7.07	4	0.3%
7.50	3	0.2%
7.52	10	0.8%
7.66	8	0.6%
7.71	2	0.2%
7.79	6	0.5%
7.88	13	1.0%
8.00	11	0.8%
8.36	2	0.2%
8.43	4	0.3%
8.46	6	0.5%
8.66	6	0.5%
8.86	5	0.4%
9.00	9	0.7%
9.19	5	0.4%
9.40	8	0.6%
9.53	5	0.4%
9.64	5	0.4%
9.85	10	0.8%
9.96	3	0.2%
10.00	1	0.1%
10.28	3	0.2%
10.34	7	0.5%
10.39	3	0.2%
10.50	1	0.1%
10.72	3	0.2%
10.83	6	0.5%
11.00	3	0.2%
11.26	2	0.2%
11.28	5	0.4%
11.49	5	0.4%
11.82	5	0.4%
12.00	5	0.4%
12.12	3	0.2%
12.21	1	0.1%
12.22	3	0.2%
12.26	5	0.4%
12.80	3	0.2%
12.86	1	0.1%
12.99	2	0.2%
13.00	3	0.2%
13.16	2	0.2%

13.50	2	0.2%
13.79	5	0.4%
13.86	2	0.2%
14.00	4	0.3%
14.10	2	0.2%
14.55	1	0.1%
14.72	1	0.1%
14.77	5	0.4%
15.04	1	0.1%
15.32	1	0.1%
15.76	2	0.2%
16.09	1	0.1%
16.45	1	0.1%
16.74	1	0.1%
16.85	1	0.1%
16.91	2	0.2%
17.00	2	0.2%
17.85	2	0.2%
18.00	1	0.1%
18.79	1	0.1%
19.28	1	0.1%
19.73	1	0.1%
19.92	1	0.1%
20.68	2	0.2%
20.78	1	0.1%
21.45	1	0.1%
21.61	1	0.1%
22.00	2	0.2%
23.38	1	0.1%
23.75	1	0.1%
24.51	1	0.1%
29.13	1	0.1%
33.77	1	0.1%
Total	1297	100.0%

Note. There were no missing data for the crosswind component variable.

Table C8

Numerical Table of UTC Time of Accident

Type of Runway Lighting	*N*	Percentage
0000	8	0.6%
0003	1	0.1%
0005	1	0.1%
0008	2	0.2%
0010	1	0.1%
0015	4	0.3%
0020	3	0.2%
0024	1	0.1%
0027	1	0.1%
0030	12	0.9%
0031	1	0.1%
0035	2	0.2%
0036	1	0.1%
0040	2	0.2%
0045	1	0.1%
0047	2	0.2%
0048	1	0.1%
0050	1	0.1%
0055	1	0.1%
0100	4	0.3%
0105	2	0.2%
0108	1	0.1%
0110	4	0.3%
0115	4	0.3%
0118	1	0.1%
0119	2	0.2%
0120	2	0.2%
0124	1	0.1%
0130	6	0.5%
0135	1	0.1%
0140	1	0.1%
0145	6	0.5%
0148	1	0.1%
0150	1	0.1%
0153	1	0.1%
0156	1	0.1%
0200	9	0.7%
0209	1	0.1%

0210	2	0.2%
0215	1	0.1%
0225	1	0.1%
0230	5	0.4%
0240	2	0.2%
0245	2	0.2%
0250	1	0.1%
0257	1	0.1%
0300	3	0.2%
0310	1	0.1%
0313	1	0.1%
0314	1	0.1%
0315	4	0.3%
0325	1	0.1%
0330	7	0.5%
0335	1	0.1%
0350	1	0.1%
0355	1	0.1%
0400	1	0.1%
0401	1	0.1%
0407	1	0.1%
0420	1	0.1%
0440	1	0.1%
0500	1	0.1%
0506	1	0.1%
0523	1	0.1%
0540	1	0.1%
0553	1	0.1%
0600	2	0.2%
0622	1	0.1%
0630	1	0.1%
0639	1	0.1%
0648	1	0.1%
0653	1	0.1%
0715	1	0.1%
0722	1	0.1%
0800	1	0.1%
0810	1	0.1%
0815	1	0.1%
0850	1	0.1%

0913	1	0.1%
1000	1	0.1%
1013	1	0.1%
1017	1	0.1%
1051	1	0.1%
1056	1	0.1%
1100	1	0.1%
1120	1	0.1%
1130	2	0.2%
1140	1	0.1%
1148	1	0.1%
1200	1	0.1%
1210	1	0.1%
1222	1	0.1%
1230	5	0.4%
1231	1	0.1%
1242	1	0.1%
1245	5	0.4%
1249	1	0.1%
1250	2	0.2%
1258	1	0.1%
1300	6	0.5%
1303	1	0.1%
1310	1	0.1%
1313	1	0.1%
1315	5	0.4%
1320	1	0.1%
1327	1	0.1%
1330	11	0.8%
1333	1	0.1%
1335	1	0.1%
1342	3	0.2%
1345	6	0.5%
1347	1	0.1%
1350	3	0.2%
1357	1	0.1%
1400	13	1.0%
1410	2	0.2%
1415	10	0.8%
1418	1	0.1%
1420	2	0.2%
1425	3	0.2%
1427	1	0.1%

1428	1	0.1%
1430	23	1.8%
1433	1	0.1%
1434	1	0.1%
1435	1	0.1%
1436	1	0.1%
1437	1	0.1%
1438	2	0.2%
1439	1	0.1%
1440	1	0.1%
1445	6	0.5%
1446	1	0.1%
1450	2	0.2%
1451	1	0.1%
1453	1	0.1%
1455	4	0.3%
1458	3	0.2%
1500	34	2.6%
1502	2	0.2%
1505	1	0.1%
1507	1	0.1%
1508	1	0.1%
1510	1	0.1%
1515	7	0.5%
1517	1	0.1%
1518	2	0.2%
1520	4	0.3%
1525	2	0.2%
1530	24	1.9%
1531	1	0.1%
1534	2	0.2%
1535	4	0.3%
1536	1	0.1%
1540	2	0.2%
1545	11	0.8%
1550	4	0.3%
1555	2	0.2%
1600	28	2.2%
1601	1	0.1%
1602	1	0.1%
1605	5	0.4%
1607	1	0.1%
1610	3	0.2%

1614	1	0.1%
1615	7	0.5%
1618	4	0.3%
1620	2	0.2%
1621	1	0.1%
1622	1	0.1%
1625	2	0.2%
1626	1	0.1%
1630	35	2.7%
1631	1	0.1%
1635	5	0.4%
1642	1	0.1%
1643	1	0.1%
1644	2	0.2%
1645	7	0.5%
1650	5	0.4%
1655	1	0.1%
1659	1	0.1%
1700	32	2.5%
1701	1	0.1%
1702	1	0.1%
1705	2	0.2%
1708	1	0.1%
1709	1	0.1%
1710	1	0.1%
1715	8	0.6%
1716	1	0.1%
1718	1	0.1%
1720	1	0.1%
1723	1	0.1%
1725	4	0.3%
1730	33	2.5%
1733	2	0.2%
1735	1	0.1%
1738	1	0.1%
1740	4	0.3%
1745	6	0.5%
1746	1	0.1%
1747	1	0.1%
1750	5	0.4%
1752	1	0.1%
1758	2	0.2%
1800	31	2.4%

1802	1	0.1%
1803	1	0.1%
1805	3	0.2%
1806	2	0.2%
1810	4	0.3%
1811	1	0.1%
1812	1	0.1%
1815	6	0.5%
1817	1	0.1%
1818	1	0.1%
1820	7	0.5%
1824	1	0.1%
1826	1	0.1%
1827	1	0.1%
1828	1	0.1%
1830	28	2.2%
1831	2	0.2%
1834	1	0.1%
1835	4	0.3%
1839	1	0.1%
1840	2	0.2%
1843	1	0.1%
1845	9	0.7%
1850	4	0.3%
1852	1	0.1%
1854	1	0.1%
1856	1	0.1%
1858	2	0.2%
1900	44	3.4%
1905	3	0.2%
1906	1	0.1%
1908	1	0.1%
1909	1	0.1%
1910	3	0.2%
1913	1	0.1%
1915	4	0.3%
1916	1	0.1%
1917	1	0.1%
1919	1	0.1%
1920	4	0.3%
1922	1	0.1%
1924	1	0.1%
1925	4	0.3%

1928	1	0.1%
1929	1	0.1%
1930	21	1.6%
1932	1	0.1%
1935	1	0.1%
1937	1	0.1%
1940	4	0.3%
1943	1	0.1%
1945	9	0.7%
1950	5	0.4%
1952	2	0.2%
1953	2	0.2%
1954	1	0.1%
1955	2	0.2%
1956	1	0.1%
2000	34	2.6%
2004	1	0.1%
2005	1	0.1%
2006	2	0.2%
2007	2	0.2%
2010	3	0.2%
2012	1	0.1%
2015	13	1.0%
2018	1	0.1%
2020	12	0.9%
2023	1	0.1%
2025	1	0.1%
2026	1	0.1%
2027	1	0.1%
2029	1	0.1%
2030	34	2.6%
2031	1	0.1%
2035	1	0.1%
2040	3	0.2%
2041	1	0.1%
2043	4	0.3%
2045	5	0.4%
2047	2	0.2%
2050	1	0.1%
2053	1	0.1%
2055	1	0.1%
2057	4	0.3%
2100	19	1.5%

2104	1	0.1%
2105	2	0.2%
2109	1	0.1%
2110	3	0.2%
2112	1	0.1%
2115	9	0.7%
2116	1	0.1%
2117	1	0.1%
2119	1	0.1%
2120	6	0.5%
2121	1	0.1%
2125	3	0.2%
2130	18	1.4%
2133	1	0.1%
2134	1	0.1%
2136	1	0.1%
2138	2	0.2%
2140	3	0.2%
2142	1	0.1%
2143	1	0.1%
2145	10	0.8%
2146	1	0.1%
2148	1	0.1%
2150	1	0.1%
2151	2	0.2%
2153	1	0.1%
2155	3	0.2%
2200	21	1.6%
2201	1	0.1%
2205	1	0.1%
2208	1	0.1%
2210	5	0.4%
2212	1	0.1%
2214	1	0.1%
2215	7	0.5%
2217	1	0.1%
2218	1	0.1%
2220	4	0.3%
2225	5	0.4%
2227	1	0.1%
2230	20	1.5%
2235	3	0.2%
2240	7	0.5%

2242	1	0.1%
2243	1	0.1%
2245	5	0.4%
2246	1	0.1%
2247	1	0.1%
2250	6	0.5%
2252	1	0.1%
2255	2	0.2%
2300	20	1.5%
2304	1	0.1%
2305	2	0.2%
2306	1	0.1%
2310	2	0.2%
2312	1	0.1%
2313	1	0.1%
2315	2	0.2%
2316	1	0.1%
2318	1	0.1%
2320	6	0.5%
2321	2	0.2%
2325	2	0.2%
2328	1	0.1%
2330	19	1.5%
2332	1	0.1%
2335	3	0.2%
2340	2	0.2%
2342	1	0.1%
2345	6	0.5%
2350	2	0.2%
2355	1	0.1%
2359	1	0.1%
Total	1297	100.0%

Note. Time was reported on the NTSB accident reports in the 24-hour format from four zeros, midnight, to 2359. There were no missing data for the UTC time of accident variable.

Table C9

Numerical Table of Transformed UTC Time of Accident

UTC Time of Accident Grouped by Hour	*N*	Percentage
0000 - 0059	46	3.5%
0100 – 0159	39	3.0%
0200 – 0259	25	1.9%
0300 – 0359	21	1.6%
0400 – 0459	5	0.4%
0500 – 0559	5	0.4%
0600 – 0659	7	0.5%
0700 – 0759	2	0.2%
0800 – 0859	4	0.3%
0900 – 0959	1	0.1%
1000 – 1059	5	0.4%
1100 – 1159	6	0.5%
1200 – 1259	19	1.5%
1300 – 1359	43	3.3%
1400 – 1459	83	6.4%
1500 – 1559	107	8.2%
1600 – 1659	117	9.0%
1700 – 1759	112	8.6%
1800 – 1859	120	9.3%
1900 – 1959	124	9.6%
2000 – 2059	133	10.3%
2100 – 2159	96	7.4%
2200 – 2259	98	7.6%
2300 – 2359	79	6.1%
Total	1297	100.0%

Note. Time was grouped into one hour time periods. For example, accidents between 2000 and 2059 were all grouped into the 2000-hour block. Midnight was reported as four zeros and included in the four zero group.

Table C10

Severity of Aircraft Damage Training: Confusion Matrix

			Actual Values			
	Kernel	Severity of Aircraft Damage	None	Minor	Substantial	Destroyed
Predicted Values	Linear	None	972	0	0	0
		Minor	0	972	0	0
		Substantial	7	26	735	230
		Destroyed	0	0	218	694
	Polynomial	None	972	0	0	0
		Minor	0	972	0	0
		Substantial	0	2	984	11
		Destroyed	0	0	287	625
	Radial Basis Function	None	972	0	0	0
		Minor	0	972	0	0
		Substantial	1	2	904	91
		Destroyed	0	0	0	912
	Sigmoid	None	972	0	0	0
		Minor	0	972	0	0
		Substantial	22	86	564	326
		Destroyed	0	147	392	373

Table C11

Severity of Aircraft Damage Test: Confusion Matrix

			Actual Values			
	Kernel	Severity of Aircraft Damage	None	Minor	Substantial	Destroyed
Predicted Values	Linear	None	20	0	0	0
		Minor	0	30	0	0
		Substantial	8	8	194	40
		Destroyed	0	0	13	25
	Polynomial	None	20	0	0	0
		Minor	0	30	0	0
		Substantial	2	1	246	1
		Destroyed	0	0	20	18
	Radial Basis Function	None	20	0	0	0
		Minor	0	30	0	0
		Substantial	0	1	227	22
		Destroyed	0	0	0	38
	Sigmoid	None	20	0	0	0
		Minor	15	15	0	0
		Substantial	17	38	113	82
		Destroyed	1	10	16	11

Table C12

Severity of Aircraft Damage Test: Classification Report

Kernel / Accuracy	Severity of Aircraft Damage	Precision	Recall	F1-Score	Support
	None	0.71	1.00	0.83	20
Linear	Minor	0.79	1.00	0.88	30
	Substantial	0.94	0.78	0.85	250
	Destroyed	0.38	0.66	0.49	38
Accuracy				0.80	338
Macro Average		0.71	0.86	0.76	338
Weighted Average		0.85	0.80	0.81	338
	None	0.91	1.00	0.95	20
Polynomial	Minor	0.97	1.00	0.98	30
	Substantial	0.92	0.98	0.95	250
	Destroyed	0.95	0.47	0.63	38
Accuracy				0.92	338
Macro Average		0.94	0.86	0.88	338
Weighted Average		0.93	0.93	0.92	338
	None	1.00	1.00	1.00	20
Radial Basis	Minor	0.97	1.00	0.98	30
Function	Substantial	1.00	0.91	0.95	250
	Destroyed	0.63	1.00	0.78	38
Accuracy				0.93	338
Macro Average		0.90	0.98	0.93	338
Weighted Average		0.96	0.93	0.94	338
	None	0.38	1.00	0.55	20
Sigmoid	Minor	0.24	0.50	0.32	30
	Substantial	0.88	0.45	0.60	250
	Destroyed	0.12	0.29	0.17	38
Accuracy				0.47	338
Macro Average		0.40	0.56	0.41	338
Weighted Average		0.70	0.47	0.52	338

Table C13

Severity of Aircraft Damage Optimization Test: Confusion Matrix

			Actual Values			
	Kernel	Severity of Aircraft Damage	None	Minor	Substantial	Destroyed
Predicted Values	Optimization B	None	20	0	0	0
		Minor	0	25	5	0
		Substantial	0	1	241	8
		Destroyed	0	0	1	37
	Optimization D	None	20	0	0	0
		Minor	0	25	5	0
		Substantial	0	1	241	8
		Destroyed	0	0	0	38
	Optimization E	None	20	0	0	0
		Minor	0	25	5	0
		Substantial	0	1	241	8
		Destroyed	0	0	1	37
	Optimization F	None	20	0	0	0
		Minor	0	25	5	0
		Substantial	0	1	242	7
		Destroyed	0	0	2	36

Table C14

Severity of Personal Injury Training: Confusion Matrix

			Actual Values			
	Kernel	Severity of Personal Injury	None	Minor	Serious	Fatal
Predicted Values	Linear	None	302	251	126	169
		Minor	196	453	147	130
		Serious	63	208	360	99
		Fatal	90	190	51	538
	Polynomial	None	806	34	3	5
		Minor	507	405	7	7
		Serious	463	0	267	0
		Fatal	499	0	0	370
	Radial Basis Function	None	497	162	111	78
		Minor	126	684	44	72
		Serious	16	34	672	8
		Fatal	10	55	22	782
	Sigmoid	None	196	289	186	177
		Minor	202	298	222	204
		Serious	125	204	225	140
		Fatal	146	282	178	263

Table C15

Severity of Personal Injury Test: Confusion Matrix

			Actual Values			
	Kernel	Severity of Personal Injury	None	Minor	Serious	Fatal
Predicted Values	Linear	None	83	60	32	34
		Minor	39	125	46	34
		Serious	8	37	106	19
		Fatal	23	51	11	136
	Polynomial	None	196	12	0	1
		Minor	138	104	1	1
		Serious	111	0	59	0
		Fatal	103	0	0	118
	Radial Basis Function	None	131	38	26	14
		Minor	34	186	13	11
		Serious	0	6	164	0
		Fatal	0	11	5	205
	Sigmoid	None	62	66	44	38
		Minor	72	67	63	42
		Serious	27	56	55	32
		Fatal	52	76	36	57

Table C16

Severity of Personal Injury Test: Classification Report

Kernel / Accuracy	Severity of Personal Injury	None	Minor	Serious	Fatal
	None	0.54	0.40	0.46	209
Linear	Minor	0.46	0.51	0.48	244
	Serious	0.54	0.62	0.58	170
	Fatal	0.61	0.62	0.61	221
Accuracy				0.53	844
Macro Average		0.54	0.54	0.53	844
Weighted Average		0.54	0.53	0.53	844
	None	0.36	0.94	0.52	209
Polynomial	Minor	.90	0.43	0.58	244
	Serious	0.98	0.35	0.51	170
	Fatal	0.98	0.53	0.69	221
Accuracy				0.57	844
Macro Average		0.81	0.56	0.58	844
Weighted Average		0.80	0.57	0.58	844
	None	0.79	0.63	0.70	209
Radial Basis	Minor	0.77	0.76	0.77	244
Function	Serious	0.79	0.96	0.87	170
	Fatal	0.89	0.93	0.91	221
Accuracy				0.81	844
Macro Average		0.81	0.82	0.81	844
Weighted Average		0.81	0.81	0.81	844
	None	0.29	0.30	0.29	209
Sigmoid	Minor	0.25	0.27	0.26	244
	Serious	0.28	0.32	0.30	170
	Fatal	0.34	0.26	0.29	221
Accuracy				0.29	844
Macro Average		0.29	0.29	0.29	844
Weighted Average		0.29	0.29	0.29	844

Table C17

Optimization of All SVM Models with RBF Kernel for Severity of Personal Injury (Test)

σ	C	Misclassification Rate	Accuracy	Precision	Sensitivity / Recall	F1-Score
0.03	1	0.19	0.81	0.81	0.82	0.81
0.1	1	0.12	0.88	0.87	0.93	0.89
0.1	10	0.07	0.93	0.93	0.96	0.94
0.1	20	0.07	0.93	0.92	0.96	0.94
0.2	1	0.06	0.94	0.94	0.96	0.95
0.2	10	0.04	0.96	0.96	0.97	0.96
0.2	20	0.04	0.96	0.96	0.97	0.97
0.3	1	0.04	0.96	0.95	0.97	0.96
0.3	10	0.04	0.96	0.96	0.97	0.97
0.3	20	0.04	0.96	0.96	0.98	0.97
0.4	1	0.04	0.96	0.96	0.97	0.97
0.4	10	0.03	0.97	0.97	0.98	0.97
0.4	20	0.03	0.97	0.97	0.98	0.97
0.5	1	0.03	0.97	0.98	0.98	0.98
0.5	10	0.02	0.98	0.98	0.98	0.98
0.5	20	0.02	0.98	0.99	0.98	0.98
0.6	10	0.02	0.98	0.99	0.98	0.98
0.6	20	0.02	0.98	0.99	0.98	0.98
0.6	30	0.02	0.98	0.99	0.98	0.98
0.6	40	0.02	0.98	0.99	0.98	0.98
0.65	10	0.02	0.98	0.99	0.98	0.99
0.65	20	0.02	0.98	0.99	0.98	0.99
0.65	30	0.02	0.98	0.99	0.98	0.99
0.65	40	0.02	0.98	0.99	0.98	0.99
0.7	10	0.02	0.98	0.99	0.98	0.99
0.7	20	0.02	0.98	0.99	0.98	0.99
0.7	30	0.02	0.98	0.99	0.98	0.99
0.8	1	0.02	0.98	0.99	0.98	0.99
0.8	10	0.02	0.98	0.99	0.98	0.99
0.8	20	0.02	0.98	0.99	0.98	0.99
0.9	10	0.03	0.97	0.98	0.97	0.98
10	100	0.41	0.59	0.88	0.41	0.44

Table C18

Subcategory Factor Importance for the Severity of Aircraft Damage

Variable Subcategory	Importance
Pilot's Total Flight Hours	0.12214
Single-Engine Land Certificate	0.1184
Time of Accident	0.11376
Pilot's Age	0.10108
Crosswind Component	0.07759
Runway Number	0.06643
Any Obstacle Penetration	0.0559
FAA Policy 2018 – 19	0.04707
Sport Rating	0.0401
20:1 Obstacle Penetration	0.03263
Instrument Rating	0.02989
Part 91 Mission	0.02982
FAA Policy 2014 – 15	0.02768
PAPI 2	0.02557
No Obstacle Penetration	0.0246
34:1 Obstacle Penetration	0.02327
Reciprocal Engine	0.02195
Crew Number	0.02188
FAA Policy 2016 – 17	0.02167
Part 121 Mission	0.01925
Number of Engines	0.01436
PAPI 4	0.01335
Approach Light System	0.01322
Turbo Fan Engine	0.01172
Private Pilot Rating	0.01088
No Approach Lighting	0.01038
Commercial Rating	0.0096
Airline Transport Rating	0.00934
Multiengine Land Certificate	0.00901
VASI 2	0.00776
Flight Instructor Rating	0.00663
Student Rating	0.0061
Turbo Prop Engine	0.00589
VASI 4	0.00526
Part 135 Mission	0.00432

Turbo Jet Engine	0.00389
Part 137 Mission	0.00005
Recreational Rating	0
Part 129 Mission	0

Note. Pilot flight hours, time of day, number of crew, number of engines, pilot's age, runway number, and crosswind component have no subcategories.

Table C19

Subcategory Factor Importance for the Severity of Personal Injury

Variable Subcategory	Importance
Time of Accident	0.13608
Pilot's Total Flight Hours	0.13368
Crosswind Components	0.12436
Pilot's Age	0.12298
Runway Number	0.10273
Any Obstacle Penetration	0.04086
20:1 Obstacle Penetration	0.02495
PAPI 2	0.02359
FAA Policy 2016 - 17	0.02302
FAA Policy 2014 - 15	0.02258
PAPI 4	0.02256
Instrument Rating	0.02101
FAA Policy 2018 - 19	0.01963
Private Pilot Rating	0.01747
No Approach Lighting	0.01644
Multiengine Land Certificate	0.01614
No Obstacle Penetration	0.01602
34:1 Obstacle Penetration	0.01591
Single-Engine Land Certificate	0.01498
Approach Light System	0.01483
Number of Engines	0.01448
Flight Instructor Rating	0.01420
Commercial Rating	0.01291
VASI 2	0.01172
VASI 4	0.01002
Airline Transport Rating	0.00843
Sport Rating	0.00737
Student Rating	0.00683
Turbo Prop Engine	0.00639
Reciprocal Engine	0.00614
Turbo Fan Engine	0.00454
Part 91 Mission	0.00251
Part 135 Mission	0.00194
Crew Number	0.00137
Part 121 Mission	0.00115

Turbo Jet Engine	0.00056
Part 137 Mission	0.00043
Recreational Engine	0.00005
Part 129 Mission	0.00000

Note. Pilot flight hours, time of day, number of crew, number of engines, pilot's age, runway number, and crosswind component have no subcategories.

Appendix D

Figures

Figure D1

Severity of Aircraft Damage Test Confusion Matrix Image

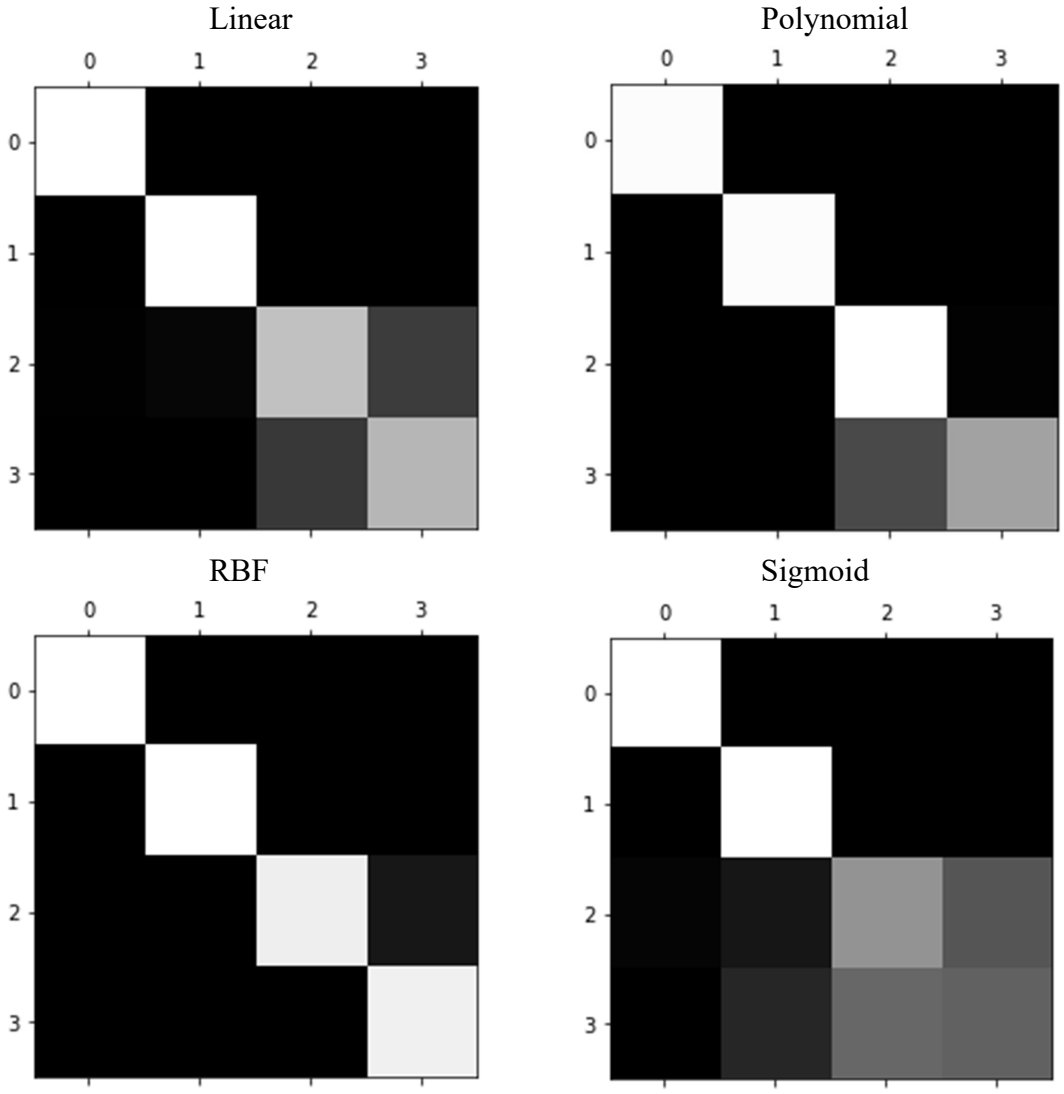

Note. RBF = Radial Basis Function.

Figure D2

Severity of Personal Injury Test Confusion Matrix Image

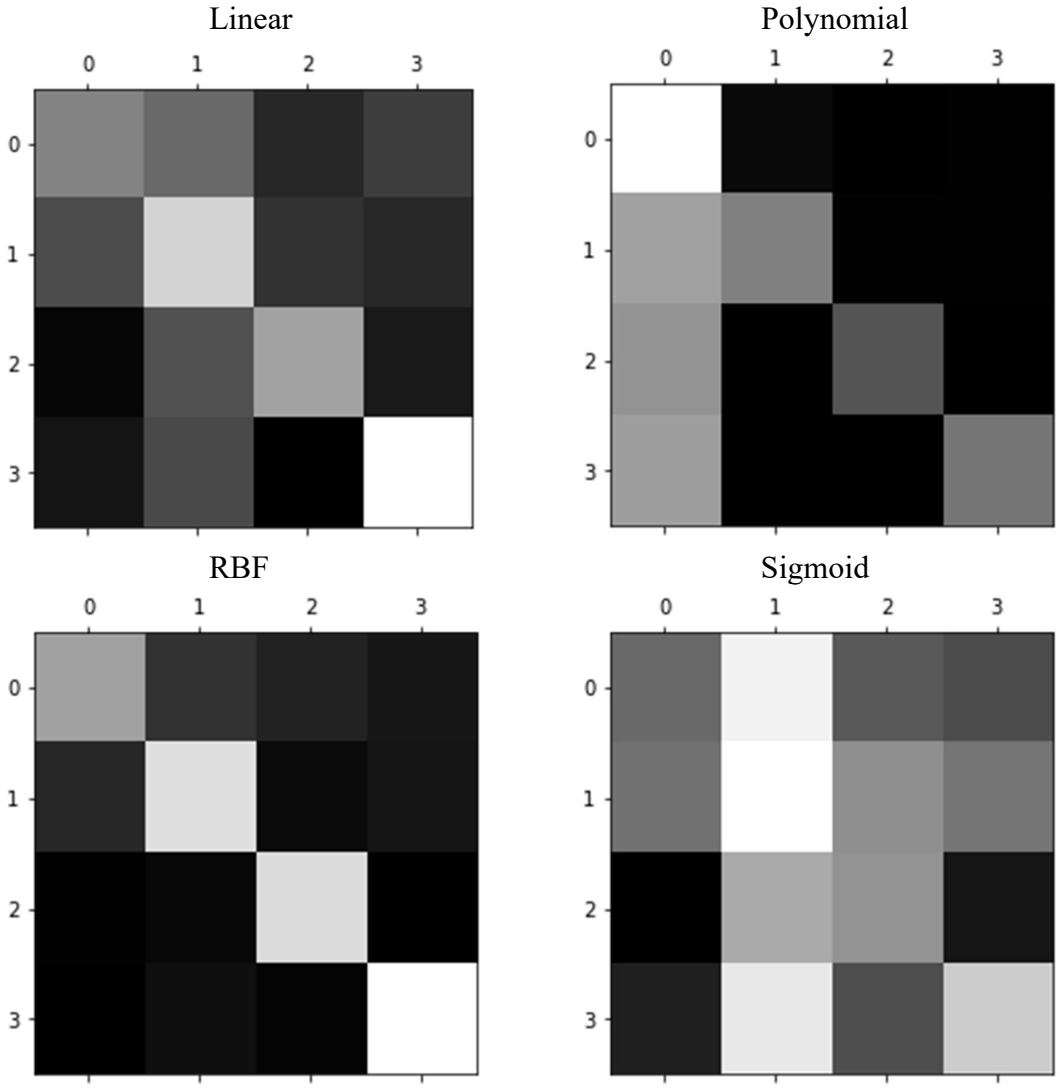

Note. RBF = Radial Basis Function.